THE IBY AND ALADAR FLEISCHMAN FACULTY OF ENGINEERING

The Zandman-Slaner Graduate School of Engineering

NOISE PROPAGATION ON RELATIVISTIC ELECTRON BEAM AND COHERENCE LIMITS OF FREE ELECTRON LASERS

By

Egor Dyunin

THESIS SUBMITTED TO THE SENATE OF TEL-AVIV UNIVERSITY

in partial fulfillment of the requirements for the degree of
"DOCTOR OF PHILOSOPHY"

Under the Supervision of Prof. Avi Gover

February 2013

Acknowledgments

First, I would like to express my gratitude to my supervisor Prof. Avi Gover, for his patience, strong support and useful suggestions, and for giving me the opportunity to work independently.

Special thanks to my friends and colleagues Dr. Alexey Shashurin and Dr. Inna Nusinsky-Shamuilov. Their criticisms repeatedly disturbed my equilibrium and forced me to think. I value their friendship.

I would like to express my deep gratitude to my mother Nina and mother-in- law Irina. Their help allowed me to completely devote my time to this work, especially during the writing phase.

Finally, my endless gratitude to my wife Julia and sons Jakov, Arie and Nisim. Their presence fills my life with meaning and they are my true inspiration. This work I dedicate to them.

Abstract

In this work I investigate the collective microdynamics in charged particle beams, particularly the stochastic microdynamics (noise development) at optical frequencies in modern high quality high current electron beams, used in Free Electron Lasers (FEL). I also analyze the generation of incoherent radiation in FELs, taking into consideration the stochastic microdynamics of noise development in the electron beam before it is injected into the FEL and within it.

The main assertion of this thesis is that electron beam noise can be controlled, even at optical frequencies, by adjusting the e-beam parameters, their drift length and use of dispersive magnetic elements. In particular, contrary to common belief, electron beam current shot-noise can be suppressed by collective effects below the classical shot noise limit of Poisson statistics. Since current-shot noise is the source of incoherent spontaneous radiation emission and self amplified spontaneous emission (SASE), the proposed scheme offers a way to control and suppress the radiation noise (and thus enhance the coherence) of seed-injected FELs.

The formulation used to establish the noise suppression theory is based on a one- dimensional linear solution of the beam plasma equations, combined with a modal excitation solution of Maxwell's equations. The stochastic signal formulation is based on the extension to relativistic beam energies and optical frequencies of the early microwave vacuum tube theory of Haus and others. The analysis of the collective microdynamics in the beam is a distributed circuit ("transmission line") model, which contrary to the short interaction length model used in conventional analysis of microbunching instability, is valid for multiple plasma wave oscillation lengths, and specifically for quarter plasma oscillation, where maximum noise suppression takes place in a free drifting beam.

The validity limits of the fluid plasma analysis and the noise suppression scheme are delineated. Necessary conditions of initial current-noise dominance (over velocity noise), ballistic thermal electrons phase spread neglect, and Landau damping neglect are identified and their relations are established. Finally, the theory is used to identify the technical and fundamental limits of coherence of short wavelength FELs analogously to the Schawlow-Towns limit for atomic lasers. It is found that after shot-noise suppression, the radiation noise in FEL is limited by the beam axial velocity spread, and fundamentally limited in the X-Ray regime by quantum noise.

Parts of this work are published in the following refereed journals:

1. A. Gover, E. Dyunin, Y. Lurie, Y.Pinhasi, M.V. Krongauz, “Superradiant and stimulated-superradiant emission in prebunched electron-beam II. Radiation enhancement schemes” Physical Review Special Topics-Accelerators and Beams, **8**, p.030702 (2005)

2. E. Dyunin, A.Gover, “The general velocity and current modulation linear transfer matrix of FEL and control over SASE power in the collective regime” Nucl. Instrum. Methods Phys. Res. A, **593**, p.49 (2008)

3. A. Gover, E. Dyunin, “Collective-Interaction Control and Reduction of Optical Frequency Shot Noise in Charged-Particle Beams” Phys. Rev. Lett. **102**, p.154801 (2009)

4. A. Gover, E. Dyunin, “Coherence limits of free electron lasers” IEEE J. Quantum Electron., **46**, p. 1511 (2010)

5. A. Nause, E. Dyunin, A. Gover, “Optical frequency shot-noise suppression in electron beams: three-dimensional analysis” J. Appl. Phys., **107**, p.103101 (2010)

6. A.Gover, E.Dyunin, T.Duchovni, A.Nause, “Collective microdynamics and noise suppression in dispersive electron beam transport” Physics of Plasmas, **18**, p.123102 (2011)

7. A. Gover, A. Nause, E. Dyunin, M. Fedurin, “Beating the shot-noise limit” Nature Physics, **8**, p.877 (2012)

The following were presented in international conferences:

1. Avi Gover, Egor Dyunin, “Coherence of e-beam radiation sources and FELs – A theoretical overview”**,** Proceedings of FEL 2006, BESSY, Berlin, Germany, MOAAU01

2. A. Gover, E. Dyunin, “FEL coherence below shot-noise limit and its fundamental limits”, Proceedings of FEL08, Gyeongju, Korea MOCAU02

3. A. Nause, E. Dyunin, A. Gover, “Shot-noise control and reduction by collective Coulomb interactions: 3D simulations evidence”, Proceedings of FEL2009, Liverpool, UK, MOPC01

4. A. Gover, E. Dyunin, “Sub-radiance and the coherence limits of FEL”**,** Proceedings of FEL2010, Malmö, Sweden, MOOC3

Table of Contents

List of Symbols

$\mathbf{A}$	vector potential
A	term of ABCD-transfer matrix
A_1	coefficient in the solution of the linear set of differential equations
A_2	coefficient in the solution of the linear set of differential equations
A_e	beam effective cross section
A_{em}	electromagnetic wave effective cross section
A_x	x-component of the vector potential
A_y	y-component of the vector potential
a_w	wiggler's normalized transverse momentum amplitude
$a_\perp$	normalized transverse momentum parameter
$\mathbf{B}$	external magnetic field
B	term of ABCD-transfer matrix
$\tilde{\tilde{\mathbf{B}}}$	magnetic field in phasor relation
B_1	coefficient in the solution of the linear set of differential equations
B_2	coefficient in the solution of the linear set of differential equations
$\mathbf{B}_{self}$	self magnetic field of the beam
$\mathbf{B}_{tot}$	total magnetic field
B_w	amplitude of the wiggler magnetic field
C	term of ABCD-transfer matrix
$\tilde{\tilde{C}}_q$	slow-varying amplitude of the electromagnetic mode q in phasor relation
c	speed of light in vacuum
D	term of ABCD-transfer matrix
$\mathbf{E}_0$	time-averaged (DC) electric field
$\mathbf{E}_1$	time- varying electric field
$\tilde{\tilde{\mathbf{E}}}$	electric field in phasor relation
$\breve{\mathbf{E}}$	Fourier transform of the electric field
E_{kin}	kinetic energy of electron beam
$\tilde{\tilde{\mathbf{E}}}_{pm}$	ponderomotive field in the phasor relation
$\hat{\tilde{\mathbf{E}}}_{pm}$	Laplace transform of phasor relation of ponderomotive force
$\tilde{\tilde{\mathbf{E}}}_{q\perp}$	transversal profile of the electromagnetic mode q
$\mathbf{E}_\mathrm{rad}$	traveling wave spectral radiation fields
$\tilde{\tilde{\mathbf{E}}}_{sc}$	space charge field in phasor relation
$\hat{\tilde{\mathbf{E}}}_{sc}$	Laplace transform of phasor relation of space charge field
$\mathbf{E}_{tot}$	total electric field
e	elementary charge
$\hat{\mathbf{e}}_x$	unit vector co-directional with x-axes
$\hat{\mathbf{e}}_y$	unit vector co-directional with y-axes

$\hat{\mathbf{e}}_z$ unit vector co-directional with z-axes

F noise figure parameter

$\tilde{\mathbf{F}}$ transfer matrix of free electron laser in terms of normalized detuning functions

$\tilde{\mathbf{f}}$ zero order transfer matrix of free electron laser in terms of normalized detuning functions

$\hat{\tilde{f}}$ Laplace transform of a function f

G gain parameter of amplifier

$\breve{\mathbf{H}}$ Fourier transform of the magnetic field

$\mathbf{H}_{\mathrm{FEL}}$ general transfer matrix of free electron laser

$\tilde{\mathbf{H}}_T$ 3x3 transfer matrix of free drift section

$\tilde{\mathbf{h}}$ transfer matrix of free electron laser with dimensional variables

$\tilde{I}$ small signal current modulation in phasor relation

$\breve{I}$ beam current spectrum

$\hat{\tilde{I}}$ Laplace transform of phasor relation of electron beam current

I_0 beam current

I_1 time- varying small signal beam current

I_A Alfven current (~17 kAmp)

i imaginary unit

$\breve{i}$ slow amplitude small signal current

$\tilde{i}$ slow amplitude small signal current in phasor relation

$\tilde{i}_1^{disp}$ slow amplitude small signal beam current in dispersive section presented in phasor relation

j and j' indexes of particle in an ensemble

$\mathbf{J}_0$ time-averaged (DC) beam current density

$\mathbf{J}_1$ time- varying beam current density

$\tilde{J}_z$ z-component of the beam current density in phasor relation

$\hat{\tilde{J}}_z$ Laplace transform of phasor relation of axial electron beam current density

$\mathbf{j}$ beam current density

$\tilde{j}$ slow amplitude small signal current density in phasor relation

K real function

K_1 modified Bessel function of the second kind

$\mathbf{k}$ optical wavenumber

k_B Boltzmann constant

k_b axial wavenumber of a spatial modulation in a beam

k_{qz} axial wavenumber of the electromagnetic mode q

k_w wiggler wavenumber

L_{acc} length of accelerator

L_d length of non-dissipative free drift section

L_{d1} length of the first drift section on the LCLS injector

L_{d2} length of the second drift section on the LCLS injector

L_{disp} – length of dispersive section

L_{Landau} Landau damping length, inverse of Landau damping parameter

$\mathbf{M}$ transfer matrix for a general non-dissipative system

$\mathbf{M}_{acc}$ transfer matrix of acceleration section

$\mathbf{M}_{acc}^{(1)}$ transfer matrix of acceleration section in first order

$\mathbf{M}_{\mathrm{d1}}$ transfer matrix of the first drift section on the LCLS injector

$\mathbf{M}_{\mathrm{d2}}$ transfer matrix of the second drift section on the LCLS injector

$\mathbf{M}_{drift}$ transfer matrix of uniform drift section

$\mathbf{M}^{LCLS}$ total transfer matrix of the LCLS injector

$\mathbf{M}_{acc}^{LCLS}$ transfer matrix of the acceleration section on the LCLS injector

$\mathbf{M}_{disp}^{LCLS}$ transfer matrix of the dispersion section on the LCLS injector

$\mathbf{M}_{shortdisp}$ transfer matrix of short dispersive section

m_0 electron rest mass

N noise dominance factor

N_D Landau damping parameter

N_T total number of electrons crossing the plane z within time T

$\hat{\tilde{n}}$ Laplace transform of phasor relation of e-beam density

$\tilde{n}$ small signal density modulation (in phasor relation)

n density of electrons

n_0 time-averaged (DC) electron's density

n_1 time- varying small signal electron's density

$\breve{n}_1$ small signal density modulation (in Fourier relation)

$\mathbf{P}$ canonical momentum of the electron

P_{in} input power

P_k small signal kinetic power

$\breve{P}_k$ spectral parameters of the absolute value squared kinetic power

P_{NEP} noise equivalent power parameter

P_{out} output power

$(P_{out})^{noise}$ output power due to the noise input source

P_q q-mode's normalized power

P_x x-component of the canonical momentum of the electron

P_y y-component of the canonical momentum of the electron

P_z z-component of the canonical momentum of the electron

$\mathbf{p}$ momentum of an electron

$\mathbf{p}_0$ momentum of the design particle

Q_b bunch charge

$\mathbf{R}$ 6D particle transport matrix

$\mathbf{r}$ radius vector

r_0 radius of an electron beam in the waist

$\mathbf{r}_\perp$ radius vector in transverse plane (*xy*-plane)

r_b beam cross section radius

r_j position of j^{th} particle

r_p plasma reduction factor

S noise suppression parameter

S_k small signal kinetic power density

S_j roots of the Free Electron Laser cubic dispersion equation (Pierce dispersion equation)

S_{10}, S_{20}, S_{30} zero order term of the Free Electron Laser cubic dispersion equation (Pierce dispersion equation) roots

s variable in Laplace space

T time duration, larger than the coherence time of the signal

T_A ambient temperature

T_c cathode temperature

t time

t_1 arrival time of the 1^{st} electron to the dispersive section entrance

t_2 arrival time of the 2^{nd} electron to the dispersive section entrance

$t_j(z)$ moment when the j^{th} particle cross the plane "z"

t_p bunch duration

$\mathbf{u}$ beam velocity

$\tilde{u}$ small signal axial beam velocity in phasor relation

$\mathbf{u}_0$ time-averaged (DC) beam velocity

u_{01} axial velocity of 1^{st} electron

u_{02} axial velocity of 2^{nd} electron

u_{0z} axial component of the velocity

$\mathbf{u}_1$ time- varying small signal beam velocity

$\breve{u}_1$ small signal velocity modulation (in Fourier relation)

$\mathbf{u}_j$ velocity of the j^{th} particle

u_{jz} axial velocity of the j^{th} particle

u_{th} velocity spread defined from the beam distribution function

$\hat{\tilde{u}}_z$ Laplace transform of phasor relation of electron beam axial velocity

V_1 Chu's small signal kinetic voltage

$\tilde{V}$ slow amplitude small signal kinetic voltage in the phasor relation

$\hat{\tilde{V}}_z$ Laplace transform of phasor relation of kinetic voltage

$\tilde{v}$ slow amplitude small signal kinetic voltage in phasor relation

$\tilde{v}^{disp}$ slow amplitude small signal kinetic voltage in dispersive section presented in phasor relation

W real function

W_d e-beam modulation (wave-) impedance in a uniform section

W_w plasma wave impedance in wiggler

$\breve{X}, \breve{Y}$	Fourier transform of quiescent variables *X* and *Y* respectively
X_1	quiescent variable
$\tilde{\tilde{X}}$	quiescent variable in phasor relation
x	x-Cartesian coordinate
y	y-Cartesian coordinate
Z_0	characteristic impedance of free space
Z_q	wave impedance of mode q
z	z-Cartesian coordinate
z'	integration variable z-Cartesian coordinate
z''	integration variable z-Cartesian coordinate
z_{in}	axial coordinate of the entrance of a dispersive section
z_j	axial coordinate of the j^{th} particle
z_{OTR}	OTR screen's axial position
z_{out}	axial coordinate of the exit of a dispersive section
z_{waist}	electron beam waist length
β	velocity in terms of the speed of light
β_0	time-averaged (DC) velocity in terms of the speed of light
β_{0z}	axial velocity in terms of light velocity
β_1	time- varying velocity in terms of the speed of light
β_{th}	velocity spread defined from the beam distribution function in terms of the speed of light
Γ	gain parameter in the Free Electron Laser cubic dispersion equation (Pierce dispersion equation)
γ	relativistic Lorentz factor
γ_0	time-averaged (DC) relativistic Lorentz factor
γ_{0z}	axial relativistic Lorentz factor
γ_1	time- varying relativistic Lorentz factor
γ'	acceleration gradient
ΔE_c	spread of kinetic energy on the cathode
Δf	frequency bandwidth
$\Delta\omega_{HG}$	FWHM spectral width of the high gain Free Electron Laser
δE_k	slice energy spread
δp	difference in momentum between the examined particle and the design one
δu_j	particular particle deviation velocity from the ensemble average
ε_0	dielectric permittivity of vacuum
ε_n	beam normalized slice emittance
θ	detuning parameter
θ_p	longitudinal plasma oscillation wavenumber
θ_p^{disp}	longitudinal plasma oscillation wavenumber in dispersive section
θ_{pr}^{disp}	reduced longitudinal plasma oscillation wavenumber in dispersive section

θ_{pr} reduced longitudinal plasma oscillation wavenumber

θ_{prw} reduced longitudinal plasma oscillation wavenumber in wiggler

λ optical wavelength in free space

λ_b beam modulation wavelength in lab frame

λ_b' beam modulation wavelength in moving frame

λ_w period of wiggler

μ_0 magnetic permittivity of vacuum

ρ Pierce parameter

σ standard deviation for a Gaussian distribution

$\sigma_{x,y,r,x',\beta z}$ variance of the beam distribution in *x*-, *y*-, *r*-, *x'*- and β_z dimension respectively

τ electron transit time through a dispersive section

ϕ real function

ϕ_A complex phase of the term A in ABCD-transfer matrix

ϕ_B complex phase of the term B in ABCD-transfer matrix

ϕ_C complex phase of the term C in ABCD-transfer matrix

ϕ_D complex phase of the term D in ABCD-transfer matrix

ϕ_{prd} plasma wave accumulation phase in free drift section (plasma reduction factor is taken into account)

ω Signal angular frequency

ω_p plasma frequency

φ electric potential

φ^E phase of the input radiation field

φ^I phase of the input current prebunching wave

$\frac{dP_{NEP}}{d\omega}$ spectral density Noise Equivalent Power

$\left(\frac{dP_{NEP}}{d\omega}\right)^I$ current noise spectral density Noise Equivalent Power

$\left(\frac{dP_{NEP}}{d\omega}\right)^V$ velocity noise spectral density Noise Equivalent Power

$\left(\frac{dP_{NEP}}{d\omega}\right)^{IV}$ kinetic power noise spectral density Noise Equivalent Power

List of Abbreviations

1D/2D/3D/6D	one/two/three/six dimensional
ATF	Advanced Test Facility, international research center in USA
BESSY	Berliner Elektronen-Speicherring Gesellschaft für Synchrotronstrahlung, international research center in Germany
COTR	Coherent Optical Transition Radiation
CSR	Coherent Synchrotron Radiation
DESY	Deutsches Elektronen-Synchrotron, international research center in Germany
FEL	free electron laser
FWHM	full width half maximum
HGHG	harmonic generation and high gain
HHG	high harmonic generation
IR	infra-red
LCLS	Linac Coherent Light Source, international research center in Germany
LINAC	linear accelerator
LSC	longitudinal space charge
NEP	Noise Equivalent Power
OTR	Optical Transition Radiation
RF-LINAC	Radio-Frequency Linear Accelerator
r.h.s	right hand side
rms	root means square
SASE	Self Amplified Spontaneous Emission
SCSS	SPring-8 Compact SASE Source, international research center in Japan
SLAC	Stanford Linear Accelerator Center, National Lab, USA
SPARC	Sorgente Pulsata Auto-amplificata di Radiazione Coerente, international research center in Italy

TESLA	Teraelectronvolt Energy Superconducting Linear Accelerator, international research center in Germany
TWT	travelling wave tube
UV	ultra-violet

List of Figures

1 Introduction

Free Electron Laser (FEL) is a source of high power coherent radiation. The FEL operates as a converter of the kinetic energy of accelerated electrons to radiation. The free electrons (emitted from a thermionic or photo-cathode electron gun) are accelerated in an accelerator up to a relativistic energy. It is well known that an electron which moves uniformly in a free space does not radiate, because frequency (ω) and wavenumber (k) of any electromagnetic wave are not synchronous to the electron. The synchronism is done by different mechanisms of interaction between electromagnetic fields and high energy accelerated electron beams in electron tubes, synchrotrons, and Free Electron Lasers (FELs).

In the case of FEL, the electrons are passed through a periodical external field (magnetic, electric or electromagnetic) and efficiently radiate electromagnetic waves (Figure 1-1). The FEL is a coherent radiation device in which the energy of a relativistic electron beam is partially converted to electromagnetic wave energy. The radiation is emitted at a wavelength (λ), specified by a synchronism condition between the electromagnetic wave, the electron beam energy and the parameters of a periodic magnetic field structure (wiggler or undulator) in which it propagates: the period of the wiggler λ_w and the wiggler strength a_w (see Figure 1-2). The wiggler strength parameter a_w will be defined in Chapter 3.

Comprehensive reviews of the physics and technology of FELs can be found in [1, 2, 3, 4, 5, 6]. Figure 1-2 shows the worldwide radiation achievements based on FEL technologies as of 2002 [7, 8]. The figure shows the radiation wavelength as a function of accelerating energy. The experimental data in this figure shows the inverse proportion dependence of the radiation wavelength on the square of the acceleration energy. The wide spectral range (six orders of magnitude) of FEL devices and the wide tuning range of some of them are remarkable. Accelerators with energies of several megavolts can be used as coherent radiation source in the microwave range, millimeter wave, and sub-millimeter (THz) wavelengths. Accelerators providing e-beams of tens of mega electron volts enable operation in the visible and infrared range. Use of accelerators in the range of Giga electron volts enables achievement of X- and UV-radiation in the front-line range up to 1 Å = 100 pm and beyond. Today there are no other useful coherent lasers in this range; FELs, developed in big research laboratories in the USA (LSLS-SLAC, Stanford), in Germany (DESY-Hamburg, BESSY-Berlin), and in Japan (SCSS, Spring 4), have already demonstrated radiation sources in the X-ray range with a brightness at least 6 orders of magnitude higher than the synchrotron radiation sources seen in Figure 1-3.

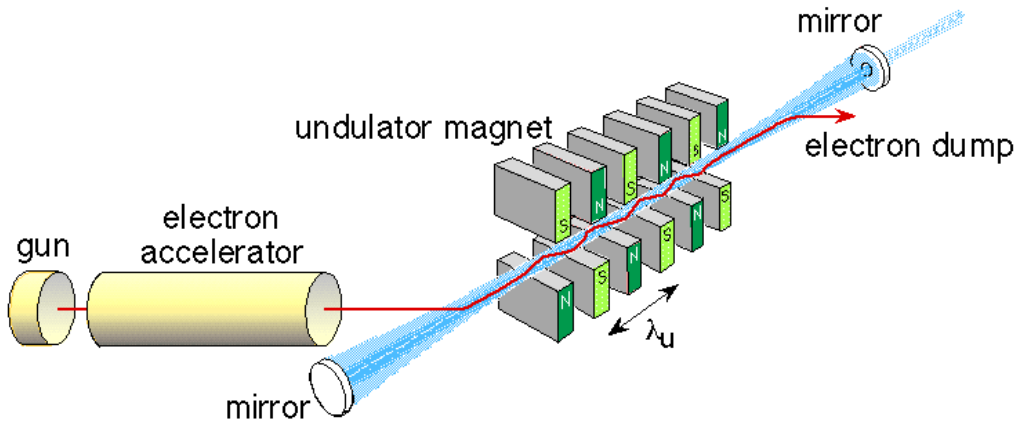

Figure 1-1 Scheme of Free Electron Laser (picture used from [9]).

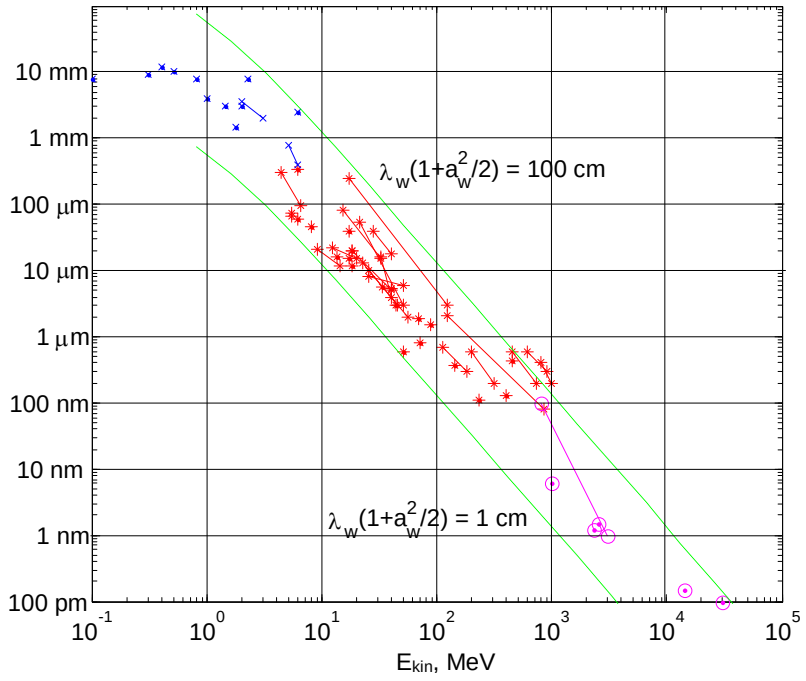

Figure 1-2 A graph of FEL radiation devices (world wide): radiation wavelength (λ) vs. accelerator energy (E_{kin}). Taken from [1].

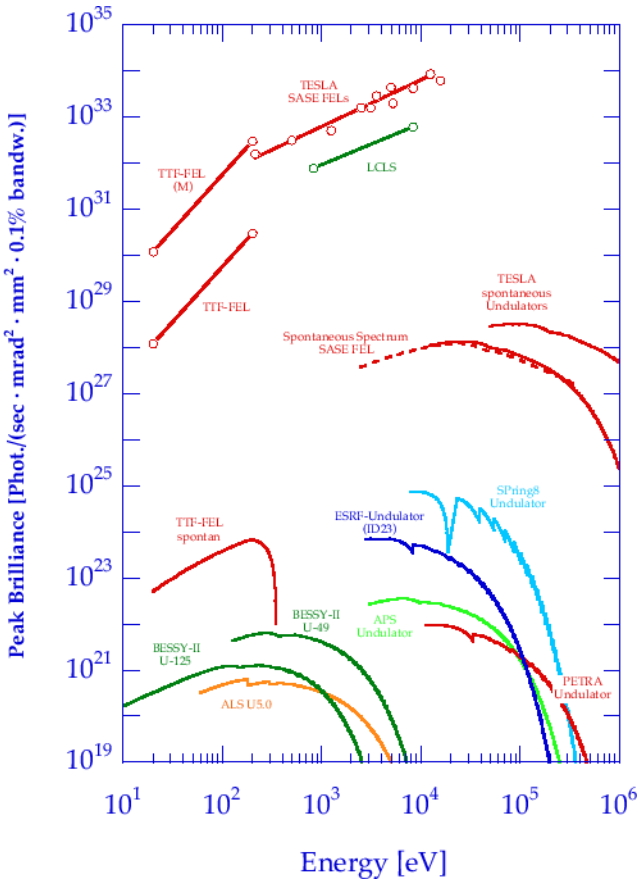

Figure 1-3 A comparison of Synchrotron sources of X and UV radiation with FELs. Brightness of FEL sources is 6 orders of magnitude greater.

The most impressive achievement so far in the field of FELs is the demonstration of a first X-ray laser (λ = 1.5 Å) in LCLS in 2011 [10]. This achievement is expected to lead to most important scientific applications in biological and other sciences and fields [11, 12, 13, 14, 15]. In this dissertation, I develop the linear theory of coherent and incoherent radiation emission of FEL starting from first principles. The analysis is then used to study the dynamics of noise evolution in electron beams and its implication to the generation of incoherent radiation in FELs. This radiation noise sets limits on the coherence of FEL, if operated as a coherent laser. My analysis and study led to new understanding of the coherence limits of FEL devices, and to discovery of new ways for controlling the FEL noise and arriving to its fundamental coherence limits.

The coherence of the radiation beam is one of the important parameters of any laser, and we expect that it would be important for FELs as well. Some early work has been done on the coherence of FEL oscillators [16], where coherence limits, similar to the Schawlow-Townes limit of conventional atomic lasers [17], were identified. However, the main interest in the FEL scientific field is currently in high gain FEL amplifiers, because they can operate at short wavelengths, down to X-rays. Most of these FELs have been operated in a Self Amplified Spontaneous Emission (SASE) mode [18, 19, 20]. Namely, they amplify the incoherent radiation noise generated by the e-beam noise. The reason has been the absence of coherent radiation X-ray sources to be amplified. On the other hand, construction of FEL oscillators in the X-ray regime has been difficult because of the lack of appropriate mirrors. Consequently, most of the present FELs in the X-UV and X-ray regime are temporally incoherent. They are very bright because of their very high power and an effect of optical guiding [21, 22] that maintains high spatial coherence of the radiation beam (Figure 1-3). However, now there is also great interest in turning these exceptional X-UV FEL radiation sources into temporally coherent sources with unprecedented spectral brightness.

With the recent striking development of high power ultra-short pulsed solid-state lasers, new schemes for coherent radiation sources in the X-UV regime have emerged. These can now be used as coherent signal sources (seed) in high gain FEL amplifiers. In recent years, a number of coherent seeding schemes have been developed in order to overcome the shot-noise (SASE) coherence limitation of FELs in the X-UV regime. These include a scheme of injection of X-UV seed radiation, produced by High Harmonic Generation (HHG) in gas, using an intense femtoSecond laser beam [23, 24]; and a scheme for pre-bunching the e-beam by consecutive Harmonic Generation and High Gain amplification (HGHG) [25] in wiggler structures. In these schemes, coherence is expected to be achieved if the injected coherent harmonic signal (of radiation or current modulation) is strong enough to significantly exceed the shot-noise equivalent-input-radiation power (SASE) [26].

HGHG pre-bunching has been demonstrated in the visible wavelength regime [24]. HHG coherent radiation injection into an FEL was demonstrated at a

wavelength of $\lambda = 49$ nm in the Spring-8 FEL facility in Japan [23] and at $\lambda = 133$ nm in SPARC, Italy [27]. In both of these coherent signal-injection schemes, it is difficult to produce an intense coherent injection signal which dominates the SASE radiation. This becomes harder at short wavelengths, as one gets closer to the desirable X-UV regime.

In this dissertation, an extensive linear formulation for analyzing both coherent and incoherent radiation in FEL is developed. A large section of the work is dedicated to the dynamics of incoherent current fluctuations (noise) in the electron beam prior to injection into the FEL wiggler. This is important because the main source of radiation noise in FELs (SASE) is the e-beam shot-noise (Figure 1-4). The study of the collective interaction noise dynamics in electron beam transport enabled me, as part of our FEL research group, to propose in this dissertation new concepts for controlling and suppressing electron beam noise [28, 29, 30, 31], as well as radiation noise [32, 33].

In this work I was highly inspired by the earlier work and theoretical formulation that was developed in the middle of the 20^{th} century in connection with microwave tubes (with non-relativistic beams) and is well presented in the books of J.R.Pierce and H.Haus [34, 35, 36], two of the a-vanguard leaders of this field.

The formulation of signal propagation on an electron beam in microwave vacuum tubes was expressed in terms of an equivalent analog transmission line [37, 38]. Thus, the propagation of signals – either coherent or stochastic - on electron beam flow was described in terms of propagation of "current modulation" and "kinetic voltage modulation" waves in analogy to current and voltage signal propagation on electric transmission lines. As a result of such formulation, the transmission of the signals (current modulation and kinetic voltage modulation) on the e-beam can be presented on a Smith-chart [39] and be described in terms of "wave impedance", "wave transducer", etc.

Using the transmission line model, an elegant mathematical formalism was developed by Haus and others to describe the propagation of coherent current and velocity (kinetic voltage) waves, and was then further extended by them to the case of stochastic wave propagation. This extension made it possible to understand the sources of noise in microwave tubes (TWT, klystron, etc.) and eventually to find ways to minimize them [40, 41].

The intrinsic limit of an electronic amplifier of gain G in the microwave regime has been considered to be the Nyquist noise [42]

$$P_{out} = G k_B T_A \Delta f \qquad 1\text{-}1$$

where k_B is the Boltzmann constant, Δf the amplifier frequency bandwidth, and $T_A = 290^{o}$K is the ambient room temperature. This corresponds to a model in which the black-body radiation per a single transverse radiation mode:

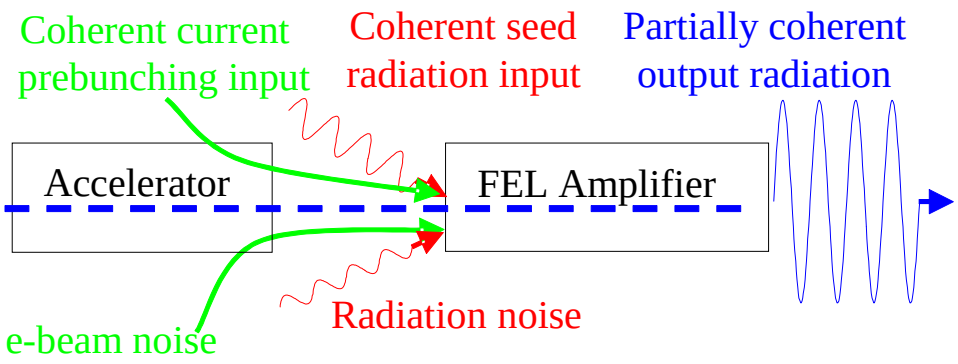

Figure 1-4 Scheme of diferent sources of coherent and incoherent radiation in Free Electron Laser: beam current prebunching and beam noise (green); coherent seed signal and incoherent thermal radiation (red). The partially coherent output radiation signal is shown in blue.

$$P_{in} = k_B T_A \Delta f \qquad 1\text{-}2$$

is injected into the RF-input of the amplifier.

In practice, the output power of microwave tube amplifiers was always higher than the Nyquist limit, because the electron beam, which is injected into the tube, generates noise by itself. This noise originated from fluctuation in the beam current due to two random processes: the random timing of electrons emission from the cathode and the random velocity in which they are emitted from the hot cathode with kinetic energy spread $\Delta E_c = k_B T_c$ (where T_c is the hot cathode temperature).

The noise of a practical amplifier is often characterized by the Noise Equivalent Power (P_{NEP}) parameter, which is the equivalent input radiation noise power that would produce at the amplifier output the actual measured incoherent output radiation power (noise).

$$P_{NEP} = \left(P_{out}\right)^{noise} \Big/ G \qquad 1\text{-}3$$

Further, the quality of the amplifier as a low noise device was characterized in terms of the noise figure parameter *F,* which is the ratio between the total measured output power noise of the practical amplifier to the output of this same amplifier if it had no internal noise (e-beam related) contribution (except for the intrinsic Nyquist Radiation noise). In terms of the input noise equivalent power, this parameter is defined as [43]

$$F = \frac{P_{NEP}}{P_{in}} = \frac{P_{NEP}}{k_B T_A \Delta f} \qquad 1\text{-}4$$

This noise figure of merit always satisfies $F > 1$, where $F = 1$ corresponds to an ideal amplifier with no excess noise besides the intrinsic Nyquist noise.

In the microwave tube art, it was found that usually $F >> 1$ and the major source of the excess amplifier noise is the shot-noise in the electron beam originating from current (or charge density) fluctuations due to random arrival of electrons into the amplifier tube. This noise is normally much larger than the velocity that originates from the random velocity of electrons emitted from a thermionic cathode with a finite energy spread ΔE_c.

Learning the dynamics of collective space charge interaction of current fluctuations in an electron beam that involve transfer of energy and development of statistical correlation between current noise and velocity noise, the microwave tube engineers and scientists found schemes to reduce the shot noise of the beam to a level in which the beam noise would be limited by the initially smaller velocity noise [44, 45]. Indeed, low noise microwave amplifiers were shown to be limited only by the cathode temperature with minimum noise figure as low a $F \sim 6$ dB.

With the development of accelerator technology, a variety of radiation sources have been discovered and developed. These include synchrotron sources, Cerenkov radiation sources, Optical Transition Radiation, undulator radiation and

more. Some of these sources that are primarily spontaneous emission radiation sources, were also developed into stimulated emission devices – amplifiers and oscillators [46, 47, 48]. Because accelerator energies can be considerably higher (MeVs to tens of GeV) than the electron guns used in microwave tubes (keV to tens of keV), the spectral radiation range of these relativistic e-beam radiation sources is at much shorter wavelengths - from optical to X-Ray (see Figure 1-2). Consequently, the development of the technology and the theory of these devices were historically quite divorced from the earlier development of electron tubes, which were originally derived only for non-relativistic electron beams and for radiation in the microwave frequencies.

The first works on undulator radiation using accelerator beams were based on spontaneous emission [49, 50, 51]. They were carried out without reference to the prior microwave tube discipline [52]. The first modern time optical frequency experiments of FEL stimulated emission devices, both amplifier [53] and oscillator [48], were operated in the low gain regime, and therefore their connection to the high gain microwave tube field was overseen. They were interpreted and analyzed in terms of laser physics theory [47]. In fact, the connection of FEL theory has become apparent as soon as it was recognized that the linear dynamics of all of these devices is described by the "Pierce cubic equation" [54, 55].

Just as in the theoretical treatment of coherent signal amplification in FELs, there is much to learn and benefit from the early theoretical formulation and analysis of noise processes in non-relativistic electron guns and electronic microwave tubes. Effects of optical frequency current fluctuation dynamics in transport of high quality (small energy spread and emittance) e-beams are now understood to be related to the corresponding e-beam noise processes in electron tubes. Processes, such as "Microbunching instabilities", were discovered in transport of such high energy beams upon passage through energy-dispersive insertion devices (bending magnet, chicane). These turn out to be important issues affecting efficiency of beam transport and functionality of beam diagnostics. Substantial research is invested in this effect and a series of symposia is currently dedicated to it [56].

Accelerator physics linear transport formulation of single electron dynamics in magnetic elements has been used to describe the "microbunching instability" effect [24, 57, 58]. Its emergence has been related to a number of processes including Coherent Synchrotron Radiation (CSR) and wake-field interaction. The dominant contribution to this instability is related to a collective microdynamic process of Coulomb interaction between the electrons in the beam, exacerbated by the dispersion in the magnetic structures [59].

While the common analytical approach to the microbunching dynamics is perturbative (assuming small space-charge microdynamic effect in the drift section), I analyze in this work the collective interaction process, using the microwave tube noise formulation of coupling between stochastic current modulation, and velocity modulation (longitudinal plasma oscillation) along the beam transport line. In this work I have extended some of the earlier formulation of

Haus, and employed it to transport and development of coherent and incoherent stochastic beam modulation and radiation processes in various relativistic beam transport lines (drift, acceleration, dispersive magnet sections), and in FEL. The extended formulation makes it possible to present in a unified model coherent radiation emission processes in FEL (low and high gain FELs, prebunched beam and superradiant FELs), as well as incoherent electron-beam noise processes (stochastic microbunching), and radiation noise processes (SASE).

The main innovative contribution of this work is the discovery that collective interaction noise suppression processes can be employed, even at optical frequencies and in a relativistic electron beam, and consequently suggesting schemes for control and suppression of radiation noise (SASE) in FEL. These concepts were inspired by the earlier concepts of current noise and radiation noise suppression in microwave tubes, and I employed the extended microwave-tube formulation to analyze these processes and to determine the fundamental coherence limits of FELs.

The hypothesis that noise control and suppression is possible in relativistic electron beams, more than four orders of magnitude energy than the beams in electronic tube guns, and at optical frequencies – seven orders of magnitude higher than the earlier microwave tube art - is not straightforward and it required derivation from first principles of a new formulation that is given in Chapter 2 of this dissertation. Also the further extension of the low noise microwave tubes concept to the idea of suppression of FEL radiation noise (SASE), at optical frequencies by controlling the e-beam noise, required a new detailed theoretical analysis corresponding to the very different operating regime of FELs, and it is presented in Chapter4. Indeed, the first theoretical claims of our group [28 - 33], faced some objections and controversy. However, most recently my theory for electron beam current noise suppression has received experimental confirmation in two independent experiments performed at optical frequencies: in an experiment of our group conducted by transport of an e-beam in a drift section [63], and an experiment in LCLS, conducted by transport of an e-beam in a dispersive section [64].

The relativistic formulation development in the present dissertation is based on analytical solution of the linearized fluid plasma equations (including space-charge effect) for the electron beam, and on a modal expansion solution of Maxwell's equations for the generation of radiation in the FEL wiggler. This provides a rigorous basis for the analysis of the problem of e-beam current and FEL radiation noise control and suppression.

Our analysis of radiation noise (SASE) control and suppression [28, 29, 32, 33], which is detailed in Chapters 3 and 4, is in current research interest in the field in connection to seed injection FELs, and in connection to determining the coherence limits of FEL. This radiation noise suppression process (suppression of spontaneous synchrotron undulator radiation or SASE emission from an undulator) has not yet been demonstrated experimentally in a FEL. Hopefully, the better understanding of the processes we helped to provide, and the recent demonstration

of optical frequency beam current noise suppression, will spur further research with the goal of demonstrating and controlling this SASE suppression effect, and determining its short wavelength limits of applicability.

Putting the subject of radiation noise suppression in a wider scientific context, we point out that the somewhat unexpected effect of current noise suppression, which takes place due to collective interaction, is the demonstration of Sub-Poissonian particle number statistics, which is well known in the context of "photon squeezing" [60].

Normally, the squared average of the current fluctuations of an electron beam, ($\overline{\left|\tilde{i}\right|^2}$), with average current I_0 is believed to be given by the classical shot-noise formula (see Chapter 2.3.1., Eq. 2-113):

$$\overline{\left|\tilde{i}\right|^2} = eI_0\Delta f \qquad 1\text{-}5$$

This is often believed to be a fundamental limit, because it is a direct consequence of the Poisson statistics that governs the density distribution of a random ensemble of particles. However, as we show in this work, this limit can be surpassed if the particles are charged. In this case, their collective Coulomb interaction makes it possible to homogenize the beam charge density [29], and exhibit sub-Poisson density distribution and a consequent excision of the shot-noise limit (Eq. 1-5).

The effect of radiation noise suppression can be related to the fundamental effect of Dicke's sub-radiance [61], which corresponds to a process of suppression of spontaneous emission in an ensemble of atomic dipoles. The SASE radiation noise limits the coherence of FEL amplifiers, and its suppression may help approach the fundamental coherence limits of FELs as a laser [33, 26], similarly to the Schalow-Townes limit for the coherence of conventional lasers [17].

The electron beam noise suppression problem has received theoretical attention and analysis in parallel and follows our work and publications on the subject. Rosenzweig et al have referred to the possibility of noise suppression and charge homogenization in the context of a "crystalline beam" [62]. Ratner and Stupakov have presented a 1-D analysis of beam current suppression by means of a dispersive section using a disk-charge model of single particle interaction [29]. This follows a similar modeling of another proposed concept of narrow band e-beam noise suppression effect using an FEL [63]. A more advanced 3-D formulation of microbunching analysis was introduced by Marinelli et al [64], using Vlasov equations (see Appendix 1) to extend and determine the limits of the cold beam microdynamic analysis due to Landau damping (in the transverse [65] and longitudinal [66] dimensions). The Landau damping effect, due to finite energy spread and emittance of the beam, would limit the validity of the fluid plasma analysis and the frequency range of the beam noise suppression process (see discussion in Appendix 8).

In comparing this work to other formulations, I point out that the microwave tube terminology and parameterization that we use are somewhat

different from the accelerator physics terminology. In this connection, we point out that what is termed in accelerator physics, "energy or velocity microbunching modulation", is equivalent to kinetic voltage modulation and kinetic voltage noise in microwave tube terminology. The concepts of "kinetic voltage" modulation and noise, that were defined by Chu in the nonrelativistic limit [67], is identical in the case of laminar flow to energy modulation and energy microbunching, normalized to voltage units (see discussion in Chapter 2). Our formulation extends the concept of kinetic voltage to describe relativistic longitudinal voltage modulation and fluctuations, so that it includes the contribution to the velocity noise (or the kinetic voltage noise) due to both energy spread and angular spread of the beam.

Another distinction between the accelerator physics terminology and the microwave tube terminology that we use is in the definition of beam longitudinal space-charge (LSC) beam impedance [see for example 68]. This difference, which is discussed in Chapter 2, originates from the difference between the approximate "lumped circuit" approach, which is currently commonly used in connection to analysis of "microbunching instability", as opposed to the more general "transmission line" model of longitudinal plasma wave interaction dynamics, that I use in the present formulation.

This different approach and the natural extension of the transmission line analysis to stochastic signals lead also to another distinction between the current work and other noise suppression analyses. In the noise suppression analysis of Ratner et al [69, 70], the total current noise of the beam is presented as a sum of unperturbed (incoherent) random electron position modulation (neglecting the effect of inter-particle interaction), and a "coherent" position perturbation due to the inter-particle Coulomb interaction, which in the case of noise suppression conspire to reduce the radiation noise. In the stochastic wave propagation formulation in the microwave tube transmission line model used, the current and velocity noise parameters in the context of single transverse mode analysis represent both terms in a unified manner, and represent the evolution of the total noise parameters due to the inter-particle interaction along the beam transport line, including the case of transport through a dispersive magnetic section.

The dissertation is organized as follows: In Chapter 2 I present the general formalism of signal propagation in non-dissipative electron transport beam sections. In such transport sections the stored energy in the electron beam waves is conserved – no interaction with radiation. The formulation is derived in terms of the electron fluid plasma parameters (moments of the distribution function): current modulation and kinetic voltage modulation. The solution of the wave propagation in the small-signal linear regime is presented in terms of 2D transfer matrices for different sections: free drift, acceleration section and dispersive magnetic section (neglecting synchrotron radiation effect).

The linear signal transfer formulation is subsequently extended to include stochastic modulation and is used for description of noise propagation on a general e-beam. I demonstrate the use of this formulation by employing it for interpreting the Coherent Optical Transition Radiation (COTR) effect (coherent in the

transverse dimensions) observed in LCLS [71]. The effect of amplification of the current noise, due to transfer of the velocity fluctuation to current fluctuation in a dispersive bend magnet, is described in terms of my theoretical model. The validity conditions of the presented single-mode linear theory are discussed at the end of the chapter.

In Chapter 3, the fluid plasma formulation is extended to include a radiative section (FEL) using modal expansion formulation of Maxwell's equations and the coupled system is solved within a single transverse mode model. The formalism is applied for two different schemes of FEL operation:

- coherent operation mode, namely FEL radiation by stimulated emission (laser amplification or seed-injection) and by superradiance (pre-bunched beam)
- incoherent radiation schemes, including spontaneous emission of radiation and Self Amplified Spontaneous Emission (SASE).

I then compare the stimulated and spontaneous emission levels in a conventional FEL amplifier (seed-injected FEL), and derive the coherence conditions (the condition on the seeding power level) for conventional seeded FELs.

In Chapter 4, the system of an FEL and an electron beam drift section preceding the FEL wiggler is analyzed in a unified formulation that combines the e-beam stochastic microdynamic formulation of Chapter 2, and the radiation emission formulation of Chapter 3. The conditions for minimizing radiation noise in such a combined system are derived, and consequently, the fundamental coherence limits of FEL at different wavelength regimes are derived. These limits would be theoretically attainable if the e-beam noise contribution to radiation noise is minimized by the proposed collective interaction electron beam noise suppression process.

Some important derivations and calculations are presented in the Appendices.

2 Small signal propagation of space-charge wave on an electron beam in a non-dissipative transport section

2.1 General formulation

In this work we shall analyze the dynamics of the electron charge distribution in an electron beam using plasma fluid (moment) equations: the force equation, the continuity equation, Gauss's law:

$$\frac{d\mathbf{p}(\mathbf{r},t)}{dt} = -e\left(\mathbf{E}_{tot}(\mathbf{r},t) + \left[\mathbf{u}(\mathbf{r},t)\times\mathbf{B}_{tot}(\mathbf{r},t)\right]\right) \quad 2\text{-}1$$

$$e\frac{\partial n(\mathbf{r},t)}{\partial t} + \nabla\cdot en(\mathbf{r},t)\mathbf{u}(\mathbf{r},t) = 0 \quad 2\text{-}2$$

$$\mathrm{div}\,\mathbf{E}_{tot}(\mathbf{r},t) = -\frac{en(\mathbf{r},t)}{\varepsilon_0} \quad 2\text{-}3$$

where $\mathbf{p}$ is the momentum of an electron, ($-e$) is the charge of an electron, $\mathbf{E}_{\mathrm{tot}}$ and $\mathbf{B}_{\mathrm{tot}}$ are the total electric and magnetic fields respectively, n is the density of electrons in the beam, $\mathbf{u}$ is the beam velocity, ε_0 is the dielectric permittivity of vacuum. In this work, we neglect the self magnetic field ($\mathbf{B}_{\mathrm{self}}$) when we discuss about signal propagation, but save it when we discuss a beam envelop evolution (in Chapter 2.4 and Appendix 5).

The momentum of an electron is:

$$\mathbf{p}(\mathbf{r},t) = \gamma(\mathbf{r},t)m_0\mathbf{u}(\mathbf{r},t) \quad 2\text{-}4$$

where m_0 is the electron rest mass, γ is the relativistic Lorentz factor:

$$\gamma(\mathbf{r},t) = \frac{1}{\sqrt{1-\left(\frac{\mathbf{u}(\mathbf{r},t)}{c}\right)^2}} \quad 2\text{-}5$$

Here c is the speed of light in a vacuum.

In the small-signal approximation, we can express all parameters in the fluid equations as the sum of two terms: a time-averaged term and a time-varying term whose amplitude is much smaller than the time-averaged one. Moreover, cross products of two “small signal” time-varying parts are neglected. As a result of these assumptions, we can write a linear expansion of all quantities (electron density n, beam velocity $\mathbf{u}$, beam current density $\mathbf{j}$, relativistic Lorentz factor γ and electric field $\mathbf{E}_{tot}$ respectively):

$$n(\mathbf{r},t) = n_0(\mathbf{r}) + n_1(\mathbf{r},t) \quad 2\text{-}6$$

$$\mathbf{u}(\mathbf{r},t) = \mathbf{u}_0(\mathbf{r}) + \mathbf{u}_1(\mathbf{r},t) \qquad 2\text{-}7$$

$$\mathbf{j}(\mathbf{r},t) = -en(\mathbf{r},t)\mathbf{u}(\mathbf{r},t) = -en_0(\mathbf{r})\mathbf{u}_0(\mathbf{r}) - e\left(n_1(\mathbf{r},t)\mathbf{u}_0(\mathbf{r}) + n_0(\mathbf{r})\mathbf{u}_1(\mathbf{r},t)\right) = \mathbf{J}_0(\mathbf{r}) + \mathbf{J}_1(\mathbf{r},t) \qquad 2\text{-}8$$

$$\gamma(\mathbf{r},t) = \gamma_0(\mathbf{r}) + \gamma_1(\mathbf{r},t) \qquad 2\text{-}9$$

$$\mathbf{E}_{tot}(\mathbf{r},t) = \mathbf{E}_0(\mathbf{r}) + \mathbf{E}_1(\mathbf{r},t) \qquad 2\text{-}10$$

We insert these expressions in the continuity equation (Eq. 2-2):

$$-e\frac{\partial n_1(\mathbf{r},t)}{\partial t} + \nabla\cdot\left(\mathbf{J}_0(\mathbf{r}) + \mathbf{J}_1(\mathbf{r},t)\right) = 0 \qquad 2\text{-}11$$

The time-independent term of the current is the steady state DC beam current distribution (invariant with time if the transport of the electron beam is free of leakage current and gas ionization),:

$$\mathbf{J}_0(\mathbf{r}) = -en_0(\mathbf{r})\mathbf{u}_0(\mathbf{r}) = const(t) \qquad 2\text{-}12$$

The small-signal time-varying continuity equation is:

$$-e\frac{\partial n_1(\mathbf{r},t)}{\partial t} + \nabla\cdot\left(\mathbf{J}_1(\mathbf{r},t)\right) = 0 \qquad 2\text{-}13$$

Gauss's law (Eq. 2-3) is separable into two equations:

$$\operatorname{div}\mathbf{E}_0(\mathbf{r}) = \frac{-en_0(\mathbf{r})}{\varepsilon_0} \qquad 2\text{-}14$$

$$\operatorname{div}\mathbf{E}_1(\mathbf{r},t) = \frac{-en_1(\mathbf{r},t)}{\varepsilon_0} \qquad 2\text{-}15$$

For a volume free of magnetic fields, the force equation (Eq. 2-1) is transformed to:

$$m_0\frac{d\gamma_0(\mathbf{r})\mathbf{u}_0(\mathbf{r})}{dt} = -e\mathbf{E}_0(\mathbf{r}) \qquad 2\text{-}16$$

$$m_0\frac{d\left(\gamma_0(\mathbf{r})\mathbf{u}_1(\mathbf{r},t) + \gamma_1(\mathbf{r},t)\mathbf{u}_0(\mathbf{r})\right)}{dt} = -e\mathbf{E}_1(\mathbf{r},t) \qquad 2\text{-}17$$

where γ_0 is the DC part of the relativistic Lorentz factor:

$$\gamma_0(\mathbf{r}) = \frac{1}{\sqrt{1-\left(\frac{u_0(\mathbf{r})}{c}\right)^2}} \qquad 2\text{-}18$$

Multiplying the continuity equation (Eq. 2-13) by the average beam velocity ($\mathbf{u}_0(\mathrm{r})$), and using the time-varying current definition (Eq. 2-8), we obtain a modified small-signal continuity equation:

$$\frac{\partial \mathbf{J}_1(\mathbf{r},t)}{\partial t} + \mathbf{u}_0(\mathbf{r})\left(\nabla \cdot \left(\mathbf{J}_1(\mathbf{r},t)\right)\right) = -en_0(\mathbf{r})\frac{\partial \mathbf{u}_1(\mathbf{r},t)}{\partial t} \qquad 2\text{-}19$$

The set of equations (Eqs. 2-12, 2-14, 2-16) for the time-independent (DC) variables ($\mathbf{J}_0(\mathbf{r})$, $n_0(\mathbf{r})$, $\mathbf{u}_0(\mathbf{r})$, $\mathbf{E}_0(\mathbf{r})$), and a linear set of equations (Eqs. 2-15, 2-17, 2-19) for the small signal time-dependent variables ($\mathbf{J}_1(\mathbf{r},\mathrm{t})$, $n_1(\mathbf{r},\mathrm{t})$, $\mathbf{u}_1(\mathbf{r},\mathrm{t})$, $\mathbf{E}_1(\mathbf{r},\mathrm{t})$), will be employed in our analysis.

2.1.1 One dimensional model

The time-independent set of equations (Eqs. 2-12, 2-14, and 2-16) describes the global transport of an electron beam in a transport line that can include also acceleration or deceleration. Assuming that the electric field in an accelerator is known and that the potential distribution ($\varphi(z)$) along the beam propagation is described by:

$$\varphi(z) - \varphi(0) = \int_0^z \mathbf{E}_0(z') \cdot \hat{\mathbf{e}}_z dz',$$

where $\hat{\mathbf{e}}_z$ is the unit vector parallel with the z-axes, we can integrate the force equation (Eq. 2-16) and obtain:

$$\gamma_0(z) = \gamma_0(0) + \frac{e\left(\varphi(z) - \varphi(0)\right)}{m_0 c^2} \qquad 2\text{-}20$$

Based on the definition of the relativistic Lorentz factor (Eq. 2-18) and the DC beam current distribution (Eq. 2-12), we obtain respectively:

$$u_0(z) = \frac{c\sqrt{\gamma_0^2(z)-1}}{\gamma_0(z)} = \frac{c}{\gamma_0(0) + \frac{e\left(\varphi(z)-\varphi(0)\right)}{m_0 c^2}} \sqrt{\left(\gamma_0(0) + \frac{e\left(\varphi(z)-\varphi(0)\right)}{m_0 c^2}\right)^2 - 1} \qquad 2\text{-}21$$

$$n_0(z) = \frac{n_0(0)u_0(0)}{u_0(z)} \qquad 2\text{-}22$$

In this derivation, we assumed that the electron beam is transported in the "+z" direction ($\mathbf{u}(\mathbf{r},t) \equiv u(z,t)\hat{\mathbf{e}}_z$, $u(z,t) > 0$). In this case, the full differential with respect to time can be written as:

$$\frac{d}{dt} = \frac{\partial}{\partial t} + \frac{\partial}{\partial z} u_0 \qquad 2\text{-}23$$

We assume that the time-independent variables (n_0, u_0) are known functions. Therefore, we substitute them into the small-signal force equation (Eq. 2-17):

$$\frac{m_0c^2}{e\beta_0 c}\frac{\partial}{\partial t}(\gamma_0^3\beta_0\beta_1)+\frac{m_0c^2}{e}\frac{\partial}{\partial z}(\gamma_0^3\beta_0\beta_1)=-E_1(z,t) \qquad 2\text{-}24$$

where $\beta_0 = u_0/c$, $\beta_1 = u_1/c$. Note:

$$\frac{d}{dt}(\gamma\beta)=(\gamma+\gamma^3\beta^2)\frac{d}{dt}(\beta)=\gamma^3\frac{d}{dt}(\beta).$$

We introduce a relativistic definition of Chu's small signal kinetic voltage V_1 [67]:

$$V_1=-\frac{m_0c^2}{e}\gamma_0^3\beta_0\beta_1 \qquad 2\text{-}25$$

This useful parameter can also be interpreted as small signal kinetic energy modulation expressed in units of voltage:

$$V_1=-\frac{m_0c^2}{e}\frac{\partial\gamma}{\partial\beta}\beta_1=-\frac{m_0c^2}{e}\gamma_1 \qquad 2\text{-}26$$

Representation in terms of this parameter makes it possible to write the modified small-signal continuity equation (Eq. 2-19) and the force equation (Eq. 2-24) in a compact way:

$$\frac{\partial J_1(z,t)}{\partial t}+c\beta_0(z)\frac{\partial J_1(z,t)}{\partial z}=\frac{e^2n_0(z)}{m_0c\gamma_0^3\beta_0(z)}\frac{\partial V_1(z,t)}{\partial t} \qquad 2\text{-}27$$

$$\frac{1}{\beta_0(z)c}\frac{\partial V_1(z,t)}{\partial t}+\frac{\partial V_1(z,t)}{\partial z}=E_1(z,t) \qquad 2\text{-}28$$

We introduce the longitudinal plasma oscillation wavenumber:

$$\theta_p(z)=\frac{\omega_{p0}(z)}{c\beta_0(z)}=\sqrt{\frac{e^2n_0(z)}{\varepsilon_0m_0c^2\gamma_0^3(z)\beta_0^2(z)}} \qquad 2\text{-}29$$

and consequently obtain a simple set of coupled differential equations for the small-signal electron beam amplitudes in the time domain:

$$\frac{\partial J_1(z,t)}{\partial z}+\frac{1}{c\beta_0(z)}\frac{\partial J_1(z,t)}{\partial t}=\varepsilon_0\theta_p^2\frac{\partial V_1(z,t)}{\partial t} \qquad 2\text{-}30$$

$$\frac{\partial V_1(z,t)}{\partial z}+\frac{1}{\beta_0(z)c}\frac{\partial V_1(z,t)}{\partial t}=E_1(z,t) \qquad 2\text{-}31$$

In the linear analysis for the steady state single-frequency case, we shall use a phasor relation. Each variable X_1 is given as a function of time by:

$$X_1(z,t) = \mathrm{Re}\left(\tilde{X}(z,\omega)\exp(-i\omega t)\right) \qquad 2\text{-}32$$

where ω is an angular frequency and i is an imaginary unit ($i = \sqrt{-1}$). Therefore, partial time differentiation is equivalent to multiplication by $-i\omega$:

$$\frac{\partial}{\partial t} X(t) \rightarrow -i\omega \tilde{X}(\omega) \qquad 2\text{-}33$$

and partial space differentiation is equivalent to full space differentiation:

$$\frac{\partial}{\partial z} \rightarrow \frac{d}{dz}$$

From Gauss's law (Eq. 2-15), and from the continuity equation (Eq. 2-13), we obtain:

$$\tilde{E} = -\frac{i}{\omega\varepsilon_0}\tilde{J}_z(z) + const \qquad 2\text{-}34$$

Using the Maxwell equation $\nabla \times \tilde{\mathbf{B}} = \mu_0 \tilde{\mathbf{J}} - i\omega\mu_0\varepsilon_0\tilde{\mathbf{E}}$ and the one-dimensional approximation ($d/dx=d/dy=0$), there is no z-component of $\nabla \times \tilde{\mathbf{B}}$; we define the constant to be equal to zero. Thus, we get a set of differential equations for the small-signal current density modulation and the kinetic voltage parameter:

$$\frac{\partial \tilde{J}(z,\omega)}{\partial z} - \frac{i\omega}{c\beta_0(z)}\tilde{J}(z,\omega) = -i\omega\varepsilon_0\theta_p^2(z)\tilde{V}(z,\omega) \qquad 2\text{-}35$$

$$\frac{\partial \tilde{V}(z,\omega)}{\partial z} - \frac{i\omega}{c\beta_0(z)}\tilde{V}(z,\omega) = -\frac{i}{\omega\varepsilon_0}\tilde{J}(z,\omega) \qquad 2\text{-}36$$

The solution of the small signal set of equations may be presented in terms of slow amplitude variables:

$$\tilde{j}(z,\omega) = \tilde{J}(z,\omega)\exp\left(i\omega\int_{-\infty}^{z}\frac{1}{c\beta_0(z')}dz'\right) \qquad 2\text{-}37$$

$$\tilde{v}(z,\omega) = \tilde{V}(z,\omega)\exp\left(i\omega\int_{-\infty}^{z}\frac{1}{c\beta_0(z')}dz'\right) \qquad 2\text{-}38$$

Therefore, we get:

$$\frac{d\tilde{j}(z,\omega)}{dz} = -i\omega\varepsilon_0\theta_p^2(z)\tilde{v}(z,\omega) \qquad 2\text{-}39$$

$$\frac{d\tilde{v}(z,\omega)}{dz} = -\frac{i}{\omega\varepsilon_0}\tilde{j}(z,\omega) \qquad 2\text{-}40$$

2.1.2 Relativistic extension of Chu's theorem

Let us define the multiplication of the kinetic voltage ($\tilde{V}$) with the complex conjugate of the current density modulation ($\tilde{J}^*$) as the kinetic power density. It was shown by Chu [72] that the real part of kinetic power density ($\tilde{V}\tilde{J}^*$) in a non-relativistic e-beam is a motion conserved parameter (independent of "z"). Using the definition of kinetic voltage (Eq. 2-25), and plasma wave number (Eq. 2-29) for relativistic beams, we can obtain Chu's conservation theorem for relativistic beams as well.

We take the complex conjugate of the small-signal current modulation equation (Eq. 2-35), and multiply it by the kinetic voltage parameter ($\tilde{V}$). We multiply the small-signal kinetic voltage parameter equation (Eq. 2-36) by the complex conjugate of the current modulation ($\tilde{J}^*$) and sum-up the two equations. We obtain:

$$\frac{d(\tilde{V}\tilde{J}^*)}{dz} = i\omega\theta_p^2\left|\tilde{V}\right|^2 - \frac{i}{\omega\varepsilon_0}\left|\tilde{J}\right|^2 \qquad 2\text{-}41$$

The real part of this equation results in a conservation theorem defined for the small signal kinetic power density:

$$S_k = \tfrac{1}{2}\mathrm{Re}(\tilde{V}\tilde{J}^*) = const \qquad 2\text{-}42$$

2.1.3 Small signal space-charge wave propagation on a finite cross section beam

We extend our analysis to the case of a beam of finite cross section. We take a model of constant density and velocity distribution across the beam cross section:
($n_0(\mathbf{r})$ = const($\mathbf{r}_\perp$) and $u_0(\mathbf{r})$ = const($\mathbf{r}_\perp$) for $|\mathbf{r}_\perp| \le r_b$, where r_b is the beam radius).

We expect that the small signal space-charge field will be, however, modified due to fringing of the field lines. Let ω be the angular frequency of electron density modulation $\tilde{n}$, and $\lambda = 2\pi c/\omega$ - the free space optical wavelength corresponding to this frequency. If the beam drifts at velocity u_0, then in addition to time modulation, the beam has spatial modulation with an axial wavenumber $k_b = \omega/u_0$. Therefore, the beam modulation wavelength is $\lambda_b = \lambda\beta_0$. Using the Lorentz transformation, we obtain that the beam modulation wavelength λ_b' in the moving-frame (where the beam average velocity is zero) (see Figure 2-1a) is:

$$\lambda_b^{'} = \lambda\beta_0\gamma_0$$

If the beam moving-frame wavelength λ_b' is smaller than the beam radius r_b, (see Figure 2-1b), the space charge field is uniform and axially oriented across the beam and the situation is nearly the 1D case. However, if the beam radius is small (Figure 2-1c), or the conductive walls are near to the beam (Figure 2-1d), the space charge fringes and consequently the effective average longitudinal field is smaller than that predicted by the 1D model.

A detailed solution of this problem would result in a solution of Langmuir plasma-wave eigenmodes of specific transverse profiles and specific plasma wavenumbers [73, 74]. In an approximate model, one may keep the one dimensional model of the previous section and neglect derivatives in terms of the transverse coordinates. In a single transverse mode approximation, the reduction of the space charge force due to fringing of the electric field is taken into account by means of a plasma reduction factor $r_p^2 \le 1$. This means that the longitudinal plasma wavenumber is essentially reduced by the plasma reduction factor r_p:

$$\theta_{pr} = r_p\theta_p \qquad 2\text{-}43$$

The plasma reduction factor was calculated by various workers for Langmuir waves in different configurations (uniform and non-uniform current distributions, propagation in conductive enclosure or in open space, etc.) [74]. In the case of a relativistic pencil beam of transverse uniform distribution and radius r_b, propagating in free space (without outer wall), the reduction factor of the fundamental Langmuir mode is given by [75, 29]:

$$r_p^2 = 1 - \frac{kr_b}{\beta_0\gamma_0} K_1\left(\frac{kr_b}{\beta_0\gamma_0}\right) \qquad 2\text{-}44$$

where $K_1(x)$ is the modified Bessel function of the second kind and k is the optical wave-number ($k = 2\pi/\lambda$) (see Figure 2-2, blue curve).

Recently, the plasma correction factor of the fundamental Langmuir mode was calculated by Marinelli et al [64] for a Gaussian beam distribution (with a transverse size variance σ_x) using the variation method [76, 77, 18] (see Figure 2-2, green curve):

$$r_p = \frac{2k\sigma_x}{\beta_0\gamma_0 + 2k\sigma_x} \qquad 2\text{-}45$$

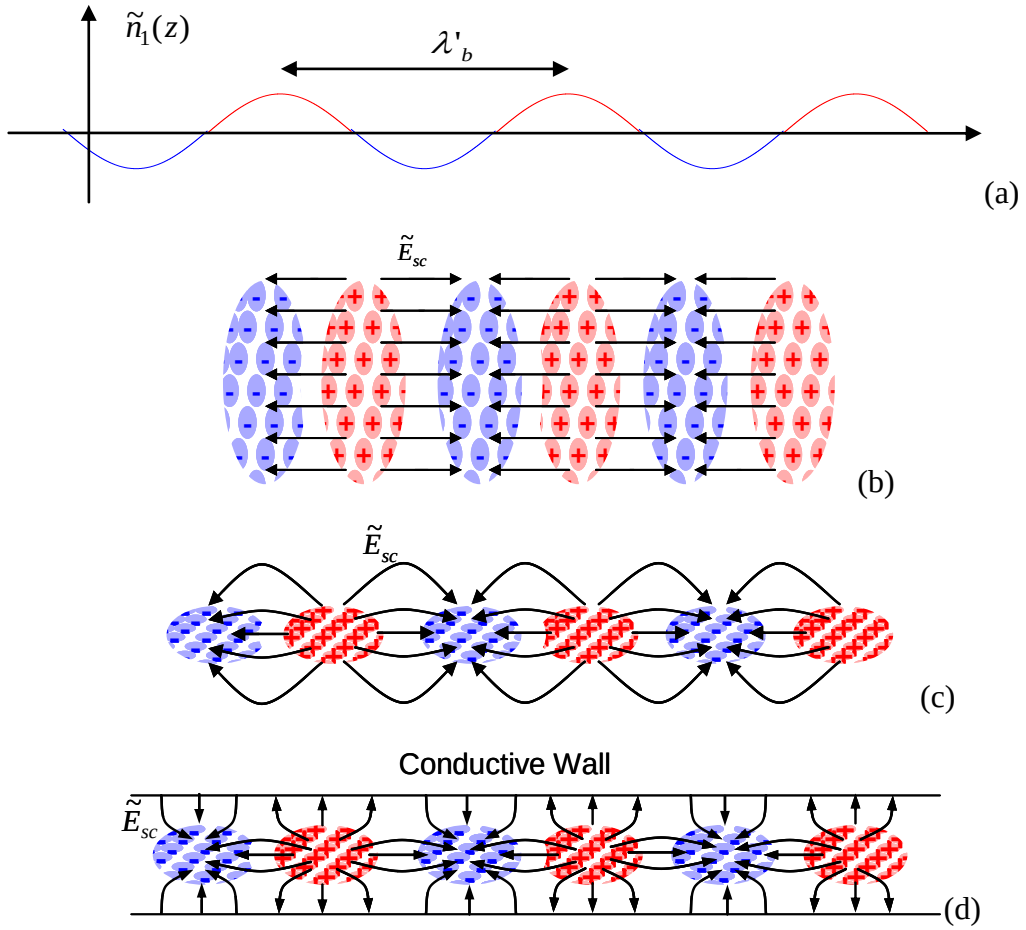

Figure 2-1 Small amplitude density modulation (a) and illustrations of the space charge field distribution in different finite cross section geometries: (b) approximately 1D case corresponding to a beam radius bigger than the moving frame modulation wavelength λ'_b, (c) significantly fringing field in the case that the beam radius is smaller than the moving frame modulation wavelength, (d) fringing due to proximity of a conductive wall.

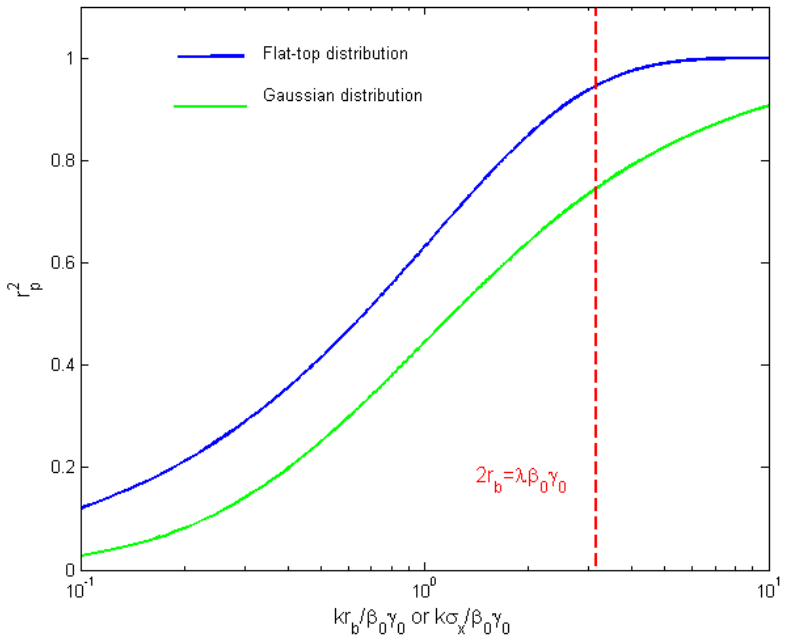

Figure 2-2 Longitudinal plasma reduction factor as a function of the beam parameters and modulation frequency for a flat-top distribution (blue curve, see Eq. 2-44) and for a Gaussian distribution (green curve, Eq. 2-45).

In the present work, we assume a known plasma reduction factor r_p, and we assume excitation of a single (fundamental) Langmuir mode in the beam. From the calculation of the plasma reduction factor (Eq. 2-44), it is seen (Figure 2-2) that in the limit where the beam radius is large relative to the beam bunching period in the beam rest frame (λ'):

$$2r_b >> \frac{2\pi c}{\omega}\beta_0\gamma_0 \qquad 2\text{-}46$$

r_p tends to a value of 1. This obviously is consistent with the fringing field effect being negligible in the 1D limit.

Based on these observations, we generalize the 1-D equations of the previous section to a finite beam case. We integrate all equations over the transverse coordinates, which corresponds to a multiplying of all equations by the beam effective cross section A_e:

$$A_e = \pi r_b^2$$

We define a small signal current modulation parameter as:

$$\tilde{I}(z) = \int \tilde{J}(x,y,z)dxdy = A_e\tilde{J}(0,0,z) \qquad 2\text{-}47$$

Using the definitions above (Eq. 2-47), the equation for the evolution of the small-signal current density (Eq. 2-35) turns into an expression for the small-signal current:

$$\frac{d\tilde{I}(z,\omega)}{dz} - \frac{i\omega}{c\beta_0(z)}\tilde{I}(z,\omega) = -i\omega\varepsilon_0 A_e\theta_p^2(z)\tilde{V}(z,\omega) \qquad 2\text{-}48$$

We now assert that Gauss's law (Eq. 2-34) in the finite cross-section beam case is modified into:

$$\tilde{E}(z) = -\frac{ir_p^2}{\omega\varepsilon_0 A_e}\tilde{I} \qquad 2\text{-}49$$

and the r.h.s. of the small signal kinetic voltage equation (Eq. 2-36) is also modified correspondingly:

$$\frac{d\tilde{V}(z,\omega)}{dz} - \frac{i\omega}{c\beta_0(z)}\tilde{V}(z,\omega) = -\frac{ir_p^2}{\omega\varepsilon_0 A_e}\tilde{I}(z,\omega) \qquad 2\text{-}50$$

In terms of slow varying amplitude parameters:

$$\tilde{i}(z,\omega) = A_e\tilde{j}(z,\omega) = \tilde{I}(z,\omega)\exp\left(i\omega\int_{-\infty}^{z}\frac{1}{c\beta_0(z')}dz'\right) \qquad 2\text{-}51$$

$$\tilde{v}(z,\omega) = \tilde{V}(z,\omega)\exp\left(i\omega\int_{-\infty}^{z}\frac{1}{c\beta_0(z')}dz'\right) \qquad 2\text{-}52$$

we obtain (compare to Eqs. 2-39, 2-40, 2-42):

$$\frac{d\tilde{i}(z,\omega)}{dz} = -i\omega\varepsilon_0 A_e \theta_p^2(z)\tilde{v}(z,\omega) \qquad 2\text{-}53$$

$$\frac{d\tilde{v}(z,\omega)}{dz} = -\frac{ir_p^2}{\omega\varepsilon_0 A_e}\tilde{i}(z,\omega) \qquad 2\text{-}54$$

$$\mathrm{Re}\,P_k = \frac{1}{2}\mathrm{Re}\left(\tilde{v}\tilde{i}^*\right) = const \qquad 2\text{-}55$$

where $P_k = A_e S_k$ is the small signal kinetic power.

Notes:

We can still permit, within our approximations, situations in which the current density is not necessarily transversely uniform and the beam cross section A_e varies slowly in the propagation direction z. We may generalize the definition of the beam cross section A_e for the case of general transverse current distribution as

$$A_e(z) = \frac{I_0}{J_0(0,0,z)}. \qquad 2\text{-}56$$

For example, for a transverse profile with a round Gaussian shape of the beam with standard deviation σ, we obtain the beam cross section area A_e is:

$$A_e = 2\pi\sigma^2 \qquad 2\text{-}57$$

This procedure of defining the beam cross section area (Eq. 2-56) makes it possible to use the same 1D model equations (Eqs. 2-53 and 2-54) for various transverse current density profiles. However, the plasma reduction factor r_p must be a given parameter for any current transverse distribution ($\mathbf{J}(\mathbf{r}_\perp)$).

The 1D finite cross section beam model and equations 2-53 and 2-54 can be employed also in transport cases in which the beam cross section dimensions vary slowly as a function of z, conditioned stipulated that the parameter dependences $A_e(z)$, $r_p(z)$ are known.

2.2 The transfer matrix for a non-dissipative e-beam transport section

2.2.1 Properties of the general transfer matrix of a non-dissipative transport section

Since the set of single mode small-signal differential equations (Eqs. 2-53 and 2-54) is linear, it is possible to write the parameters $\tilde{i}(z)$ and $\tilde{v}(z)$ in terms of their initial values and a general 2 x 2 ABCD-transfer matrix:

$$\begin{pmatrix} \tilde{i}(z) \\ \tilde{v}(z) \end{pmatrix} = \begin{pmatrix} A(z) & B(z) \\ C(z) & D(z) \end{pmatrix} \begin{pmatrix} \tilde{i}(0) \\ \tilde{v}(0) \end{pmatrix} \qquad 2\text{-}58$$

The matrix must satisfy some symmetry conditions which can be derived directly from the generalized theorem (Eq. 2-55). In Appendix 3 we derive the symmetry form of the transfer matrix for a general non-dissipative system:

$$\mathbf{M}(z) = \begin{pmatrix} K(z)\cos(\phi(z)) & \mp\frac{i}{W(z)}\sin(\phi(z)) \\ \mp iW(z)\sin(\phi(z)) & \frac{1}{K(z)}\cos(\phi(z)) \end{pmatrix} \exp\left(i\phi_A(z)\right) \qquad 2\text{-}59$$

where $K(z)$, $W(z)$ and $\varphi(z)$ are real functions. Note, that the determinant of the general transfer matrix is equal to 1:

$$\det(\mathbf{M}(z)) \equiv 1 \qquad 2\text{-}60$$

In the following sections we shall find the specific transfer matrices for the useful cases of a free drift region, an acceleration section and a magnetic dispersive beam transport section.

2.2.2 Uniform drift section

We assume that in a drifting beam transport section, the DC beam parameters are constant. Therefore, the single mode slow varying small-signal differential equations (Eqs. 2-53 and 2-54) reduce into simple constant coefficient 2nd order ordinary differential equations:

$$\frac{d^2\tilde{i}(z,\omega)}{dz^2} + \theta_{pr}^2(z)\tilde{i}(z,\omega) = 0 \qquad 2\text{-}61$$

$$\frac{d^2\tilde{v}(z,\omega)}{dz^2} + \theta_{pr}^2(z)\tilde{v}(z,\omega) = 0 \qquad 2\text{-}62$$

and their solutions are:

$$\tilde{i}(z,\omega) = A_1\cos(\theta_{pr}z) + A_2\sin(\theta_{pr}z) \qquad 2\text{-}63$$

$$\tilde{v}(z,\omega) = B_1 \sin(\theta_{pr} z) + B_2 \cos(\theta_{pr} z) \qquad 2\text{-}64$$

Using Eqs. 2-53, 2-54 and expressing A_1, A_2, B_1, B_2 in terms of the initial conditions, the solution for the slow varying parameters is [32]:

$$\tilde{i}(z,\omega) = \cos(\theta_{pr} z)\tilde{i}(0,\omega) - \frac{i}{W_d}\sin(\theta_{pr} z)\tilde{v}(0,\omega) \qquad 2\text{-}65$$

$$\tilde{v}(z,\omega) = -iW_d \sin(\theta_{pr} z)\tilde{i}(0,\omega) + \cos(\theta_{pr} z)\tilde{v}(0,\omega) \qquad 2\text{-}66$$

where

$$W_d = \frac{r_p^2 \sqrt{\mu_0/\varepsilon_0}}{k\theta_{pr} A_e} \qquad 2\text{-}67$$

is the e-beam modulation impedance in a uniform section, μ_0 is the magnetic permeability of vacuum. In matrix form the solution is:

$$\begin{pmatrix} \tilde{i}(z,\omega) \\ \tilde{v}(z,\omega) \end{pmatrix} = \mathbf{M}_{drift}(z) \begin{pmatrix} \tilde{i}(0,\omega) \\ \tilde{v}(0,\omega) \end{pmatrix} = \\ = \begin{pmatrix} \cos(\theta_{pr} z) & \frac{-i}{W_d}\sin(\theta_{pr} z) \\ -iW_d \sin(\theta_{pr} z) & \cos(\theta_{pr} z) \end{pmatrix} \begin{pmatrix} \tilde{i}(0,\omega) \\ \tilde{v}(0,\omega) \end{pmatrix} \qquad 2\text{-}68$$

There is full consistency with the symmetry properties of the general transfer matrix (Eq. 2-59) with $K(z) = 1$, $W(z) = W_d$, $\phi(z) = \theta_{pr} z$.

2.2.3 Space charge interaction in an e-beam acceleration section

When the beam is transported in an axial acceleration or deceleration section, the time-independent beam parameters (n_0, u_{0z}) vary as a function of z (Eqs. 2-21 and 2-22). Therefore, the slow-amplitude small-signal set of differential equations (Eqs. 2-53 and 2-54) have z dependent coefficients. Substitution of these equations results in general 2nd order differential equations for $\tilde{v}(z,\omega)$ and $\tilde{i}(z,\omega)$ for the case of z-dependent coefficients:

$$\frac{d^2\tilde{v}(z,\omega)}{dz^2} + \theta_{pr}^2(z)\tilde{v}(z,\omega) = 0 \qquad 2\text{-}69$$

$$\frac{d^2\tilde{i}(z,\omega)}{dz^2} + \frac{d}{dz}\ln\left(\frac{1}{\theta_p(z)}\right)\frac{d\tilde{i}(z,\omega)}{dz} + \theta_{pr}^2(z)\tilde{i}(z,\omega) \qquad 2\text{-}70$$

The coupled slow varying amplitude first order differential equations, Eqs. 2-53, 2-54, can be written in an integrated form:

$$\tilde{v}(z) = \tilde{v}(0) + \int_0^z \frac{r_p^2(z)}{i\omega\varepsilon_0 A_e(z)} \tilde{i}(z')dz' \qquad 2\text{-}71$$

$$\tilde{i}(z) = \tilde{i}(0) - \int_0^z i\omega\varepsilon_0 A_e(z')\theta_p^2(z')\tilde{v}(z')dz' \qquad 2\text{-}72$$

This presentation invites a general solution by an iterative process of substituting one equation into the other. This process converges well if the slow varying optical frequency components $\tilde{v}(z,\omega)$ and $\tilde{i}(z,\omega)$ do not change much during transport through the transport section (e.g. for fast acceleration through a short length or small collective interaction effects).

We perform here a first order iteration by substituting $\tilde{i}(z',\omega) = \tilde{i}(0,\omega)$ and $\tilde{v}(z',\omega) = \tilde{v}(0,\omega)$ in Eqs. 2-71, 2-72 respectively:

$$\tilde{i}(z) = \left(1 - \int_0^z A_e(z')\theta_p^2(z')\left(\int_0^{z'} \frac{r_p^2(z'')}{A_e(z'')}dz''\right)dz'\right)\tilde{i}(0) - \left(i\omega\varepsilon_0 \int_0^z A_e(z')\theta_p^2(z')dz'\right)\tilde{v}(0) \qquad 2\text{-}73$$

$$\tilde{v}(z) = -\left(\int_0^z \frac{ir_p^2(z')}{\omega\varepsilon_0 A_e(z')}dz'\right)\tilde{i}(0) + \left(1 - \int_0^z \frac{r_p^2(z')}{A_e(z')}\left(\int_0^{z'} A_e(z'')\theta_p^2(z'')dz''\right)dz'\right)\tilde{v}(0) \qquad 2\text{-}74$$

Assuming that the plasma reduction factor r_p and the e-beam cross section area A_e do not change significantly along the acceleration section, the transfer matrix for "fast acceleration" in the 1st iteration step is:

$$\mathbf{M}_{acc}^{(1)}(L_{acc}) = \begin{pmatrix} 1 - \int_0^{L_{acc}} z'\theta_{pr}^2(z')dz' & -i\frac{kA_e}{Z_0}\int_0^{L_{acc}} \theta_p^2(z')dz' \\ -ir_p^2\frac{Z_0}{kA_e}L_{acc} & 1 - \int_0^{L_{acc}}\int_0^{z'} \theta_{pr}^2(z'')dz''dz' \end{pmatrix} \qquad 2\text{-}75$$

where L_{acc} is the accelerator length, $Z_0 = \sqrt{\frac{\mu_0}{\varepsilon_0}} = 120\pi\ Ohm$ is the characteristic impedance of free space.

We further note that because of the kinetic power conservation theorem (Chu's theorem), the determinant of the transfer matrix is equal to 1. Thus we can provide a criterion for the validity of the first order iterative expression (Eq. 2-75):

$$\left|\det\left(\mathbf{M}_{acc}^{(1)}(L_{acc})\right)-1\right| = \left| -\int_0^{L_{acc}} z'\theta_{pr}^2(z')dz' - \int_0^{L_{acc}}\int_0^{z'} \theta_{pr}^2(z'')dz''dz' + r_p^2 L_{acc}\int_0^{L_{acc}} \theta_p^2(z')dz' + \right.$$
$$\left. + \int_0^{L_{acc}} z'\theta_{pr}^2(z')dz' \int_0^{L_{acc}}\int_0^{z'} \theta_{pr}^2(z'')dz''dz' \right| << 1 \qquad 2\text{-}76$$

If

$$\left(\max_{0<z<L_{acc}}\left(\theta_{pr}(z)\right)L_{acc}\right)^2 << 1 \qquad 2\text{-}77$$

then each integral in Eq. 2-76 is small than 1:

$$\int_0^{L_{acc}}\int_0^{z'} \theta_{pr}^2(z'')dz''dz' < \int_0^{L_{acc}} z'\max_{0<z<z'}\left(\theta_{pr}^2(z)\right)dz' < \max_{0<z<L_{acc}}\left(\theta_{pr}^2(z)\frac{L_{acc}^2}{2}\right) << 1$$

$$\int_0^{L_{acc}} z'\theta_{pr}^2(z')dz' < \int_0^{L_{acc}} z'\max_{0<z<z'}\left(\theta_{pr}^2(z)\right)dz' < \max_{0<z<L_{acc}}\left(\theta_{pr}^2(z)\frac{L_{acc}^2}{2}\right) << 1$$

$$L_{acc}\int_0^{L_{acc}} \theta_{pr}^2(z')dz' < \max_{0<z<L_{acc}}\left(\theta_{pr}^2(z)L_{acc}^2\right) << 1$$

For the case of axial linear acceleration, based on Eq. 2-20, we can rewrite the plasma wave number (Eq. 2-29) as:

$$\theta_p^2(z) = \frac{I_0 Z_0}{\frac{m_0c^2}{e}A_e(z)}\frac{1}{\left(\gamma_0(z)\beta_0(z)\right)^3} = \frac{I_0 Z_0}{\frac{m_0c^2}{e}A_e(z)}\frac{1}{\left((\gamma_0(0)+\gamma' z)^2-1\right)^{3/2}} \qquad 2\text{-}78$$

where γ' is the acceleration gradient [78]. From this relation, it is evident that the plasma wave number (θ_p) achieves the maximum value at the lowest energy. In Appendix 4 we evaluate explicitly the 1st order transfer matrix expression (Eq. 2-75) for the case of linear acceleration and negligible dependence of the plasma reduction factor (r_p), and the e-beam cross section area (A_e) on beam energy (γ). The result is (see Eqs. A0-21 – 23 in Appendix 4), note $\gamma\beta = \sqrt{\gamma^2-1}$:

$$M_{acc}^{(1)}(L_{acc}) = \begin{pmatrix} 1-\left(\frac{I_0 Z_0 r_p^2}{\frac{mc^2}{e}A_e(\gamma')^2}\right)\left(\frac{\gamma_0(0)\gamma_0(L_{acc})-1}{\gamma_0(L_{acc})\beta_0(L_{acc})}-\gamma_0(0)\beta_0(0)\right) & i\frac{kA_e}{Z_0}\left(\frac{I_0 Z_0}{\frac{mc^2}{e}A_e\gamma'}\right)\left(\frac{1}{\beta_0(L_{acc})}-\frac{1}{\beta_0(0)}\right) \\ -ir_p^2\frac{Z_0}{kA_e}L_{acc} & 1+\frac{I_0 Z_0 r_p^2}{\frac{mc^2}{e}A_e\gamma'}\left(\frac{\gamma_0(L_{acc})\beta_0(L_{acc})-\gamma_0(0)\beta_0(0)}{\gamma'}-\frac{L_{acc}}{\beta_0(0)}\right) \end{pmatrix}$$

2-79

Using the e-beam wave impedance W_d, in terms of the plasma wave number at the entrance to the accelerator ($\theta_{pr}(0)$), for the case when the e-beam is relativistic before and after an accelerator ($\gamma_0(0) >> 1$ and $\gamma_0(L_{acc}) >> 1$), keeping the second order term ($1/\gamma^2$) only, we obtain:

$$\mathbf{M}_{acc}^{(1)}(L_{acc})=\begin{pmatrix} 1-\frac{\theta_{pr}^2(0)L_{acc}^2}{2}\frac{\gamma_0^2(0)\beta_0^3(0)}{\gamma_0^2(L_{acc})} & -i\frac{\theta_{pr}(0)L_{acc}}{W_d(0)}\left(\frac{\gamma_0(0)}{\gamma_0(L_{acc})}\frac{\left(\gamma_0(L_{acc})+\gamma_0(0)\right)}{2\gamma_0(L_{acc})}\beta_0^3(0)\right) \\ -iW_d(0)\theta_{pr}(0)L_{acc} & 1-\frac{\theta_{pr}^2(0)L_{acc}^2}{2}\frac{\gamma_0(0)\beta_0^3(0)}{\gamma_0(L_{acc})} \end{pmatrix}$$

The same result in terms of the plasma wave number at the end of the accelerator ($\theta_{pr}(L_{acc})$) is given by:

$$\mathbf{M}_{acc}^{(1)}(L_{acc})=\begin{pmatrix} 1-\frac{\theta_{pr}^2(L_{acc})L_{acc}^2}{2}\frac{\gamma_0(L_{acc})\beta_0^3(L_{acc})}{\gamma_0(0)} & -i\frac{\theta_{pr}(L_{acc})L_{acc}}{W_d(L_{acc})}\left(\frac{\gamma_0(L_{acc})}{\gamma_0(0)}\frac{\left(\gamma_0(L_{acc})+\gamma_0(0)\right)}{2\gamma_0(0)}\beta_0^3(L_{acc})\right) \\ -iW_d(L_{acc})\theta_{pr}(L_{acc})L_{acc} & 1-\frac{\theta_{pr}^2(L_{acc})L_{acc}^2}{2}\frac{\gamma_0^2(L_{acc})\beta_0^3(L_{acc})}{\gamma_0^2(0)} \end{pmatrix}$$

2.2.4 Dispersive section without space charge effects

Electron-optical elements can be dispersive. Dispersive sections (like chicanes, bending magnets, etc.) are characterized by dependence of the particle transit time on its energy. Conventional theory often describes such devices by means of a "6D particle transport matrix" **R**. This matrix describes the transformation between the differential positions and angles (in 6D-phase space) of the single particle at the entrance and at the exit of the section [78]. Our most relevant term is R_{56}. The term R_{56} gives the difference in the spatial position along the z-axis between two particles at the system exit entering it with different energy.

In our model, the kinetic voltage wave (or, in other words, velocity modulation) propagates in (and with) the e-beam, the electrons have different energies at the maximum and minimum of this wave. Therefore, a dispersive section is an effective transformer of the kinetic voltage wave into a current modulation.

In this section we match our plasma parameterization to the conventional single particle parameterization in the case of the absence of space-charge effects. If we examine two electrons arriving to the entrance of a dispersive section (z_{in}) at different times (t_1 and t_2), with different velocities (energies), then at the exit (at z_{out}), each of them arrives at time $t_1+\tau(u_{01})$ and $t_2+\tau(u_{02})$ respectively, where $\tau(u)$ is a transit time and defined by the dispersive properties of the section.

Therefore, the output current (defined as charge per unit time) relative to the input current is given as:

$$\frac{I(z_{out},t+\tau)}{I(z_{in},t)}=\frac{\Delta t}{\Delta t+\Delta\tau}=\frac{1}{1+\frac{\Delta\tau}{\Delta t}} \qquad 2\text{-}80$$

where $\Delta t=t_2-t_1$ and $\Delta\tau=\tau(u_{02})-\tau(u_{01})$.

For the case of small spread of electron velocities (energies), we obtain:

$$\frac{I(z_{out},t+\tau)}{I(z_{in},t)}=\frac{1}{1+\frac{\Delta\tau(u)}{\Delta u}\frac{\Delta u}{\Delta t}}\cong 1-\frac{\Delta\tau(u)}{\Delta u}\frac{\Delta u}{\Delta t} \qquad 2\text{-}81$$

On the other hand, the dispersive term of the "particle transport matrix" R_{56} is defined [78]:

$$R_{56}=-u_0\frac{\partial\tau}{\partial\left(\frac{\delta p}{p_0}\right)}=-u_0 p_0\frac{\partial\tau}{\partial u}\frac{\partial u}{\partial p} \qquad 2\text{-}82$$

where p_0 is the momentum of the design particle (a particle with average parameters of the trajectories), δp is the difference in momentum between the examined particle and the design one.

Using this definition to Eq. 2-81, we obtain:

$$\frac{I(z_{out},t+\tau)}{I(z_{in},t)}\cong 1-\frac{\Delta\tau(u)}{\Delta u}\frac{\Delta u}{\Delta t}=1-\frac{1}{p_0u_0}R_{56}\frac{dp}{du}\frac{du}{dt}=1-\frac{{\gamma_0}^2}{u_0^2}R_{56}\frac{du}{dt} \qquad 2\text{-}83$$

In the small signal limit, we obtain:

$$I(z_{out},t)=\left(1-\frac{{\gamma_0}^2}{u_0^2}R_{56}\frac{du}{dt}\right)\left(I_0(z_{in})+I_1(z_{in},t)\right) \qquad 2\text{-}84$$

Thus, using the single frequency expansion (Eq. 2-33), we receive:

$$\tilde{i}(z_{out})=\left(\tilde{i}(z_{in})+i\omega I_0R_{56}\frac{\gamma_0^2}{u_0^2}\tilde{u}(z_{in})\right) \qquad 2\text{-}85$$

Therefore, using the kinetic voltage definition (Eq. 2-25), we obtain the transfer matrix for a short dispersive section (if the space charge effects do not change the particle trajectories):

$$\begin{pmatrix}\tilde{i}(z_{out})\\ \tilde{v}(z_{out})\end{pmatrix}=\mathbf{M}_{shortdisp}\begin{pmatrix}\tilde{i}(z_{in})\\ \tilde{v}(z_{in})\end{pmatrix}=\begin{pmatrix}1 & -i\omega I_0R_{56}\frac{e}{mc^3\gamma_0\beta_0^3}\\ 0 & 1\end{pmatrix}\begin{pmatrix}\tilde{i}(z_{in})\\ \tilde{v}(z_{in})\end{pmatrix} \qquad 2\text{-}86$$

Taking into account definitions of plasma wavenumber (θ_p) (Eq. 2-78) and e-beam wave impedance in drift section (W_d) (Eq. 2-67), we obtain:

$$\mathbf{M}_{shortdisp}=\begin{pmatrix}1 & -i\frac{\theta_{pr}(z_{in})\gamma_0^2R_{56}}{W_d(z_{in})}\\ 0 & 1\end{pmatrix} \qquad 2\text{-}87$$

2.2.5 Analysis of a dispersive section with space charge

In the previous section, the common case of a short dispersive section with negligible space charge microdynamics effects was discussed. With recent technological availability of high quality high current e-beams (based on photocathode injectors), it is conceivable that collective microdynamics can take place throughout a long dispersive section (e.g. a chicane). For this reason, we extend our collective microdynamics analysis in this section to the case of a long dispersive section.

We start again from the 3D Lorentz equation (Eq. 2-1), but this time permit the presence of a magnetic field, and express the beam parameters as a sum of time-independent and time dependent (small signal parts):

$$m_0 \frac{d}{dt}\left(\gamma_0 \mathbf{u}_0(\mathbf{r}) + \gamma_0 \mathbf{u}_1(\mathbf{r},t) + \gamma_1 \mathbf{u}_0(\mathbf{r})\right) = -e\mathbf{E}_1(\mathbf{r},t) - e\left(\mathbf{u}_0(\mathbf{r}) + \mathbf{u}_1(\mathbf{r},t)\right)\times \mathbf{B}(\mathbf{r}) \quad 2\text{-}88$$

where **B**(**r**) is the external magnetic field. Taking into account the time differential presentation (Eq. 2-23)), the time independent and time-varying parts of the Lorentz equation (Eq. 2-88) are:

$$m_0(\nabla \cdot \mathbf{u}_0(\mathbf{r}))(\gamma_0 \mathbf{u}_0(\mathbf{r})) = -e\mathbf{u}_0(\mathbf{r}) \times \mathbf{B}(\mathbf{r}) \quad 2\text{-}89$$

$$m_0 \frac{\partial(\gamma_0 \mathbf{u}_1(\mathbf{r},t) + \gamma_1 \mathbf{u}_0(\mathbf{r}))}{\partial t} + m_0(\nabla \cdot \mathbf{u}_0(\mathbf{r}))(\gamma_0 \mathbf{u}_1(\mathbf{r},t) + \gamma_1 \mathbf{u}_0(\mathbf{r})) = -e\mathbf{E}_1(\mathbf{r},t) - e\mathbf{u}_1(\mathbf{r},t) \times \mathbf{B}(\mathbf{r}) \quad 2\text{-}90$$

The first equation (Eq. 2-89) shows the general particle trajectory in an external magnetic field, the second equation (Eq. 2-90) expresses the wave interaction dynamics along the beam in the presence of a time dependent space-charge field ($\mathbf{E}_1(\mathbf{r},t)$).

We may represent the external magnetic field (**B**) in terms of the vector potential **A**:

$$\mathbf{B}(\mathbf{r}) = \nabla \times \mathbf{A}.$$

and assume that the external magnetic field has a transverse (x-y) component only. We also assume that the magnetic field is uniform across the beam, namely:

$$\mathbf{A}(z) = A_x \hat{\mathbf{e}}_x + A_y \hat{\mathbf{e}}_y \quad 2\text{-}91$$

where $\hat{\mathbf{e}}_x$ and $\hat{\mathbf{e}}_y$ are the unit vectors parallel with the x- and y-axes respectively.

Neglecting the synchrotron radiation emission in the dispersive element, the motion of the electron is derived from the Hamiltonian:

$$c\sqrt{m^2c^2 + \left|\mathbf{P} - e\mathbf{A}\right|^2} = \gamma mc^2 \quad 2\text{-}92$$

where $\mathbf{P} = P_x \hat{\mathbf{e}}_x + P_y \hat{\mathbf{e}}_y + P_z \hat{\mathbf{e}}_z$ is the canonical momentum of the electron:

$$P_x = \gamma mc\beta_x + eA_x$$

$$P_y = \gamma mc\beta_y + eA_y \qquad \text{2-93}$$

$$P_z = \gamma mc\beta_z$$

Assuming that the amplitude of the magnetic field is small and the electron beam transits in the "+z" direction (the electron beam does not turn back), the axial Lorentz factor, defined as:

$$\gamma_z = \frac{1}{\sqrt{1-\beta_z^2}} \qquad \text{2-94}$$

is found to be:

$$\gamma_z(z) = \frac{\gamma_0}{\sqrt{1+\left(\frac{\left|\mathbf{P}_\perp - e\mathbf{A}(z)\right|}{mc}\right)^2}}$$

The transverse canonical momentum is conserved. If a vector potential field, with no transverse coordinates dependence (Eq. 2-91), and a beam angular spread is negligible, we may set the canonical momentum to be zero ($\mathbf{P}_\perp = 0$). Therefore, the axial Lorentz factor may be written as:

$$\gamma_z^2(z) = \frac{\gamma_0^2}{1+a_\perp^2(z)} \qquad \text{2-95}$$

where

$$a_\perp^2(z) = \left(\frac{e}{mc}\right)^2\left(\left(\int_{z_{in}}^{z} B_x(z')dz'\right)^2 + \left(\int_{z_{in}}^{z} B_y(z')dz'\right)^2\right)$$

is the normalized transverse momentum parameter, z_{in} is the entrance point to the dispersive section in which the transverse magnetic field and the electron canonical momentum are equal to zero.

The complete time-differential representation (Eq. 2-23) can now be written in the form:

$$\frac{d}{dt}(\gamma\beta) = (\gamma_0 + \beta_z^2\gamma_z^2\gamma_0)\frac{d}{dt}(\beta_z) = \gamma_0\gamma_z^2\frac{d}{dt}(\beta_z)$$

For this case, we redefine the small signal kinetic voltage parameter (Eq. 2-26) and plasma wavenumber parameter (Eq. 2-29) as:

$$V_z = -\frac{m_0c^2}{e}\gamma_z^2\gamma_0\beta_{z0}\beta_{z1} \qquad \text{2-96}$$

$$\theta_p^{disp}(z)=\frac{\omega_{p0}(z)}{c\beta_z(z)}=\frac{1}{c\beta_z(z)}\sqrt{\frac{e^2 n_0(z)}{\varepsilon_0 m_0\gamma_0\gamma_z^2(z)}}=\frac{1}{\beta_z(z)\gamma_z(z)}\sqrt{\frac{I_0 Z_0}{\frac{m_0c^2}{e}\gamma_0\beta_0 A_e(z)}} \qquad 2\text{-}97$$

With these definitions we get a set of differential equations for the small-signal current modulation and the kinetic voltage parameter, which is a generalized form of (Eqs. 2-37, 2-38):

$$\frac{\partial\tilde{J}_1(z,\omega)}{\partial z}-\frac{i\omega}{c\beta_z(z)}\tilde{J}_1(z,\omega)=-i\omega\varepsilon_0\left(\theta_p^{disp}(z)\right)^2\tilde{V}^{disp}(z,\omega) \qquad 2\text{-}98$$

$$\frac{\partial\tilde{V}^{disp}(z,\omega)}{\partial z}-\frac{i\omega}{c\beta_z(z)}\tilde{V}^{disp}(z,\omega)=-\frac{i}{\omega\varepsilon_0}\tilde{J}_1(z,\omega) \qquad 2\text{-}99$$

Continuing now with the same procedure of Chapter 2.1.3, to extend the 1D-model to the case of finite cross section beam with a single Langmuir plasma wave mode, it is found that the same coupled small signal equations (Eqs. 2-35, 2-36) are applicable for the dispersive transport case with appropriate substitutions of β_z and γ_z instead β and γ.

For the slow varying beam dynamic variable $\tilde{i}_1^{disp}(z,\omega)$ and $\tilde{v}^{disp}(z,\omega)$:

$$\tilde{i}_1^{disp}(z,\omega)=A_e\tilde{j}_1(z,\omega)=\tilde{I}_1(z,\omega)\exp\left(i\omega\int_0^z\frac{1}{\beta_z(z')c}dz'\right) \qquad 2\text{-}100$$

$$\tilde{v}^{disp}(z,\omega)=\tilde{V}^{disp}(z,\omega)\exp\left(i\omega\int_0^z\frac{1}{\beta_z(z')c}dz'\right) \qquad 2\text{-}101$$

the coupled equations (Eqs. 2-98, 2-99) turn into:

$$\frac{d\tilde{i}_1^{disp}(z,\omega)}{dz}=-i\omega\varepsilon_0 A_e\left(\theta_p^{disp}(z)\right)^2\tilde{v}^{disp}(z,\omega) \qquad 2\text{-}102$$

$$\frac{d\tilde{v}^{disp}(z,\omega)}{dz}=-\frac{ir_p^2}{\omega\varepsilon_0 A_e}\tilde{i}_1^{disp}(z,\omega) \qquad 2\text{-}103$$

Thus, with these definitions of the plasma wave number (θ_p^{disp},Eq. 2-97), and the kinetic voltage slow amplitude of ($\tilde{v}_p^{disp}$,Eqs. 2-96, 2-101), also the first order iteration expression for the transfer matrix ($\mathbf{M}^{(1)}$, Eq. 2-75) applies without change (except the definitions Eqs. 2-97, 2-96) for the case of small collective interaction dynamics (short dispersive section length L_{disp}).

$$\mathbf{M}^{(1)}_{disp}(L_{disp}) = \begin{pmatrix} 1 - \int_{z_{in}}^{L_{disp}} z' \left(\theta^{disp}_{pr}(z')\right)^2 dz' & -i\frac{kA_e}{Z_0} \int_{z_{in}}^{L_{disp}} \left(\theta^{disp}_{pr}(z')\right)^2 dz' \\ -ir_p^2 \frac{Z_0}{kA_e} L_{disp} & 1 - \int_{z_{in}}^{L_{disp}} \int_{z_{in}}^{z'} \left(\theta^{disp}_{pr}(z'')\right)^2 dz'' dz' \end{pmatrix}$$

The validity of this approximation is again given by:

$$\left(\max_{0<z<L_{disp}} (\theta^{disp}_{pr}(z)) L_{disp} \right)^2 << 1$$

2.3 Collective microdynamics of noise in electron beams

The e-beam transfer matrix formulation was derived in the previous section for a coherent single frequency signal as a phasor relation. But as is well known in linear systems analysis, it can also be employed for the analysis of incoherent signals composed of random fluctuations and a wide frequency spectrum. In the present context it describes the transport of noise on electron beams.

2.3.1 Noise parameters at the cathode

Small signal wave propagation in an electron beam was presented in previous sections in terms of a phasor formalism (Eq. 2-32) for a single frequency. An alternative presentation of signals in the frequency domain is the Fourier transform presentation, which is useful for multi-frequency signals. In the small signal linear regime, the frequency domain solutions of the plasma moment equations in the Fourier transform formalism are identical to the solution in the phasor formalism. The expressions for the Fourier components of the small signal parameters:

$$\breve{X}(\omega) = \int_{-\infty}^{\infty} X(t)\exp(i\omega t)dt \qquad \text{2-104}$$

are the same as the solution expressions of the phasor components (Eq. 2-32), but their units differ by a time unit factor. We can therefore use the same transfer matrix that we derived for the single frequency coherent signal to describe also multiple frequency and incoherent signals. This applies, however, only in the linear interaction regime.

We calculate now the amplitudes of the current modulation and kinetic voltage as a function of frequency starting from a model of single particles. The actual e-beam current flow is not continuous. It consists of discrete particles (here we do not take into account any quantum effects). Therefore, we define the current density as a function of time (t) and position ($\mathbf{r}$) by:

$$\mathbf{J}(\mathbf{r},t) = -e\sum_j \delta(\mathbf{r}-\mathbf{r}_j(t))\mathbf{u}_j(\mathbf{r},t) \qquad \text{2-105}$$

where δ is the Dirac delta function, $\mathbf{u}_j$ is the velocity of the j^{th} particle and $\mathbf{r}_j(t)$ is its trajectory. Integrating the axial component of this expression over the cross section ($dxdy$), we obtain the beam current as a function of axial coordinate (z) and time (t):

$$I(z,t) = -e\int_{-\infty}^{\infty}\int_{-\infty}^{\infty}\mathbf{J}(\mathbf{r},t)\cdot\hat{\mathbf{e}}_z dxdy = -e\sum_j u_{jz}(z)\delta(z-z_j(z)) \qquad \text{2-106}$$

If $z_j(t)$ is a single valued function of t, then it can be inverted. Therefore, $t_j(z)$ is the moment when the j^{th} electron cross the plane "z". Then, using the identity:

$$\delta(z - z_j(t))dz = \frac{1}{\frac{dz_j(t)}{dt}}\delta(t - t_j(z))dt$$

and $\frac{dz_j(t)}{dt} = u_{jz}$, we obtain:

$$I(z,t) = \sum_j -e \cdot \delta(t - t_j(z)) \qquad 2\text{-}107$$

Following the Fourier transform definition (Eq. 2-104), we obtain the current spectrum:

$$\breve{I}(z,\omega) = \sum_j \int_{-\infty}^{\infty} -e\delta(t - t_j(z))\exp(i\omega t)dt = \sum_j -e\exp(i\omega t_j(z)) \qquad 2\text{-}108$$

Using the small signal current definition (Eq. 2-8), we derive an expression for the small signal velocity in the frequency domain as:

$$\breve{u}_1(z,\omega) = -\frac{\breve{I}(z,\omega)}{eA_e n_0} - \frac{\breve{n}_1 u_0}{n_0} = \frac{\breve{I}(z,\omega) + \breve{n}_1 u_0 eA_e}{-eA_e n_0 u_0} u_0 =$$

$$= \frac{\breve{I}(z,\omega) + eu_0 \sum_j \frac{1}{u_j(z)}\exp\left(i\omega t_j(z)\right)}{I_0} u_0 =$$

$$= \frac{e}{I_0}\sum_j \frac{\left(u_j(z) - u_0(z)\right)}{u_j(z)} u_0(z)\exp\left(i\omega t_j(z)\right) \qquad 2\text{-}109.$$

We represent the velocity of each particle (u_j) as the sum of the average velocity (u_0), and the particular particle deviation velocity (δu_j, $<\delta u_j>=0$) from the ensemble average:

$$u_j = u_0 + \delta u_j \qquad 2\text{-}110$$

Substituting this into our previous result (Eq. 2-109.), assuming that the particular particle deviation velocity is small compared to the average velocity ($|\delta u_j| << u_0$), we can write:

$$\breve{u}_1(z,\omega) = \frac{e}{I_0}\sum_j \left(\delta u_j - \frac{(\delta u_j)^2}{u_0}\right)\exp\left(i\omega t_j(z)\right) \qquad 2\text{-}111$$

Here we kept the second order term and neglected higher order terms.

The spectral density of the product of two random signal parameters ($\breve{X}(\omega)$ and $\breve{Y}(\omega)$) is defined as the average over an ensemble of the product $\breve{X}(\omega)\breve{Y}^*(\omega)$. For an ergodic stationary system, the average of the ensemble may be replaced by an average over time (T):

$$\overline{\breve{X}\breve{Y}^*} = \frac{1}{T}\left\langle \breve{X}\breve{Y}^* \right\rangle_T \qquad 2\text{-}112$$

where T is larger than the coherence time of the signal.

At a plane z, where the crossing times of electrons ($t_j(z)$) are statistically independent random variables, or in other words, are completely uncorrelated (for example – at the cathode plane), we obtain the spectral density of the current for shot noise (based on Eqs. 2-108 and 2-112):

$$\overline{\left|\breve{i}_1(\omega)\right|^2} = \frac{\left\langle \left|\breve{I}(\omega)\right|^2 \right\rangle_T}{T} = \frac{1}{T}\left|\sum_j -e\exp\left(-i\omega t_j(z)\right)\right|^2 = e\frac{eN_T}{T} = -eI_0 \qquad 2\text{-}113$$

where N_T is the total number of electrons crossing the plane z within time T. The conventional definition of shot-noise relates to positive frequencies only, and therefore is twice as large ($-2eI_0$). The sign "minus" here demonstrates that if an electron moves to "+z" direction, then the current I_0 is negative.

The same procedure is applied to the velocity spectrum (using Eqs. 2-110 and 2-111) assuming that the electron velocity deviations δu_j are statistically independent random variables (uncorrelated), and also are independent of their crossing times t_j. Keeping only second order terms in δu_j this results in:

$$\overline{\left|\breve{u}_1(\omega)\right|^2} = \frac{\left\langle \left|\breve{u}_1(\omega)\right|^2 \right\rangle_T}{T} = \frac{e^2}{I_0}\frac{1}{I_0 T}\sum_j \left(\delta u_j\right)^2 = -\frac{e}{I_0}\left(u_{th}\right)^2$$

where u_{th} is the velocity spread defined from the beam distribution function:

$$u_{th} = \sqrt{\frac{1}{N_T}\sum_j \left(\delta u_j\right)^2}$$

Using this result, we define the spectral density of the kinetic voltage in the frequency range $-\infty < \omega < \infty$ for an e-beam with an energy spread as:

$$\overline{\left|\breve{\gamma}(\omega)\right|^2} = \frac{\left\langle \left|\breve{\gamma}(\omega)\right|^2 \right\rangle_T}{T} = -\left(\frac{m_0 c}{e}\gamma_0^3\beta_0\right)^2 \frac{e}{I_0}u_{th}^2 \qquad 2\text{-}114$$

It is usually assumed that the electron emission from the cathode produces a beam with stochastic uncorrelated distribution of emission times t_j and initial velocities u_j. In this case, one may substitute the relation $\delta E_{th} = k_B T_c$, where T_c is the cathode temperature. We call any plane, where the crossing times t_j and the crossing velocities u_j are independent, as an "I-V-independence plane". It is important to note that the thermal energy distribution (δE_{th}) defines the kinetic voltage noise only at an I-V-independence plane. Note that spectral kinetic voltage noise (Eq. 2-114), as well as spectral energy noise ($\left|\delta\breve{\gamma}(\omega)\right|^2$), are not identical with the parameter of beam thermal energy spread. Equation 2-114 gives the value of

the noise in terms of the beam energy spread δE_{th} only at the I-V-independence plane.

The product of the kinetic voltage noise and the complex conjugate of the current noise is the kinetic power noise of the signal:

$$\breve{v}\breve{i}_1^* = -\frac{emc\gamma_0^3\beta_0}{I_0}\sum_j\left(\delta u_j - \frac{(\delta u_j)^2}{u_0}\right)\exp\left(i\omega t_j(z)\right)\cdot\sum_j\exp\left(-i\omega t_j(z)\right)=$$

$$=-\frac{emc\gamma_0^3\beta_0}{I_0}\left[\sum_j\left(\delta u_j - \frac{(\delta u_j)^2}{u_0}\right)+\sum_{\substack{j,j'\\ j\neq j'}}\left(\delta u_j - \frac{(\delta u_j)^2}{u_0}\right)\exp\left(i\omega t_j(z)-i\omega t_{j'}(z)\right)\right]$$

As was mentioned above, the electron crossing times t_j and their velocities deviations δu_j are independent at any I-V-independence plane. Because of this reason, the inter-particle summation (second term) vanishes upon averaging and also $<\delta u_j> = 0$. Therefore the kinetic voltage spectral noise is non-zero upon emission from the cathode:

$$\overline{\breve{v}\breve{i}_1^*} = \frac{1}{T}\left\langle\breve{v}\breve{i}_1^*\right\rangle = -\frac{emc\gamma_0^3\beta_0}{I_0T}\left[\sum_j\left(\delta u_j - \frac{(\delta u_j)^2}{u_0}\right)\right] = mc^2\gamma_0^3\beta_{th}^2 = \frac{mc^2\delta\gamma\beta_{th}}{\beta_0} \qquad 2\text{-}115$$

where $\beta_{th} = u_{th}c$. However, its imaginary part is identically zero at this plane.

$$\mathrm{Im}\left(\overline{\breve{v}\breve{i}_1^*}\right) = 0 \qquad 2\text{-}116$$

Note also that according to Chu's theorem (Eq. 2-55), the real part of kinetic power remains constant along the entire non-dissipative transport section, but its imaginary part may vary.

2.3.2 Collective microdynamics of e-beam noise in a non-dissipative free drift section

With the Fourier spectrum definition, (Eq. 2-104), we may replace (Eq. 2-68) with an analogous expression presenting the evolution of the spectral current ($\breve{i}_1(\omega)$) and the spectral kinetic voltage ($\breve{v}(\omega)$) in a non-dissipative free drift section of length L_d:

$$\begin{pmatrix}\breve{i}_1(L_d,\omega)\\ \breve{v}(L_d,\omega)\end{pmatrix} = \mathbf{M}_{drift}(L_d)\begin{pmatrix}\breve{i}_1(0,\omega)\\ \breve{v}(0,\omega)\end{pmatrix} = \begin{pmatrix}\cos(\phi_p) & -\frac{i}{W_d}\sin(\phi_p)\\ -iW_d\sin(\phi_p) & \cos(\phi_p)\end{pmatrix}\begin{pmatrix}\breve{i}_1(0,\omega)\\ \breve{v}(0,\omega)\end{pmatrix} \qquad 2\text{-}117$$

where $\phi_p = \theta_{pr}L_d$ is the phase shift of the plasma wave in the free drift section.

This relation can be used to describe the transport for free drift of each Fourier component of the finite duration beam modulation signal. It can also be used for describing the propagation of a random signal (noise) during some period of time T, within which the beam noise can be considered stationary and ergodic,

and is long enough to correspond to a large number of electrons (N_T). The phases of the random parameters $\breve{i}_1(\omega)$ and $\breve{v}(\omega)$ are not known then, but one can derive (from Eq. 2-117) expressions for the development of the spectral parameters of the absolute value squared current ($\breve{i}$), kinetic voltage ($\breve{v}$) and kinetic power ($\breve{P}_k$) (Eq. 2-112).

We find then the spectral power of the current noise is:

$$\overline{\left|\breve{i}_1(L_d)\right|^2} = \overline{\left|\breve{i}_1(0,\omega)\right|^2}\cos^2\phi_p + \frac{1}{{W_d}^2}\overline{\left|\breve{v}(0,\omega)\right|^2}\sin^2\phi_p + \left[i\frac{\cos\phi_p \sin\phi_p}{W_d}\overline{\left(\breve{v}(0,\omega)\breve{i}_1^{*}(0,\omega)\right)} + c.c. \right] =$$

$$\overline{\left|\breve{i}_1(0,\omega)\right|^2}\cos^2\phi_p + \frac{1}{{W_d}^2}\overline{\left|\breve{v}(0,\omega)\right|^2}\sin^2\phi_p - \frac{\sin 2\phi_p}{W_d}\operatorname{Im}\overline{\left(\breve{v}(0,\omega)\breve{i}_1^{*}(0,\omega)\right)}$$

and the spectral power of the kinetic voltage noise is:

$$\overline{\left|\breve{v}(L_d,\omega)\right|^2} = \overline{\left|\breve{v}(0,\omega)\right|^2}\cos^2\phi_p + {W_d}^2\overline{\left|\breve{i}_1(0,\omega)\right|^2}\sin^2\phi_p -$$

$$-\left[iW_d\cos\phi_p\sin\phi_p\overline{\left(\breve{v}(0,\omega)\breve{i}_1^{*}(0,\omega)\right)} + c.c. \right] =$$

$$\overline{\left|\breve{v}(0,\omega)\right|^2}\cos^2\phi_p + {W_d}^2\overline{\left|\breve{i}_1(0,\omega)\right|^2}\sin^2\phi_p + W_d\sin 2\phi_p\operatorname{Im}\overline{\left(\breve{v}(0,\omega)\breve{i}_1^{*}(0,\omega)\right)}$$

The real part of the spectral beam kinetic power at any point is:

$$\breve{P}_k = \frac{1}{2}\operatorname{Re}\overline{\left(\breve{v}(L_d,\omega)\breve{i}_1^{*}(L_d,\omega)\right)} = \frac{1}{2}\operatorname{Re}\overline{\left(\breve{v}(0,\omega)\breve{i}_1^{*}(0,\omega)\right)}$$

and it is constant because of Chu's relativistic conservation theorem (Eq. 2-42). The imaginary part of the kinetic power (the reactive kinetic power) is:

$$\operatorname{Im}\overline{\left(\breve{v}(L_d,\omega)\breve{i}_1^{*}(L_d,\omega)\right)} = \frac{1}{2}\left(W_d\overline{\left|\breve{i}_1(0,\omega)\right|^2} - \frac{1}{W_d}\overline{\left|\breve{v}(0,\omega)\right|^2} \right)\sin 2\phi_p + \operatorname{Im}\overline{\left(\breve{v}(0,\omega)\breve{i}_1^{*}(0,\omega)\right)}\cos 2\phi_p$$

2-118

If we take an I-V-independence plane as the starting point (z = 0), the spectral powers of the noise parameters are given by:

$$\overline{\left|\breve{i}_1(L_d)\right|^2} = \overline{\left|\breve{i}_1(0)\right|^2}\cos^2\phi_p + \frac{1}{W_d^2}\overline{\left|\breve{v}(0)\right|^2}\sin^2\phi_p \qquad 2\text{-}119$$

$$\overline{\left|\breve{v}(L_d)\right|^2} = \overline{\left|\breve{v}(0)\right|^2}\cos^2\phi_p + W_d^2\overline{\left|\breve{i}_1(0)\right|^2}\sin^2\phi_p \qquad 2\text{-}120$$

$$\operatorname{Im}\overline{\left(\breve{v}(L_d)\breve{i}_1^{*}(L_d)\right)} = \frac{1}{2}\left(W_d\overline{\left|\breve{i}_1(0)\right|^2} - \frac{1}{W_d}\overline{\left|\breve{v}(0)\right|^2} \right)\sin 2\phi_p \qquad 2\text{-}121$$

Here we introduce the noise dominance factor at the initial conditions N as the impedance-weighed ratio between the averaged of squares of the amplitudes of the kinetic voltage noise and current noise at z = 0. Namely:

$$N^2 \equiv \frac{\overline{\left|\breve{v}(0,\omega)\right|^2}}{\overline{\left|\breve{i}_1(0,\omega)\right|^2} W_d^2} \qquad \text{2-122}$$

Using the noise dominance factor, we can rewrite the equation for the noise intensities (Eqs. 2-119, 2-120 and 2-121) as:

$$\overline{\left|\breve{i}_1(L_d)\right|^2} = \overline{\left|\breve{i}_1(0)\right|^2}\left(\cos^2\phi_p + N^2\sin^2\phi_p\right) \qquad \text{2-123}$$

$$\overline{\left|\breve{v}(L_d)\right|^2} = W_d^2\overline{\left|\breve{i}_1(0)\right|^2}N^2\left(\cos^2\phi_p + \frac{1}{N^2}\sin^2\phi_p\right) \qquad \text{2-124}$$

$$\mathrm{Im}\left(\overline{\breve{v}(L_d)\breve{i}_1^*(L_d)}\right) = \frac{1}{2}W_d\overline{\left|\breve{i}_1(0)\right|^2}\left(1-N^2\right)\sin 2\phi_p \qquad \text{2-125}$$

The noise intensities in a free drift section with constant parameters vary periodically with the ϕ_p period π. When the current noise source, defined at I-V-independence plane, is dominant:

$$N^2 < 1 \qquad \text{2-126}$$

then the current noise spectral density decreases and the kinetic voltage noise spectral density increases until the next I-V-independence plane at the quarter plasma oscillation period point $\phi_p = \pi/2$.

$$\overline{\left|\breve{i}(\phi_p = \pi/2,\omega)\right|^2} = N^2\overline{\left|\breve{i}(0,\omega)\right|^2} < \overline{\left|\breve{i}(0,\omega)\right|^2} \qquad \text{2-127}$$

$$\overline{\left|\breve{v}(\phi_p = \pi/2,\omega)\right|^2} = \overline{\left|\breve{i}(0,\omega)\right|^2}W_d^2 > \overline{\left|\breve{v}(0,\omega)\right|^2} \qquad \text{2-128}$$

Note, that in this new I-V-independence plane, the impedance-weighed ratio between the averaged of squares of the amplitudes of the kinetic voltage noise and current noise is larger than 1:

$$\frac{\overline{\left|\breve{v}(\phi_p = \pi/2,\omega)\right|^2}}{\overline{\left|\breve{i}(\phi_p = \pi/2,\omega)\right|^2}W_d^2} = \frac{1}{N^2(\phi_p = 0)}. \qquad \text{2-129}$$

If we measure the kinetic voltage intensity with the unit of current noise intensity using the e-beam wave impedance, then the maximum of the kinetic voltage intensity is equal to the current noise intensity at the starting point (see Figure 2-3).

2.3.3 Interpreting the Coherent Optical Transition Radiation effect observed in LCLS

Based on the formulation presented in the previous section, we can explain quantitatively the phenomenon of current noise amplification that has been observed recently in several laboratories, where an intense e-beam was transported

though a dispersive section after a free space drift section. In particular, we will provide a description of an effect of Coherent Optical Transition Radiation (COTR) that was observed in the LCLS injector and was referred to at the time as "unexpected physics" (now understood to be a result of a collective interaction of spatially coherent random energy modulation in the drift section, which turned into enhanced coherent current noise in a dispersive section [71]).

The LCLS injector (Figure 2-4) is composed of a photocathode rf-gun (the output electron energy of which is 6 MeV) followed by two linac sections (L0a and L0b). The injector produces a single electron bunch (1 nC charge bunch, with duration of 10 ps) with energy of 135 MeV. The 135 MeV beam is deflected onto the main linac axis by a two-dipole 35-degree achromatic bend. After the bend, the electrons are accelerated to 250 MeV in three 3-m long S-band accelerating structures (L1S) before entering the first bunch compressor chicane (BC1).

Figure 2-5 describes the "unexpected physics" observation of LCLS [71]. In conditions of a balanced achromatic magnetic bend (the quad in the bend centered tuned properly), the integrated optical power measured from the OTR screen varied nonlinearly with the bunch charge, while in the off-balance condition, it grows linearly (Figure 2-6).

To demonstrate the use of the noise transfer formalism of Section 2.2, we now apply it to the example of the LCLS experiment. We take the output point of the injector (end of the linac L0b) as a starting point for our analysis. The e-beam parameters at this point are: the e-beam energy (E_{k1}) is 135 MeV, the bunch charge (Q_b) and the bunch duration (t_p) are 1 nC and 10 ps respectively, beam normalized slice emittance (ε_n) is 1 μm, the e-beam has a Gaussian shape for its transverse profile with radius at FWHM (r_b) 82.5 μm (σ = 70 μm), the slice energy spread (δE_k) is 3 keV [71].

After a short free drift section (Ld1 =2.5 m) where a beam is focused to a waist, electrons are transported through a bending section containing two bending magnets and one quadrupole between them. The control over the strength of the magnetic field gradient into this quadrupole makes it possible to achieve a perfect linear achromatic section, which means that the transverse position of an electron does not depend on its energy. In other words, if the bending section is perfectly linearly achromatic, then this section conserves the transverse coherence of any modulation on the e-beam. The dispersive properties of the bending section are defined by R56 = 6.3 mm, and a trajectory length of Ldisp = 1.7 m.

The bent e-beam is passed through the linear accelerator L1S (Lacc = 9 m) and accelerated to an energy (Ek) of 250 MeV. The free drift length between the linear accelerator L1S and the OTR screen is Ld2 = 6 m. A CCD camera detects the signal (see Figure 2 6a) radiated from the OTR screen at an optical wavelength (near 1 □s). It is important to note that during the reported experiments the bunch compression system (BC1) was turned off.

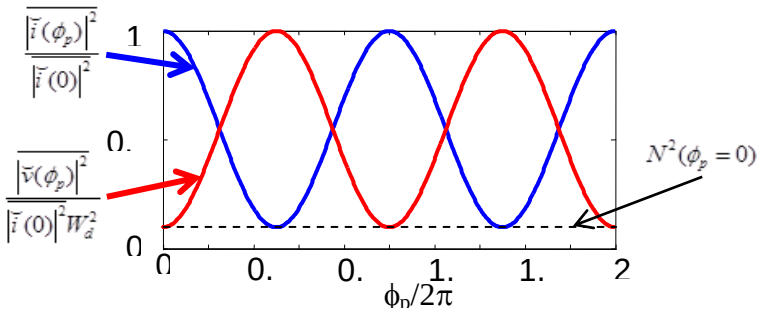

Figure 2-3 The noise intensities (current noise – blue curve, kinetic voltage noise – red curve) in a free drift section with constant impedance in a case of a current noise dominated beam (N^2 = 0.1).

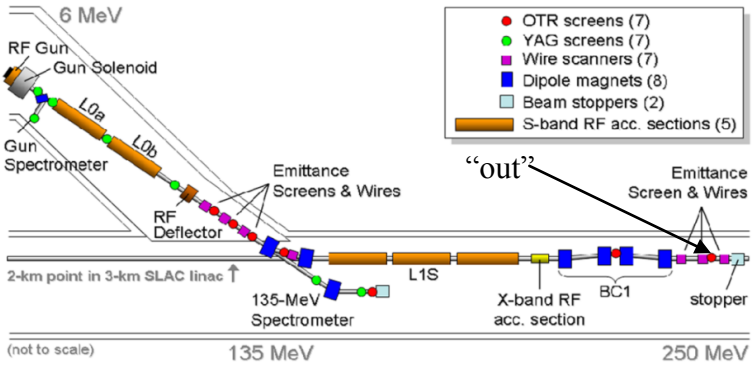

Figure 2-4 Scheme of the LCLS injector

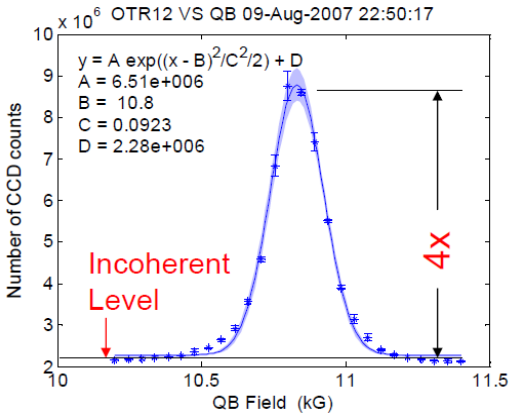

Figure 2-5 The integrated optical transition radiation signal as a function of the single quadrupole between the 17.5 degree bends. The optical signal is a maximum at the quadrupole setting which makes the DL1 bend doubly achromatic.

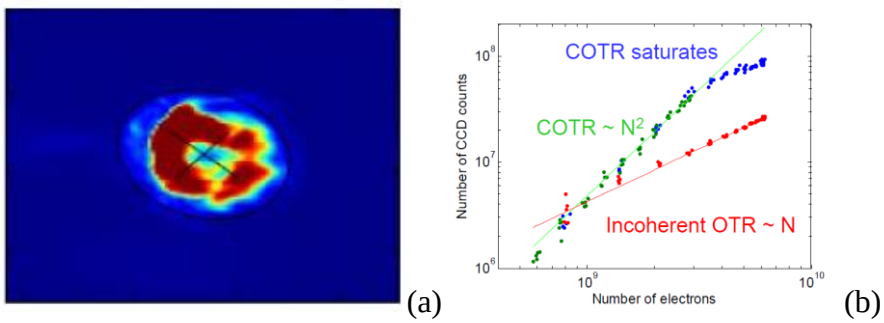

Figure 2-6 An image of the COTR radiation obtained by careful adjustment of the quadrupoles after the bunch compressor (a) and dependence the CCD counts on the e-beam current for different quadrupole strength (b) .

Thus, the electron transport line from the L0b accelerator end to the OTR screen (marked "out" in Figure 2-4) consists of four sections that can be modeled by our theory:

(A) a "drift section (L_{d1} = 2.5 m)" with starting point (z = 0)"-

(B) – a "short dispersive section (R_{56} = 6.3 mm)" –

(C) an "acceleration section (L_{acc} = 9 m)" –

(D) a "drift section (L_{d2} = 6 m)" – ends at the "OTR screen point (z = z_{OTR})".

Based on this description, we calculate the plasma wavenumber θ_p (Eq. 2-29) and the e-beam modulation impedance W_d (Eq. 2-67) for the first and the second free drift sections: θ_{p1} = 0.358 rad/m, W_{d1} = 4.293 kOhm, θ_{p2} = 0.143 rad/m, W_{d2} = 6.891 kOhm respectively. Note that we used the beam cross section area defined for a Gaussian beam (Eq. 2-57) and assume that the beam cross section area is approximately constant along the transport line. The plasma reduction factor for the first and the second free drift sections are found to be r_{p1} = 0.889 and r_{p2} = 0.71 respectively. The transfer matrices of the free drift sections are calculated from (Eq. 2-117):

$$\mathbf{M}_{d1} = \begin{pmatrix} 0.699 & -i \cdot 1.665 * 10^{-4}\ i(Ohm^{-1}) \\ -3.069 * 10^{3} i(Ohm) & 0.699 \end{pmatrix} \qquad 2\text{-}130$$

$$\mathbf{M}_{d2} = \begin{pmatrix} 0.954 & -4.341 * 10^{-5} i(Ohm^{-1}) \\ -2.062 * 10^{3} i(Ohm) & 0.954 \end{pmatrix} \qquad 2\text{-}131$$

For the dispersive section, we obtain (based on Eq. 2-86):

$$\mathbf{M}_{disp}^{LCLS} = \begin{pmatrix} 1 & -0.033 i(Ohm^{-1}) \\ 0 & 1 \end{pmatrix} \qquad 2\text{-}132$$

For the acceleration section, we obtain (based on Eqs. 2-72, 2-73):

$$\mathbf{M}_{acc}^{LCLS} = \begin{pmatrix} 0.995 & -1.714 * 10^{-5} i(Ohm^{-1}) \\ -1.114 * 10^{4} i(Ohm) & 0.86 \end{pmatrix} \qquad 2\text{-}133$$

Multiplying these transfer matrices, we obtain the total transfer matrix of the LCLS injector up to the OTR screen:

$$\mathbf{M}^{LCLS} = \mathbf{M}_{d2}\mathbf{M}_{acc}^{LCLC}\mathbf{M}_{disp}^{LCLC}\mathbf{M}_{d1} = \begin{pmatrix} 14.086 & 3.256 * 10^{-3} i(Ohm^{-1}) \\ 1.288 * 10^{6} i(Ohm) & -297.793 \end{pmatrix} \qquad 2\text{-}134$$

The complex initial amplitudes of the current and kinetic-voltage spectral densities are not known. We derive the root mean square of their averaged squared values (Eqs. 2-113 and 2-114):

$$\breve{i}_1^{LCLS}(z=0) = \sqrt{\left|\breve{i}_1(z=0)\right|^2} = \sqrt{eI_0} = 4 * 10^{-9}\, Amp \cdot s^{1/2} \qquad 2\text{-}135$$

$$\breve{v}^{LCLS}(z=0)=\sqrt{\left|\breve{v}(z=0)\right|^2}=\frac{\delta E_k}{\sqrt{eI_0}}=1.2*10^{-7}V\cdot s^{1/2} \qquad 2\text{-}136$$

Based on this, we can calculate the noise dominance factor N (Eq. 2-122) and determine that the LCLS injector operates in the current noise dominance regime:

$$N(z=0)=7*10^{-3}<<1 \qquad 2\text{-}137$$

From the general relation (Eq. 2-58) employed for random signals:

$$\overline{\left|\breve{i}_1(z_{out})\right|^2}=\overline{\left|A\breve{i}_1(z_{in})+B\breve{v}(z_{in})\right|^2}$$

It is evident from Eqs. 2-134 to 2-136 that the contribution of kinetic voltage noise is small compared to the current noise contribution ($\left|B\breve{v}(z_{in})\right|<<\left|A\breve{i}_1(z_{in})\right|$), and therefore, the current noise gain in the system is approximately:

$$\frac{\sqrt{\overline{\left|\breve{i}_1(z_{out})\right|^2}}}{\sqrt{\overline{\left|\breve{i}_1(z_{in})\right|^2}}}=A=14.1$$

Thus, the 1D linear small signal theory of noise propagation for a relativistic e-beam predicts that for the LSLC injector experiment, the current noise spectral density amplitude at the OTR screen plane should grow about 14 times, compared to the initial value (Eq. 2-122), assuming ideal electron optic elements are used.

The OTR experiment on the LCLS injector demonstrated that in the case of the linear achromatic bend structure, the integrated OTR signal grows 4 times compared to the incoherent level. The reasons for the deviation from the theoretical estimate are the degrading effects due to finite energy spread and emittance of the beam combined with non-vanishing of the $R_{i\neq j}$ coefficients [70]. Some additional degradation of the coherent microdynamics processes may be attributed to other electron-optic elements (quads, etc.) that may partially break the transverse coherence of the single plasma mode and reduce the gain of the microbunching instability.

2.4 Validity of the single Langmuir mode fluid plasma linear theory

Our single Langmuir plasma wave linear model is essentially a 1D coasting beam longitudinal interaction model. It includes, however, some 3D aspects of a finite cross section beam. In the following we analyze limitations of the validity of our fluid plasma model in the optical frequency range.

An obvious condition for the validity of the fluid plasma formulation and the longitudinal charge bunching model is multiplicity of particles per bunching wavelength $\lambda\beta_0$:

$$n_0 A_e \lambda\beta_0 >> 1 \qquad \text{2-138}$$

2.4.1 Ballistic electron phase spread condition

Another restriction to our model is a requirement that the beam is cold enough so that bunch smearing, due to electrons axial velocity spread (β_{th}), does not wash away space-charge wave bunching components at frequency ω (and wavenumber k/β) that were found to propagate on the beam (under a model of a cold beam) using the moment (fluid) equations. This condition can be expressed in terms of the optical phase spread $\Delta\varphi_b$ of the electrons along the interaction length L_d:

$$\Delta\varphi_b = kL_d\Delta(1/\beta_z) = kL_d\Delta\beta_z/\beta_z^2 = << \pi. \qquad \text{2–139}$$

This is a "ballistic-electron phase spread condition", in which one assumes that for the relevant drift length, each electron retains its velocity determined by the initial axial velocity distribution. The axial velocity spread of the beam may be owing to the beam energy spread, in which case the ballistic electron phase spread condition sets a limit on the beam energy spread:

$$\Delta\gamma/\gamma_0 << \beta_0^3\gamma_0^2\lambda/2L_d \qquad \text{2-140}$$

or owing to the angular spread of the beam $\sigma_{x'}$, that for a given beam width, σ_x sets a limit on the emittance $\varepsilon_n = \sigma_x * \sigma_{x'}$:

$$\varepsilon_n << \beta_0^2\gamma_0\sigma_{x0}(\lambda/L_d)^{1/2}. \qquad \text{2-141}$$

Note: the conditions above refer to beam propagation in a drift section. In the case of beam propagation through a magnetic dispersive section (such chicane, bend magnet, etc.) one should consider possible balistic electron phase spread due to the matrix parameter R_{56} [69]. Similarly to equation 2-139, one needs to inquire $kR_{56}\frac{\Delta\gamma}{\gamma_0} << \pi$ in order to keep the validity of the fluid model. This corresponds to:

$$\frac{\Delta\gamma}{\gamma_0} << \frac{\lambda}{2R_{56}}$$

2.4.2 Landau damping condition

The "ballistic-electron phase spread condition" (Eq. 2-139) is a plausible assumption for the validity of our electron-beam plasma wave solution in a long uniform drift section (Eqs. 2-65 and 2-66). Whereas we consider plasma wave dynamics in a short length (less than one plasma oscillation, which is the case of interest in the present work), we are mostly interested only in quarter plasma oscillation. There is, however, another well-known condition for the validity of the fluid plasma model derivation of the e-beam plasma wave solution (Eqs. 2-65 and 2-66) – "the Landau damping condition" [65, 66, 79].

The Landau damping effect, in the context of electron-beam plasma waves, and its neglected condition, are explained in Appendix 8. For its definition, one needs to assume that the plasma wave extends over at least a number of oscillations, so that its wavenumber is properly defined. The wavenumbers of the excited plasma waves can be identified when the solution (Eqs. 2-65 and 2-66) is expressed in terms of the fast varying parameters ($\tilde{I}(z,\omega)=\tilde{i}(z,\omega)\exp\left(-\frac{i\omega}{c\beta_{0z}}\right)$, $\tilde{V}(z,\omega)=\tilde{v}(z,\omega)\exp\left(-\frac{i\omega}{c\beta_{0z}}\right)$) (see Eqs. 2-51, 2-52):

$$k_z=\frac{\omega\pm\omega_{pr}}{u_{0z}}=\frac{\omega\pm\omega_{pr}}{c\beta_{0z}} \qquad 2\text{-}142$$

If the electron beam is not monoenergetic and has an axial velocity distribution of standard deviation u_{th}, there may be synchronism between the plasma wave and electrons of velocity $u_0 \pm u_{th}$, and then energy transfer from the plasma wave to the individual electrons would lead to damping of the plasma wave. This synchronism condition is depicted in Figure A0-5 and the condition for avoiding it found in Appendix 8:

$$k\Delta\beta/\beta < \theta_{pr} \qquad 2\text{-}143$$

where $k = \omega/c$.

Using the definition for the Debye wavenumber:

$$k_D=\frac{\omega_{pr}}{\Delta\beta c} \qquad 2\text{-}144$$

and defining the Landau damping parameter:

$$N_D=\frac{k}{k_D} \qquad 2\text{-}145$$

the Landau damping neglect condition is:

$$N_D<1 \qquad 2\text{-}146$$

Note, that the Landau damping argument is valid with reference to the validity of the cold beam plasma wave solution (Eqs. 2-65, 2-66) for a length of several plasma oscillations. It is not necessarily required when the interaction length is less than a plasma wavelength. The connection between the ballistic electron phase spread condition and the Landau damping condition is discussed in the next section in the context of noise suppression.

2.4.3 Space-charge dominated beam transport condition

In our analysis of beam microdynamics in free drift, we have assumed uniform beam cross-section and therefore constant plasma frequency along the drift length. This may be possible by imposing focusing (guiding) along the beam transport line. Of special interest is the case of free space drift in the absence of such continuous focusing. In this case, the beam envelope expands either due to its finite emittance or because of an average space charge repulsion force. Nevertheless, nearly uniform flow is possible if the beam is focused by electron optical elements, so that in its subsequent free space proportion, it converges to a waist of nearly uniform cross-section along its length $2z_{waist}$ (see Figure 2-7, Figure 2-8). The practical question that one may ask is whether the noise suppression effect that requires plasma phase accumulation $\phi_p = \pi/2$ (quarter plasma wave oscillation) can take place within the waist length, before the beam starts expanding, namely if one can satisfy

$$L_{\pi/2} = \pi/2\theta_{pr} < 2z_{waist} \qquad 2\text{-}147$$

In Appendix 4, we prove a new theorem that states that this condition is always satisfied if one forms a waist and if the beam envelope expansion is space charge dominated (namely the expansion effect of the emittance is negligible). It is also shown there that the plasma phase accumulation along the waist length is for $r_p = 1$ exactly $\pi/2$:

$$\int_{-z_{waist}}^{z_{waist}} \theta_p(z)dz = \pi/2 \qquad 2\text{-}148$$

Considering that some plasma phase accumulation can take place before and after the waist, we conclude that a sufficient condition for attaining quarter plasma oscillation by free drift along a beam waist is that the beam emittance is small enough to keep space charge dominated beam expansion along the waist. Using the K-V envelope equation [96], it is shown in Appendix 5 that this condition is

$$\varepsilon_n < \left(\frac{I_0}{I_A(\gamma\beta)^5}\right)^{1/2} r_b(z_{in}) \qquad 2\text{-}149$$

where $r_b(z_{in})$ is the initial beam radius after the focusing element.

For a given initial beam radius $r_b(z_{in})$ and arbitrary focusing means, assuming condition (Eq. 2-149) is satisfied, one can always form a waist of radius

$r_0 \le r_b(z_{in})/\sqrt{2}$ and length $2z_{waist}$, if enough drift length L_d is available after focusing, $\left(L_d > 2z_{waist}\right)$. Note that the parameters z_{waist} and r_0 are related by (see Appendix 5, Eq. A0-30):

$$\frac{z_{waist}}{r_0} = \sqrt{\left(\sqrt{2}-1\right)\left(\gamma_0\beta_0\right)^3 I_A/I_0} \qquad 2\text{-}150$$

Often the limiting factor in the experiment is the available drift length, while we have the freedom to extend the initial beam radius using appropriate beam optics and then focus the beam tighter to a smaller radius r_0 and shorter waist length z_{waist} (while keeping (Eq. 2-150)). In this case, the emittance condition (Eq. 2-149) can be written in terms of the available drift length L_d:

$$\varepsilon_n \le \frac{1}{\sqrt{2\left(\sqrt{2}-1\right)}} \frac{1}{\left(\gamma_0\beta_0\right)^3} \frac{I_0}{I_A} L_d \qquad 2\text{-}151$$

Notes:

(1) Condition (Eq. 2-149) or (Eq. 2-151) are sufficient conditions for attaining quarter plasma wave oscillation only if one takes advantage of them to form a waist in front of the focusing element and the emittance satisfies also condition (Eq. 2-141) (with $L_d=2z_0$), which is an entirely independent additional condition.

(2) In accelerator electron optics it is common to use the beta-function to describe the beam expansion instead of the radius. We avoided using this representation because it is limited to emittance dominated beam expansion.

(3) When the beam transport is not space-charge dominated and conditions (Eq. 2-149), (Eq. 2-151) are not satisfied, it is not possible to get quarter plasma oscillation in free drift along a waist. It is possible though to obtain smaller plasma phase accumulation, as calculated in Appendix 5, Eq. A0-36

(4) As was mentioned before, conditions Eq. 2-149 and Eq. 2-151 need to be satisfied only for a beam propagating in free space. It is not necessary if the beam is guided without expansion by means of focusing elements (solenoids or quads) or possibly by partial beam charge neutralization.

Considering again the previous example of the LCLS parameters, and given the reported emittance □n = 1 □m, I0 = 100 A, □0 = 273, one can verify that all inequalities (Eqs. 2 138 - 2 141) are satisfied except for Eq. 2 149. Therefore, if one would attempt to realize noise suppression with a beam of the same parameter values, it would require the use of a longer drift section Ld = 15m. Alternatively, a shorter drift section may be used if focusing quads can succeed to keep the beam from expanding. In this case, Eq. 2 149 is not relevant and not necessary for satisfying the quarter plasma oscillation condition.

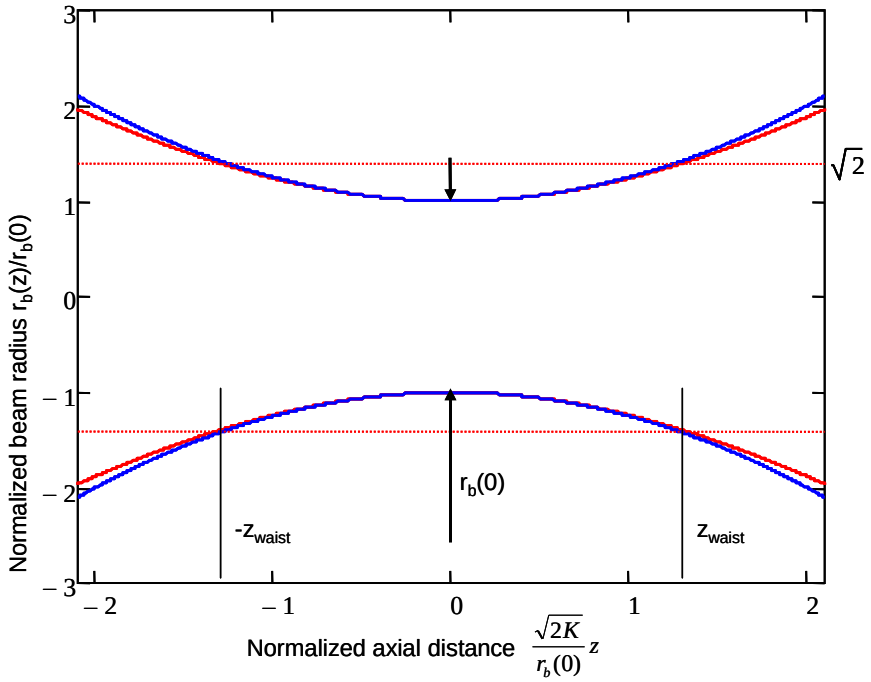

Figure 2-7 Beam envelope in a space charge dominated case: numerical solution (red curve) and approximated analytical solution (blue curve).

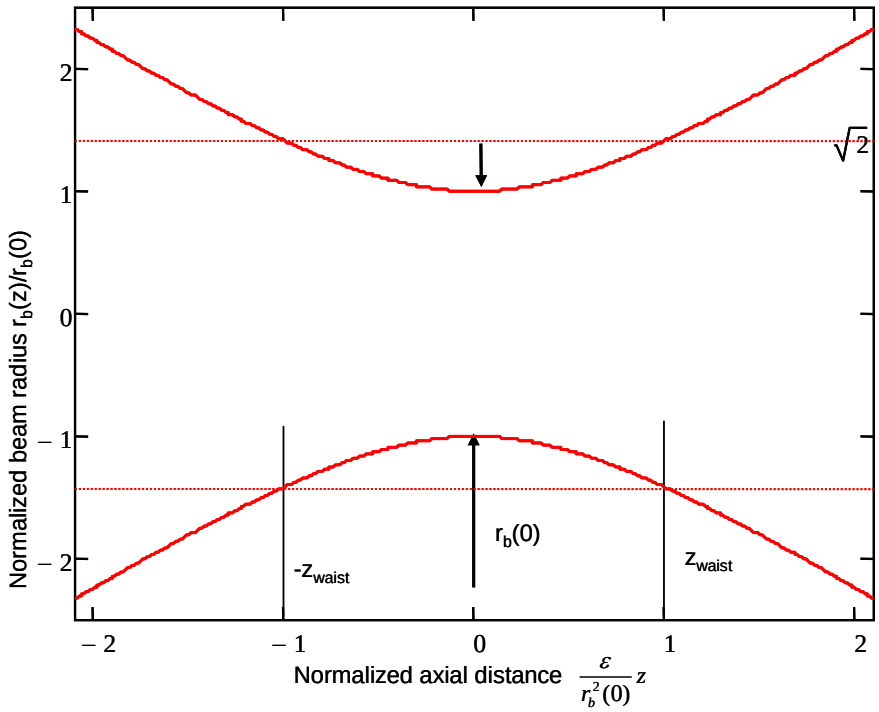

Figure 2-8 Beam envelope in an emittance dominated case. Analytical solution.

Whether noise suppression is possible to attain at frequencies beyond the IR-UV is a question of great interest. The answer depends on technological development and proper electron-optical design procedures that take into account the theoretical restrictions derived above. It should be borne in mind that the collective beam-noise interaction region in the LCLS experiment is right after the RF-LINAC injector and the noise effects were measured in the visible-IR regime. In practical X-UV FEL designs, the beam is transported through bends, chicanes and other electron-optical elements that degrade the beam parameters, and may give rise to destructive microbunching instabilities (one may consider reduction of such effects by *minimizing* the energy noise entering the dispersive section). Further theoretical and experimental studies are needed in order to understand the noise dynamics in these elements and evaluate the feasibility of the proposed scheme at frequencies beyond the visible. Note that in *seed-radiation* injection X-UV FEL schemes, one would need to diminish the beam-noise at X-UV frequencies in order to enhance the FEL radiation coherence. However in HGHG FELs, the noise reduction needs to be accomplished only at the frequency of the first laser buncher.

2.5 Landau damping and ballistic electron phase spread conditions in the context of noise suppression.

The conditions for the validity of the cold beam plasma oscillation solution (Eqs. 2-65, 2-66) at least up to a distance of quarter plasma oscillation length, are best described in terms of the "noise dominance parameter" N (see Eq. 2-122):

$$N^2 \equiv \frac{\overline{\left|\breve{v}(0,\omega)\right|^2}}{\overline{\left|\breve{i}_1(0,\omega)\right|^2} W_d^2}$$

This parameter is also useful for examining the connection of our velocity spread condition to the well-known Landau damping neglect condition (Eq. 2-146). Using the definitions of kinetic voltage noise (Eq. 2-114), current noise (Eq. 2-113), wave impedance (Eq. 2-67) and plasma wavenumber (Eq. 2-78), we obtain:

$$N^2 = \frac{-\left(\frac{m_0 c}{e}\gamma_0^3\beta_0\right)^2 \frac{e}{I_0} u_{th}^2}{-eI_0\left(\frac{r_p^2\sqrt{\mu_0/\varepsilon_0}}{k\theta_{pr}A_e}\right)^2} = \left(\frac{\frac{m_0 c^2}{e}\gamma_0^3\beta_0^3 A_e}{I_0 Z_0}\right)^2 \frac{u_{th}^2}{\beta_0^4 c^2}\left(\frac{k\theta_{pr}}{r_p^2}\right)^2 = \qquad 2\text{-}152$$

$$= \frac{1}{\theta_p^4}\frac{u_{th}^2}{\beta_0^4 c^2}\left(\frac{k\theta_{pr}}{r_p^2}\right)^2 = \frac{u_{th}^2}{\beta_0^4 c^2}\left(\frac{k}{\theta_{pr}}\right)^2 = \frac{u_{th}^2}{\beta_0^2}\left(\frac{k}{\omega_{pr}}\right)^2 = \frac{1}{\beta_0^2}\left(\frac{k}{k_D}\right)^2$$

Therefore,

$$N = \frac{N_D}{\beta_0} \approx N_D$$

Thus, we showed that the current noise dominance parameter N (Eq. 2-122) is identical with the Landau parameter N_D (Eq. 2-145). The current noise dominance condition ($N^2 < 1$, see Eq. 2-126) is not only the condition for attaining current noise suppression (Eq. 2-127), but it is also identical with the Landau damping neglect condition (Eq. 2-146) for a relativistic electron beam ($\beta_0 \sim 1$)!

This connection is not a priori obvious, considering that the noise dominance parameter N was defined only in the context of noise, while the Landau parameter N_D is defined in the context of decay of plasma wave oscillation, possibly coherent, not necessarily stochastic.

It is now interesting to reveal the connection between the different conditions for noise suppression that we discussed so far:

1. The current shot-noise dominance condition: $N << 1$.
2. The Landau damping neglect condition: $N_D << 1$.
3. The ballistic electron phase spread condition: $\Delta\varphi_b << \pi$

Following the discussion in Appendix 8 and Marinelli [65], we may write the Landau decay constant in the lab frame in the range $N < 0.5$ (which is anyway the range of interest for noise suppression) as:

$$\mathrm{Im}\,k = \theta_{pr}\sqrt{\frac{\pi}{8}}\frac{1}{N_D^3}\exp\left(-\frac{(1+3N_D^2)}{2N_D^2}\right)$$

It is intuitively convenient to express this relation in terms of the Landau decay length L_{Landau} (the e-folding decay length of the plasma wave amplitude).

$$L_{Landau} = (\mathrm{Im}\,k)^{-1} = \frac{1}{\theta_{pr}}\sqrt{\frac{8}{\pi}}N_D^3\exp\left(\frac{1}{2N_D^2}\right)\exp\left(\frac{3}{2}\right)$$

The drift length range where Landau damping is negligible is

$$L_d << L_{Landau}$$

or

$$\phi_{prd} = \theta_{pr}L_d << \sqrt{\frac{8}{\pi}}N_D^3\exp\left(\frac{1}{2N_D^2}\right)\exp\left(\frac{3}{2}\right)$$

The curve of $L_d = L_{Landau}$ is shown in Figure 2-9 (red curve). The broken line part corresponds to the numerically computed solution of the Landau damping in the range $N_D > 0.5$ [80]. Evidently in the range of interest for noise suppression $N << 1$, $0 < \phi_{prd} < \pi/2$, the neglect of Landau damping is well satisfied under the condition $N \cong N_d << 1$, which is fully consistent with the current shot noise dominance condition (Eq. 2-122).

We now examine the ballistic electron phase spread condition $\Delta\varphi_b << \pi$ (Eq. 2-139) It is instructive to express also the phase spread parameter $\Delta\varphi_b$ in terms of the Landau parameter N_D. Using the definition for the Debye wavenumber (Eq. 2-144) and relation for the noise dominance parameter (Eq. 2-152), we obtain:

$$\Delta\varphi_b = kL_d\frac{\Delta\beta_z}{\beta_z^2} = kL_d\frac{\Delta\beta_z c}{\omega_{pr}\beta_z^2}\frac{\omega_{pr}}{c} = \frac{k}{k_D}\frac{L_d\theta_{pr}}{\beta_z} = N\phi_{prd} \qquad 2\text{-}153$$

Thus the ballistic electron phase spread condition (Eq. 2-139) can be written simply as:

$$\phi_{prd} << \frac{\pi}{N} \approx \frac{\pi}{N_D}$$

The curve $\phi_{prd} = \dfrac{\pi}{N_D}$ is drawn in Figure 2-9 (blue curve). Again, it is evident that this condition is well satisfied in the range of interest $0 < \phi_{prd} < \pi/2$. For $\phi_{prd} = \dfrac{\pi}{N_D}$, it corresponds to requirement $N_D << 2$, which is automatically satisfied when the Landau damping condition $N_D << 1$ is satisfied, and for $N_D \cong N$ it is fully consistent with the current noise dominance condition $N << 1$, which satisfies all conditions for noise suppression.

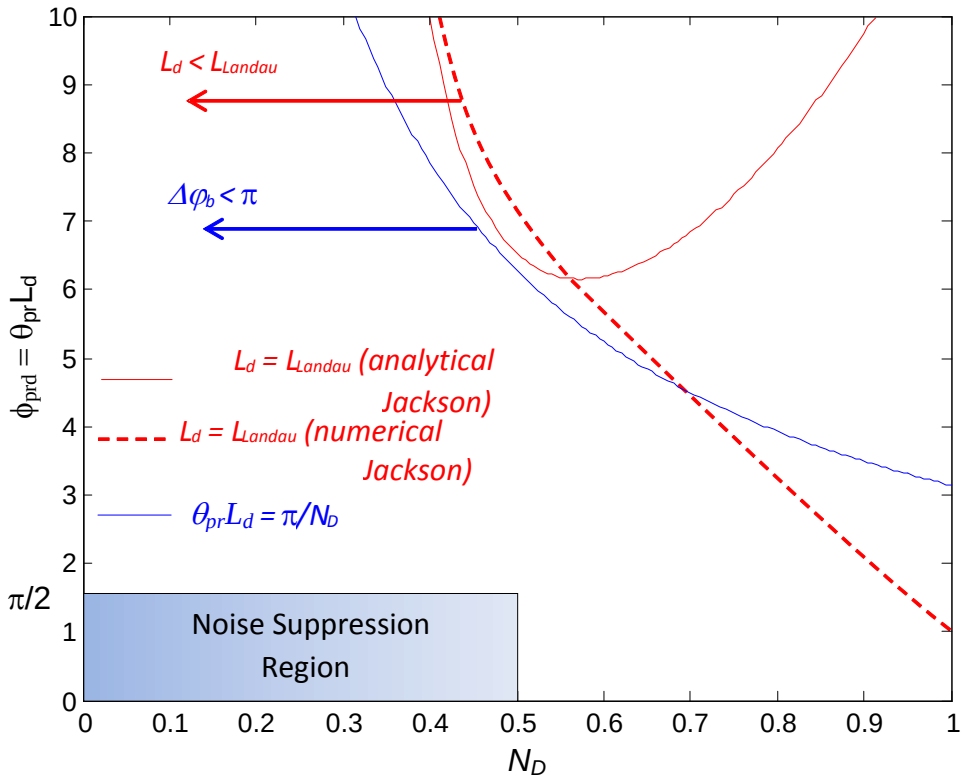

Figure 2-9 The Landau damping neglect region ($L_d < L_{Landau}$) and the ballistic electron optical phase spread region ($\Delta\varphi_b < \pi$). Both conditions are automatically satisfied in the region of interest for noise suppression: $\phi_{prd} < \pi/2$, $N \approx N_D < 0.5$ (current shot-noise dominance condition).

3 Generation of coherent and incoherent radiation in FEL

3.1 The general transfer matrix

We examined above the propagation of waves on an e-beam for non-dissipative sections (where there is no energy transfer from the e-beam to electromagnetic waves and back). E-beam transport has been considered in several passive (non-radiating) elements: the drift region, the accelerator region and the dispersive section.

In this chapter we derive the relativistic transfer matrix for an active (radiating) e-beam transport element: the wiggler. For the synchronism condition between the e-beam and the electromagnetic wave, energy transfer takes place between e-beam waves and the radiated electromagnetic waves. We use the small-signal expressions (similar to Eqs. 2-6 - 2-10) to find the stimulated radiation emission (or absorption) from e-beam radiation devices in the frequency domain (Eq. 2-32). We suppose here that the time-dependent part is a single-frequency signal:

$$n(\mathbf{r},t) = n_0(\mathbf{r}) + \frac{1}{2}\left(\tilde{n}_1(\mathbf{r},t)\exp(-i\omega t) + c.c.\right) \qquad 3\text{-}1$$

$$\mathbf{u}(\mathbf{r},t) = \mathbf{u}_0(\mathbf{r}) + \frac{1}{2}\left(\tilde{\mathbf{u}}_1(\mathbf{r},t)\exp(-i\omega t) + c.c.\right) \qquad 3\text{-}2$$

$$\begin{aligned}&\mathbf{j}(\mathbf{r},t) = -en(\mathbf{r},t)\mathbf{u}(\mathbf{r},t) \cong \\ &\cong -en_0(\mathbf{r})\mathbf{u}_0(\mathbf{r}) - \frac{1}{2}\left(e\left(\tilde{n}_1(\mathbf{r},t)\mathbf{u}_0(\mathbf{r}) + n_0(\mathbf{r})\tilde{\mathbf{u}}_1(\mathbf{r},t)\right)\exp(-i\omega t) + c.c.\right) = \\ &= \mathbf{J}_0(\mathbf{r}) + \frac{1}{2}\left(\tilde{\mathbf{J}}_1(\mathbf{r},t)\exp(-i\omega t) + c.c.\right)\end{aligned} \qquad 3\text{-}3$$

As in Chapter 2, we again assume that the electron beam propagates generally in the "+z" direction, and that the electrons in the injected beam oscillate transversely to their propagation direction (z) because of the periodic transverse Lorenz force in the static transverse magnetic field:

$$\frac{d\mathbf{p}_\perp}{dt} = u_{0z}\frac{d\mathbf{p}_\perp}{dz} = -eu_{0z}\hat{\mathbf{e}}_z \times \mathbf{B}_\perp \qquad 3\text{-}4$$

In a planar (linear) wiggler, the magnetic field on axis is approximately cosinusoidal:

$$\mathbf{B}_\perp = B_w\hat{\mathbf{e}}_y\cos(k_w z)$$

In a helical wiggler:

$$\mathbf{B}_\perp = B_w\left(\hat{\mathbf{e}}_y\cos(k_w z) + \hat{\mathbf{e}}_x\sin(k_w z)\right)$$

where B_w is the amplitude of the wiggler magnetic field, k_w is the wiggler wavenumber.

Direct integration of the force equation (Eq. 3-4) results in:

$$\mathbf{p}_\perp(z) = -e\hat{\mathbf{e}}_z \times \mathbf{B}_\perp(z)/k_w$$

We introduce the wiggler parameter a_w as the normalized transverse momentum amplitude:

$$a_w = \frac{p_\perp}{mc} = \beta_\perp \gamma = \frac{eB_w}{mck_w} \qquad 3\text{-}5$$

Therefore, based on the relation $\beta_z^2 + \beta_\perp^2 = \beta^2$, we obtain the average axial Lorentz factor (averaged over the wiggler period) along the z-axis:

$$\gamma_{0z} = \frac{1}{\sqrt{1-\beta_z^2}} = \frac{\gamma_0}{\sqrt{1+\frac{a_w^2}{2}}} \qquad 3\text{-}6$$

$$\gamma_{0z} = \frac{1}{\sqrt{1-\beta_z^2}} = \frac{\gamma_0}{\sqrt{1+a_w^2}} \qquad 3\text{-}7$$

for planar and helical wigglers respectively.

We use a formulation of modal expansion [81], where the traveling wave spectral radiation fields are expanded in terms of a complete set of transverse modes q (the beam propagation is in the z-direction):

$$\mathbf{E}_{rad}(\mathbf{r},t) = \mathrm{Re}\left(\sum_q \tilde{C}_q(z,\omega)\tilde{\mathbf{E}}_{q\perp}(\mathbf{r}_\perp)\exp(ik_{qz}z)\exp(-i\omega t) \right) \qquad 3\text{-}8$$

where $\tilde{C}_q$, k_{qz} and $\tilde{\mathbf{E}}_{q\perp}$ are the slow-varying amplitude, the axial wavenumber, and the transversal profile of the electromagnetic mode q respectively. We shall examine the interaction between the e-beam and TE-TEM modes, because these modes are commonly used in wiggler-based FELs.

The mode amplitude $\tilde{C}_q$ develops along the wiggler interaction length according to the mode excitation equation [81]:

$$\frac{d}{dz}\tilde{C}_q = -\frac{1}{4P_q}\exp(-ik_{qz}z)\iint \tilde{\mathbf{J}}(x,y,z)\cdot\tilde{\mathbf{E}}^*_{q\perp}(x,y)dxdy \qquad 3\text{-}9$$

where $P_q = -\frac{1}{2}\mathrm{Re}\iint \tilde{\mathbf{E}}_{q\perp} \times \mathbf{H}^*_{q\perp}\cdot\hat{\mathbf{e}}_z dxdy$ is the q-mode's normalized power.

The full differential with respect to time can be presented as:

$$\frac{d}{dt} = \frac{\partial}{\partial t} + \frac{\partial}{\partial z}u_z \qquad 3\text{-}10$$

where u_z is defined in Eq. 3-6 or Eq. 3-7.

$$\hat{\mathbf{e}}_z \cdot \frac{d\tilde{\mathbf{J}}}{dz} = -i\omega e\tilde{n}(z) \qquad 3\text{-}11$$

In the linear model, we assume that the average e-beam kinetic energy does not change along the wiggler. Therefore, the force equation (Eq. 2-1) and the continuity equation (Eq. 2-2) have a time-dependent part only. This formulation results in the following expression for the longitudinal part of the force equation:

$$m\gamma_0\gamma_{0z}^2\left(-i\omega+u_{0z}\frac{d}{dz}\right)\tilde{u}(z)=-e\tilde{E}_{pm}(z)-e\tilde{E}_{sc}(z) \qquad 3\text{-}12$$

The synchronous longitudinal force component on the r.h.s. of Eq. 3-12 is composed of two parts: the ponderomotive field ($\tilde{E}_{pm}$), which is due to the interaction of the electromagnetic wave and wiggler field) [21]

$$\tilde{E}_{pm}(z)=\tilde{C}_q(z)\frac{a_w}{2\gamma_0\beta_{0z}}\left(\hat{\mathbf{e}}_z\times\hat{\mathbf{e}}_w^*\right)\cdot\mathbf{E}_{q\perp}(\mathbf{r}_{e\perp})\exp(ik_{qz}z+ik_wz) \qquad 3\text{-}13$$

where $\mathbf{E}_{q\perp}(\mathbf{r}_{e\perp})$ is the mode profile field at the e-beam center ($\mathbf{r}_{e\perp}$). The second term in equation 3-12 ($\tilde{E}_{sc}$), is the self space-charge field, which is found from Gauss's law and the charge distribution along the e-beam .

$$\frac{d\tilde{E}_{sc}}{dz}=-r_p^2\frac{e\tilde{n}(z)}{\varepsilon_0} \qquad 3\text{-}14$$

where $r_p<1$ is the plasma reduction factor corresponding to a fundamental Langmuir plasma wave mode of the beam (see Chapter. 2). Using the same formalism, we obtain:

$$\tilde{E}_{sc}=-\frac{ir_p^2e}{\varepsilon_0\omega}\tilde{J}_z(z) \qquad 3\text{-}15$$

The force equation (Eq. 3-12), the excitation equation (Eq. 3-9), and the continuity equation (Eq. 3-11), with the definition of the field (Eqs. 3-13 and 3-15) form a set of linear differential equations, which should be solved self consistently. This set describes the coupling between three independent waves: electromagnetic wave ($\tilde{C}_q$), current modulation ($\tilde{\mathbf{J}}$) and kinetic voltage modulation ($\tilde{V}$).

The solution of this set may be found using the Laplace transform:

$$Laplace(\tilde{f}(z))=\hat{\tilde{f}}(s)=\int_0^z\tilde{f}(z)\exp(-sz)dz$$

The continuity equation is transformed to:

$$s\hat{\tilde{J}}(s)-\tilde{J}_z(0)=-i\omega e\hat{\tilde{n}}(s) \qquad 3\text{-}16$$

The space-charge field is:

$$\hat{\tilde{E}}_{sc}=-\frac{ir_p^2e}{\varepsilon_0\omega}\hat{\tilde{J}}_z(z)$$

The current small signal amplitude is:

$$\hat{\tilde{J}}_z(s) = -eu_{0z}\hat{\tilde{n}}(s) - en_0\hat{\tilde{u}}_z(s)$$

The force equation:

$$m\gamma_0\gamma_{0z}^2 u_{0z}\left(\left(s - i\frac{\omega}{u_{0z}}\right)\hat{\tilde{u}}_z(s) - \tilde{u}_z(0)\right) = -e\hat{\tilde{E}}_{pm}(s) - e\hat{\tilde{E}}_{sc}(s) \qquad 3\text{-}17$$

Again we recall the definition of the small signal relativistic kinetic voltage parameter in the presence of a transverse magnetic field (Eq. 2-96) with γ_{0z} given in the wiggler by equations 3-6, 3-7:

$$\tilde{V}_z(z) = -\frac{m}{e}\gamma_0\gamma_{0z}^2 u_{0z}\tilde{u}_z(z) = -\frac{mc^2}{e}\gamma_0\gamma_{0z}^2\beta_{0z}\tilde{\beta}_z(z) \qquad 3\text{-}18$$

and rewrite the force equation as:

$$\left(s - i\frac{\omega}{u_{0z}}\right)\hat{\tilde{V}}_z(s) - \tilde{V}_z(0) = \hat{\tilde{E}}_{sc}(s) + \hat{\tilde{E}}_{pm}(s) \qquad 3\text{-}19$$

The ponderomotive force is:

$$\hat{\tilde{E}}_{pm}(s) = \tilde{E}_{q\perp}^{*}\frac{a_w}{2\gamma\beta_{0z}}\hat{\tilde{C}}_q(s - ik_{qz} - ik_w) \qquad 3\text{-}20$$

The mode excitation equation (Eq. 3-9) is transformed to:

$$s\hat{\tilde{C}}_q(s) - \tilde{C}_q(0) = -\frac{1}{4P_q}\frac{a_w}{2\gamma\beta_z}\hat{\tilde{J}}_z\left(s + ik_{qz} + ik_w\right)\tilde{E}_{q\perp}^{*}(0,0)A_e$$

Here we assume that the EM-mode amplitude $\tilde{E}_{q\perp}^{*}$ does not change significantly across the e-beam transverse cross-section. Therefore, the integral over the transverse coordinates (*dxdy*) (see Eq. 2-47) was replaced by multiplication of the e-beam cross sectional area A_e.

In analogy with the e-beam one-dimensional model, definition (Eq. 2-47), we use the small signal current parameter instead of the small signal current density

$\tilde{I}(z) = A_e\tilde{J}_z(z)$.

Substituting the Laplace transformed equations, we obtain a linear set of three algebraic equations for the field amplitude $\hat{\tilde{C}}_q(s)$, the current $\hat{\tilde{I}}(s)$ and the kinetic voltage $\hat{\tilde{V}}_z(s)$, which are the Laplace transformed parameters. This set can be solved in terms of the initial conditions of these parameters at the entrance to the wiggler ($\tilde{C}_q(0), \tilde{I}(0), \tilde{V}_z(0)$). These algebraic equations may be rewritten in matrix form as a transform of the input amplitudes ($\tilde{C}_q(0), \tilde{I}(0), \tilde{V}_z(0)$) to the Laplace space $\hat{\tilde{C}}_q(s), \hat{\tilde{I}}(s), \hat{\tilde{V}}_z(s)$:

$$\begin{pmatrix} \tilde{\hat{C}}_q(s+ik_{qz}) \\ \tilde{\hat{I}}(s+ik_{qz}+ik_w) \\ \tilde{\hat{V}}_z(s+ik_{qz}+ik_w) \end{pmatrix} = \frac{1}{\Delta(s)} \begin{pmatrix} (s-i\theta)^2+\theta_{prw}^2 & -\frac{\tilde{E}^*_{q\perp}}{8P_q}\frac{a_w(s-i\theta)}{\gamma\beta_z} & \frac{i\tilde{E}^*_{q\perp}}{8P_q}\frac{a_w}{\gamma\beta_z}\frac{\theta_{prw}}{W_w} \\ i\tilde{E}_{q\perp}\frac{a_w}{2\gamma\beta_z}\frac{\theta_{prw}}{W_w} & s(s-i\theta) & -\frac{is\theta_{prw}}{W_w} \\ -\tilde{E}_{q\perp}\frac{a_w(s-i\theta)}{2\gamma\beta_z} & i\frac{W_w(i\Gamma^3-s\theta_{prw}^2)}{\theta_{prw}} & s(s-i\theta) \end{pmatrix} \begin{pmatrix} \tilde{C}_q(0) \\ \tilde{I}(0) \\ \tilde{V}_z(0) \end{pmatrix} \quad 3\text{-}21$$

where

$$\theta = \frac{\omega}{u_{0z}} - k_{qz}(\omega) - k_w$$

is the detuning parameter,

$$\theta_{prw} = \frac{\omega_{prw}}{u_{0z}} = r_p\sqrt{\frac{e^2 n_0}{\varepsilon_0 mc^2\gamma_0\gamma_{0z}^2\beta_{0z}^2}} \quad 3\text{-}22$$

is the beam plasma wavenumber in the wiggler,

$$\Gamma^3 = \frac{\theta_{prw}}{32A_{em}}\left(\frac{a_w}{\gamma_0\beta_{0z}}\right)^2\frac{Z_0}{W_w}$$

is the gain parameter

$$\Delta(s) = s\left((s-i\theta)^2+\theta_{prw}^2\right) - i\Gamma^3 \quad 3\text{-}23$$

is the determinant of the set,

$$W_w = \frac{r_p^2 Z_0}{k\theta_{prw}A_e} \quad 3\text{-}24$$

is the e-beam wave impedance in the wiggler.

The detuning parameter θ represents the deviation of the e-beam velocity from the synchronism condition for an electromagnetic wave at an angular frequency ω. The gain parameter Γ is related to the so called "Pierce parameter" [82] through

$$\Gamma = 2k_w\rho$$

We now can obtain the solutions of the set of the differential equations (Eqs. 3-9, 3-12, 3-11) by applying the inverse Laplace transform to the matrix (Eq. 3-21):

$$\tilde{f}(z) = Laplace^{-1}(\tilde{\hat{f}}(s)) = \frac{1}{2\pi i}\lim_{T\to\infty}\int_{\sigma-iT}^{\sigma+iT}\tilde{\hat{f}}(s)\exp(sz)ds \quad 3\text{-}25$$

where σ is a real number. The inverse Laplace transform can be calculated by the method of residues:

$$\tilde{f}(z) = Laplace^{-1}(\hat{\tilde{f}}(s)) = \sum_j \mathrm{Res}\left(\hat{\tilde{f}}(s)\right)\exp(S_j z) \qquad 3\text{-}26$$

where S_j (j = 1, 2, 3) are the roots (assuming non-degenerative roots) of the FEL cubic dispersion equation also named the Pierce dispersion equation:

$$\Delta(s) = 0 \qquad 3\text{-}27$$

Each cubic polynomial has 3 roots in the complex plane of numbers (including degenerate roots). Replacing the Laplace variable "s" with the variable "$i*k$", the dispersion equation is transformed to a cubic equation with real coefficients:

$$k^3 - 2\theta k^2 + (\theta^2 - \theta_{prw}^2)k + \Gamma^3 = 0 \qquad 3\text{-}28$$

As is well known, such a third order polynomial equation with real coefficients has three roots – either all real or one real and two complex (which are complex conjugates of each other). In the second case, one of the roots has a negative imaginary part, and consequently, one of the parameters S_j (because $S_j = i*k_j$) has a positive real part that corresponds to exponential growth. In this case, FEL operation is possible with high gain.

3.2 The FEL transfer matrix

The solutions of the Pierce cubic equation and their influence on the electromagnetic gain curve were investigated by [83, 84, 85]. The transfer matrix operating on the initial condition parameters can be expressed in real space as:

$$\begin{pmatrix} \tilde{C}_q(z) \\ \tilde{I}(z) \\ \tilde{V}_z(z) \end{pmatrix} = \mathbf{H}_{FEL} \begin{pmatrix} \tilde{C}_q(0) \\ \tilde{I}(0) \\ \tilde{V}_z(0) \end{pmatrix} = \tilde{\mathbf{h}} \circ \tilde{\mathbf{F}} \begin{pmatrix} \tilde{C}_q(0) \\ \tilde{I}(0) \\ \tilde{V}_z(0) \end{pmatrix} \qquad 3\text{-}29$$

where operation "$\circ$" is the Hadamard product (the element-by-element product) also known as the Schur product [86]. Matrix $\tilde{\mathbf{h}}$ includes all dimensional variables and matrix $\tilde{\mathbf{F}}$ is expressed in terms of normalized detuning functions (θ/Γ, θ_{prw}/Γ, S_j/Γ):

$$\tilde{\mathbf{h}} = \begin{pmatrix} 1 & -\frac{E_{q\perp}^*}{8P_q}\frac{a_w}{\gamma_0\beta_{0z}}\frac{1}{\Gamma} & \frac{iE_{q\perp}^*}{8P_q}\frac{a_w}{\gamma_0\beta_{0z}}\frac{\theta_{prw}}{W_w}\frac{1}{\Gamma^2} \\ iE_{q\perp}\frac{a_w}{2\gamma_0\beta_{0z}}\frac{\theta_{prw}}{W_w}\frac{\exp(-ik_w z - ik_{qz}z)}{\Gamma^2} & \exp(-ik_w z - ik_{qz}z) & -i\frac{\theta_{prw}}{W_w}\frac{\exp(-ik_w z - ik_{qz}z)}{\Gamma} \\ E_{q\perp}\frac{a_w}{2\gamma_0\beta_{0z}}\frac{\exp(-ik_w z - ik_{qz}z)}{\Gamma} & i\frac{W_w}{\theta_{prw}}\Gamma\exp(-ik_w z - ik_{qz}z) & \exp(-ik_w z - ik_{qz}z) \end{pmatrix} \qquad 3\text{-}30$$

$$\tilde{\tilde{\mathbf{F}}} = \begin{pmatrix} \sum_j \mathrm{Res}_{\frac{S_j}{\Gamma}} \left(\frac{\left(\frac{s}{\Gamma} - i\frac{\theta}{\Gamma}\right)^2 + \frac{\theta_{prw}^2}{\Gamma^2}}{\Delta\left(\frac{s}{\Gamma}\right)} \right) \exp\left(\frac{S_j}{\Gamma}\Gamma z\right) & \sum_j \mathrm{Res}_{\frac{S_j}{\Gamma}} \left(\frac{\frac{s}{\Gamma} - i\frac{\theta}{\Gamma}}{\Delta\left(\frac{s}{\Gamma}\right)} \right) \exp\left(\frac{S_j}{\Gamma}\Gamma z\right) & \sum_j \mathrm{Res}_{\frac{S_j}{\Gamma}} \left(\frac{1}{\Delta\left(\frac{s}{\Gamma}\right)} \right) \exp\left(\frac{S_j}{\Gamma}\Gamma z\right) \\ \sum_j \mathrm{Res}_{\frac{S_j}{\Gamma}} \left(\frac{1}{\Delta\left(\frac{s}{\Gamma}\right)} \right) \exp\left(\frac{S_j}{\Gamma}\Gamma z\right) & \sum_j \mathrm{Res}_{\frac{S_j}{\Gamma}} \left(\frac{\frac{s}{\Gamma}\left(\frac{s}{\Gamma} - i\frac{\theta}{\Gamma}\right)}{\Delta\left(\frac{s}{\Gamma}\right)} \right) \exp\left(\frac{S_j}{\Gamma}\Gamma z\right) & \sum_j \mathrm{Res}_{\frac{S_j}{\Gamma}} \left(\frac{\frac{s}{\Gamma}}{\Delta\left(\frac{s}{\Gamma}\right)} \right) \exp\left(\frac{S_j}{\Gamma}\Gamma z\right) \\ \sum_j \mathrm{Res}_{\frac{S_j}{\Gamma}} \left(\frac{\frac{s}{\Gamma} - i\frac{\theta}{\Gamma}}{\Delta\left(\frac{s}{\Gamma}\right)} \right) \exp\left(\frac{S_j}{\Gamma}\Gamma z\right) & \sum_j \mathrm{Res}_{\frac{S_j}{\Gamma}} \left(\frac{i - \frac{s}{\Gamma}\frac{\theta_{prw}^2}{\Gamma^2}}{\Delta\left(\frac{s}{\Gamma}\right)} \right) \exp\left(\frac{S_j}{\Gamma}\Gamma z\right) & \sum_j \mathrm{Res}_{\frac{S_j}{\Gamma}} \left(\frac{\frac{s}{\Gamma}\left(\frac{s}{\Gamma} - i\frac{\theta}{\Gamma}\right)}{\Delta\left(\frac{s}{\Gamma}\right)} \right) \exp\left(\frac{S_j}{\Gamma}\Gamma z\right) \end{pmatrix}$$

3-31

In Figure 3-1 we display the numerically computed normalized detuning function absolute value squared of the radiation matrix elements ($|F^{EE}(\theta)|^2$, $|F^{EI}(\theta)|^2$, $|F^{EV}(\theta)|^2$) in the low gain regime case ($\Gamma L = 0.6$). The curves are drawn as a function of θ for various values of plasma wavenumber parameters ($\theta_{prw}L$).

In the low gain regime, the EM-wave source gain curve for an electromagnetic input ($|F^{EE}(\theta)|^2$, Figure 3-1a) is the well-known derivative of the sinc-function [83]. The gain curves for current modulation ($|F^{EI}(\theta)|^2$, Figure 3-1b) is square of the sinc-function [83].

Note that in the general case, if different sources are used simultaneously (it will be discussed in the next sections), one must consider the phases of the input parameters and of the matrix elements, and consider cross-product terms in evaluating the output radiation power.

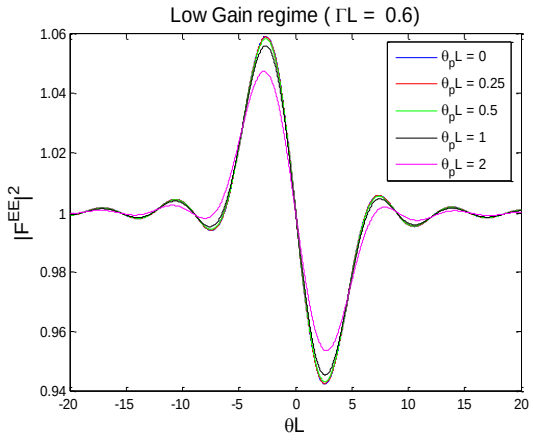

(a)

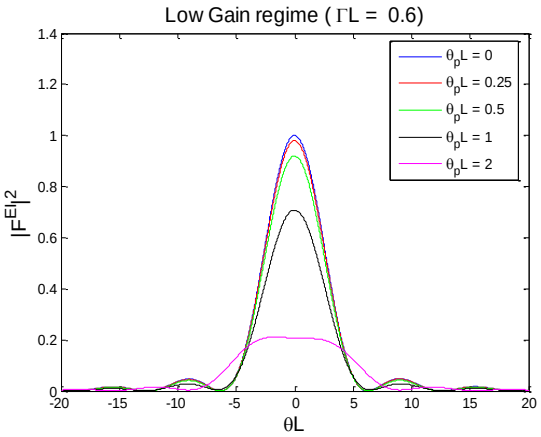

(b)

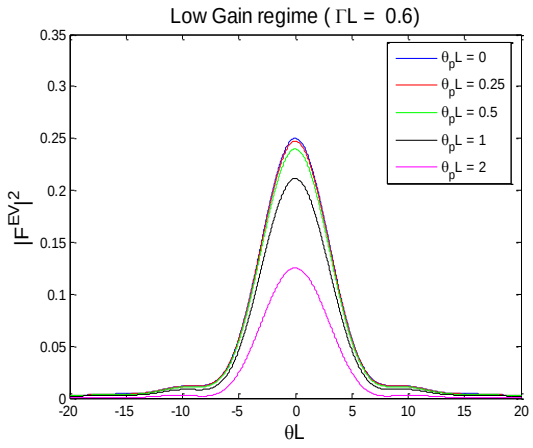

(c)

Figure 3-1 Absolute value square of the radiation terms of the transfer matrix in low gain regime for different plasma wave number: a) EM-wave source gain curve, b) current pre-modulation gain curve, c) velocity pre-modulation gain curve

3.3 High gain regime

The case of greatest interest in operating FELs is in the high gain ($\Gamma L_w >> 1$) tenuous beam ($\Gamma >> \theta_{prw}$) regime. For the synchronism condition ($\theta = 0$), and neglecting the space charge effect ($\theta_{prw} = 0$), the solutions of the Pierce equation are:

$$S_{1_0} = \frac{\sqrt{3}+i}{2}\Gamma \qquad 3\text{-}32$$

$$S_{2_0} = \frac{-\sqrt{3}+i}{2}\Gamma \qquad 3\text{-}33$$

$$S_{3_0} = -i\Gamma \qquad 3\text{-}34$$

For a given gain (Γ), the Pierce equation is an implicit function of residues (S_j), detuning parameter (θ) and plasma wave number (θ_{prw}). We can represent each residue in terms of a Taylor expansion:

$$S_j = S_{j_0} + \left.\frac{dS_j}{d\theta}\right|_{\substack{\theta=0\\ \theta_{prw}=0}} \theta + \left.\frac{dS_j}{d\theta_{prw}}\right|_{\substack{\theta=0\\ \theta_{prw}=0}} \theta_{prw} + \\ + \frac{1}{2}\left.\frac{d^2S_j}{d\theta^2}\right|_{\substack{\theta=0\\ \theta_{prw}=0}} \theta^2 + \frac{1}{2}\left.\frac{d^2S_j}{d\theta_{prw}^2}\right|_{\substack{\theta=0\\ \theta_{prw}=0}} \theta_{prw}^2 + \left.\frac{d^2S_j}{d\theta_{prw}d\theta}\right|_{\substack{\theta=0\\ \theta_{prw}=0}} \theta_{prw}\theta + \ldots \qquad 3\text{-}35$$

Using the Implicit function theorem, we define:

$$\frac{dS_j}{d\theta} = -\frac{\frac{\partial\Delta}{\partial\theta}}{\frac{\partial\Delta}{\partial s}} \qquad 3\text{-}36$$

$$\frac{dS_j}{d\theta_{prw}} = -\frac{\frac{\partial\Delta}{\partial\theta_{prw}}}{\frac{\partial\Delta}{\partial s}} \qquad 3\text{-}37$$

Based on these results, higher order differentials are given as:

$$\frac{d^2S_j}{d\theta^2} = \frac{d}{d\theta}\left(\frac{dS_j}{d\theta}\right)$$

$$\frac{d^2S_j}{d\theta_{prw}^2} = \frac{d}{d\theta_{prw}}\left(\frac{dS_j}{d\theta_{prw}}\right)$$

$$\frac{d^2S_j}{d\theta_{prw}d\theta} = \frac{d}{d\theta_{prw}}\left(\frac{dS_j}{d\theta}\right)$$

Thus, we obtain (see Appendix 9):

$$S_j = S_{j_0} + \frac{2i}{3}\theta + 0\cdot\theta_{prw} - \frac{1}{9S_{j_0}}\theta^2 - \frac{1}{3S_{j_0}}\theta_{prw}^2 + 0\cdot\theta_{prw}\theta + \ldots \qquad 3\text{-}38$$

The Tailor expansion for the roots of the Pierce equation makes possible an approximation analysis of frequency dependence for the FEL general transfer matrix. We are focusing now on the exponential growth solution (S_1) in the high gain regime ($|\theta|/\Gamma << 1$, $\theta_{prw}/\Gamma << 1$, $\Gamma z >> 1$). Because the general transfer matrix is written as inverse Laplace transform, each matrix element:

- exponentially grows up with the rate $\sqrt{3}(1-\frac{\theta_{prw}^2}{3\Gamma^2})\Gamma z/2$,
- has a phase shift (comparing to the synchronism frequency) $\frac{2}{3}(\frac{\theta}{\Gamma}+\frac{\theta_{prw}^2}{4\Gamma^2})\Gamma z$,
- is limited far from the synchronism by a Gaussian shape with FWHM $5.37(\Gamma/z)^{1/2}$,
- has a frequency chirp (an imaginary part of the Gaussian shape term in the Fourier space corresponds to the frequency shift in the time-space along the pulse).

For such a case, the FEL transfer matrix (Eq. 3-29) can be written as:

$$\begin{pmatrix} \tilde{C}_q(z) \\ \tilde{I}(z)\exp(-ik_w z - ik_{qz} z) \\ \tilde{V}_z(z)\exp(-ik_w z - ik_{qz} z) \end{pmatrix} = \tilde{\mathbf{H}}_{FEL} \begin{pmatrix} \tilde{C}_q(0) \\ \tilde{I}(0) \\ \tilde{V}_z(0) \end{pmatrix} = \frac{1}{3}\left(\tilde{\mathbf{h}}(z)^{\circ}\tilde{\mathbf{f}}\right)\begin{pmatrix} \tilde{C}_q(0) \\ \tilde{I}(0) \\ \tilde{V}_z(0) \end{pmatrix} \times$$
$$\times \exp\left(\frac{\sqrt{3}+i}{2}\Gamma z\right)\exp\left(\frac{2i}{3}\frac{\theta}{\Gamma}\Gamma z\right)\exp\left(-\frac{\sqrt{3}-i}{18}\frac{\theta^2}{\Gamma^2}\Gamma z\right)\exp\left(-\frac{\sqrt{3}-i}{6}\frac{\theta_{prw}^2}{\Gamma^2}\Gamma z\right) \qquad 3\text{-}39$$

where $\tilde{\mathbf{f}}$ is

$$\tilde{\mathbf{f}} = \begin{pmatrix} 1 & \exp\left(-i\frac{\pi}{6}\right) & \exp\left(-i\frac{\pi}{3}\right) \\ \exp\left(-i\frac{\pi}{3}\right) & 1 & \exp\left(-i\frac{\pi}{6}\right) \\ \exp\left(-i\frac{\pi}{6}\right) & \exp\left(i\frac{\pi}{6}\right) & 1 \end{pmatrix} \qquad 3\text{-}40$$

Here we neglect the frequency dependence of the fractional part in terms of matrix $\tilde{F}$ and save the phase advance in synchronism (for $\theta = 0$).

3.4 Generation of coherent radiation

From the first line of the general FEL transfer matrix (Eq. 3-29), one obtains a general expression for the amplitude of a radiation mode at the exit of the FEL ($z = L_w$) in terms of the initial conditions at the wiggler entrance ($z = 0$):

$$\tilde{C}_q(L) = H^{EE}\tilde{C}_q(0) + H^{EI}\tilde{I}(0) + H^{EV}\tilde{V}(0) \qquad 3\text{-}41$$

Assuming operating in the linear regime with a single radiation mode, the FEL power output is given by:

$$P(L) = P_q\left|\tilde{C}_q(L)\right|^2 = P_q\left|H^{EE}\tilde{C}_q(0) + H^{EI}\tilde{I}(0) + H^{EV}\tilde{V}_z(0)\right|^2 \qquad 3\text{-}42$$

For the general case, one must use the expressions of the general FEL matrix terms with all the initial amplitudes ($\tilde{C}_q(0), \tilde{I}(0), \tilde{V}_z(0)$) given both in amplitude and phase. However, for some special cases of interest, explicit expressions for the emitted power (Eq. 3-42) can be derived.

In the case of a regular FEL amplifier (no current and kinetic voltage modulation at the entrance to the wiggler), we set $\tilde{I}(0) = \tilde{V}_z(0) = 0$, and we define the FEL gain parameter as the ratio between the output radiation power ($P(L_w,\omega)$) and the input radiation power ($P(0,\omega)$):

$$G(\omega) = \frac{P(L,\omega)}{P(0,\omega)} = \left|\tilde{H}^{EE}(\omega)\right|^2 \qquad 3\text{-}43$$

In the low gain ($\Gamma L_w << 1$) tenuous beam ($\Gamma > \theta_{prw}$) regime, the FEL gain is given by the well know expression [83]:

$$G(\omega) = 1 + (\Gamma L)^3 \frac{d}{d\theta}\operatorname{sinc}^2\left(\frac{\theta(\omega)L_w}{2}\right) \qquad 3\text{-}44$$

In the high gain ($\Gamma L_w >> 1$) tenuous beam ($\Gamma > \theta_{prw}$) regime (see Eqs. 3-39 and 3-40):

$$G(\omega) = \frac{1}{9}\exp(\sqrt{3}\Gamma L_w)\exp\left(-\frac{(\omega-\omega_0)^2}{\Delta\omega_{HG}^2}\right) \qquad 3\text{-}45$$

where ω_0 is the synchronism frequency ($\theta = 0$) and

$$\Delta\omega_{HG} = 3^{3/4}\sqrt{\frac{\Gamma}{L_w}}\frac{\omega_0}{k_{qz}+k_w} \qquad 3\text{-}46$$

Another case of interest is the example of pure initial current prebunching ($\tilde{C}_q(0) = \tilde{V}_z(0) = 0$). In this case, the generated power is given by:

$$P(L_w,\omega) = P_q\left|H^{EI}\right|^2\left|\tilde{I}(0)\right|^2 = \frac{\left|\tilde{E}_q\right|^2}{64P_q}\left(\frac{a_w}{\gamma\beta_z}\right)^2\left|F^{EI}(\theta)\right|^2\left|\tilde{I}(0,\omega)\right|^2$$

In the low gain regime ($\Gamma L_w << 1$):

$$\left|F^{EI}(\theta)\right|^2 = \mathrm{sinc}^2\left(\frac{\theta(\omega)L_w}{2}\right) \qquad 3\text{-}47$$

This case of e-beam prebunching is also referred to as superradiance, since the emitted radiation power is proportional to the current modulation amplitude squared (this is similar to the effect of atomic superradiance where the coherent spontaneous emission rate is proportional to the number of atoms squared [87, 61]).

In the high gain regime

$$\left|F^{EI}(\theta)\right|^2 = \exp\left(-\frac{(\omega-\omega_0)^2}{\Delta\omega_{HG}^2}\right) \qquad 3\text{-}48$$

Note that current prebunching often involves also energy prebunching. In this case, one must keep both $\tilde{I}(0)$ and $\tilde{V}_z(0)$ and mind the phase between them:

$$P(L,\omega) = P_q\left|H^{EI}\tilde{I}(0,\omega) + H^{EV}\tilde{V}_z(0,\omega)\right|^2 = \frac{\left|E_{q\perp}\right|^2}{64P_q}\left(\frac{a_w}{\gamma_0\beta_{0z}\Gamma}\right)^2\left|\tilde{I}(0,\omega) + \frac{\theta_{prw}}{W_w\Gamma}\exp\left(-\frac{i\pi}{6}\right)\tilde{V}_z(0,\omega)\right|^2 \qquad 3\text{-}49$$

An interesting special case is the case when the input includes both coherent radiation field and beam pre-bunching. This situation, referred to as "stimulated-superradiance" [87, 88], is actually the case of the radiation section of an optical-klystron [89]. It was studied experimentally in an FEM configuration by Arbel et al [90], and recently noted to have a significant effect on the gain of long wavelength FEL oscillators [91].

For the common case where the energy modulation is small relative to the current modulation, the stimulated superradiant power term may be expressed as:

$$\Delta P = 2\,\mathrm{Re}\left[H^{EE}H^{EI*}\tilde{C}_q(0)\tilde{I}^*(0)\right] \qquad 3\text{-}50$$

or:

$$\Delta P = P_{in}(0)\left|\tilde{I}(0)\right|\frac{\tilde{\tilde{E}}_q}{8P_q}\frac{a_w}{\gamma_0\beta_{0z}\Gamma}2\,\mathrm{Re}\left(F^{EE}(\theta)F^{EI*}(\theta)\exp\left(i(\varphi^E-\varphi^I)\right)\right) \qquad 3\text{-}51$$

Note that the relative phase between the input radiation field and current prebunching φ^E-φ^I is important and determines if power is generated or absorbed ($\Delta P_q < 0$).

3.5 Generation of incoherent radiation

The radiative spontaneous emission of FEL is synchrotron undulator radiation. This radiation has been well studied, and is usually described in the framework of single particle models. However, such an approach is not sufficient for analysis of high gain Self Amplified Spontaneous Emission FELs, where multi electron cooperative emission takes place, and in high current FELs, where collective interaction takes place.

In systems with a linear response, it is possible to extend the single frequency coherent response formulation to a multi-frequency spectral response and also employ stochastic (incoherent) signal analysis. Following [72, 1] we extend the coherent linear response formulation and the FEL transfer matrix expression that we derived in the previous sections and employ them for calculating FEL spontaneous emission and self amplified spontaneous emission. These processes are described then as a linear transfer of stochastic input signals of the FEL parameters – current noise, energy noise and radiation noise.

To account for the multi-frequency situation, the single frequency radiation mode excitation model (Eqs. 3-8 and 3-9), should be modified to correspond to Fourier components of the radiation field (Eq. 2-104), rather than to phasor notation:

$$\breve{\mathbf{E}}(\mathbf{r},\omega)=\int_{-\infty}^{\infty}\mathbf{E}(\mathbf{r},\omega)\exp(i\omega t)dt \qquad 3\text{-}52$$

$$\breve{\mathbf{H}}(\mathbf{r},\omega)=\int_{-\infty}^{\infty}\mathbf{H}(\mathbf{r},\omega)\exp(i\omega t)dt \qquad 3\text{-}53$$

Instead of equations 3-8 and 3-9 the radiation mode excitation equations are then:

$$\breve{\mathbf{E}}(\mathbf{r},\omega)=\sum_{q}\breve{C}_q(z,\omega)\tilde{\mathbf{E}}_q(\mathbf{r}_\perp)\exp(ik_{qz}z) \qquad 3\text{-}54$$

$$\frac{d}{dz}\breve{C}_q(z,\omega)=\frac{1}{4P_q}\exp(-ik_{qz}z)\iint\breve{\mathbf{J}}(x,y,\omega)\cdot\tilde{\mathbf{E}}_q(x,y)dxdy \qquad 3\text{-}55$$

Note that the units of the mode's transverse profile ($\tilde{\mathbf{E}}_{q\perp}$) are voltage per unit length (V/m) and the mode's slow amplitude ($\breve{C}_q$) are time (s).

To calculate the spectral power of a stochastic radiation signal in a single mode *q*, we use the following expression (see Appendix 7):

$$\frac{dP}{d\omega}=\frac{2}{\pi}P_q\overline{\left|\breve{C}_q(\omega)\right|^2} \qquad 3\text{-}56$$

In this expression, which is analogous to Eq. 3-42 for a coherent single frequency mode, $\breve{C}_q(\omega)$ is the Fourier transform of the radiation mode amplitude, P_q is the

normalization power of the mode at the center frequency of the radiation spectrum and $\frac{dP}{d\omega}$ is the spectral power of positively-defined frequencies (in units of Watt/(rad/sec)).

The linear transfer matrix relation (Eq. 3-29) can now be written in the spectral notation:

$$\begin{pmatrix} \breve{C}_q(z) \\ \breve{I}(z) \\ \breve{V}_z(z) \end{pmatrix} = \mathbf{H}_{FEL} \begin{pmatrix} \breve{C}_q(0) \\ \breve{I}(0) \\ \breve{V}_z(0) \end{pmatrix} = \begin{pmatrix} H^{EE} & H^{EI} & H^{EV} \\ H^{IE} & H^{II} & H^{IV} \\ H^{VE} & H^{VI} & H^{VV} \end{pmatrix} \begin{pmatrix} \breve{C}_q(0) \\ \breve{I}(0) \\ \breve{V}_z(0) \end{pmatrix} \qquad 3\text{-}57$$

or, after opening the squared expression and specifying our analysis to a spectral stochastic signal (noise) formalism (Eq. 2-112):

$$\frac{dP(\omega, L_w)}{d\omega} = \frac{2}{\pi} P_q \overline{\left|\breve{C}_q(\omega, L_w)\right|^2} =$$
$$\frac{2}{\pi} P_q \left(\left|H^{EE}(\omega, L_w)\right|^2 \overline{\left|\breve{C}_q(\omega,0)\right|^2} + \left|H^{EI}(\omega, L_w)\right|^2 \overline{\left|\breve{I}(\omega,0)\right|^2} + \left|H^{EV}(\omega, L_w)\right|^2 \overline{\left|\breve{V}_z(\omega,0)\right|^2} + \right. \qquad 3\text{-}58$$
$$\left. + H^{EI}(\omega, L_w)\left(H^{EV}(\omega, L_w)\right)^* \overline{\breve{I}(\omega,0)\breve{V}_z^*(\omega,0)} + \left(H^{EI}(\omega, L_w)\right)^* H^{EV}(\omega, L_w) \overline{\breve{V}_z(\omega,0)\breve{I}^*(\omega,0)} \right)$$

Here we assumed no correlation between the input radiation field and the input beam modulation components (their products average to zero). Besides the input noise contributions of the beam current noise (Eq. 2-113), the beam energy noise (Eq. 2-114) and the beam kinetic power noise (Eq. 2-115), this expression includes also a radiation noise term. The input radiation noise can be interpreted to represent the ambient temperature black-body radiation coupling into a single transverse mode and quantum spontaneous emission. It is assumed to be given by the Bose-Einstein formula [92]:

$$\left(\frac{dP}{d\omega}\right)_{in}^{E} = \hbar\omega / \left(1 - e^{-\hbar\omega/k_B T}\right) \qquad 3\text{-}59$$

In conventional SASE FEL theory, it is assumed that the current shot-noise is dominant over all other input noise sources [20] (this assumption is justified in the next section). Consequently, we can write a simple conventional general expression for the FEL spontaneous emission and SASE radiation power in terms of the input current shot-noise (Eq. 2-113) and the normalized detuning function F^{EI}:

$$\frac{dP(L_w, \omega)}{d\omega} = \frac{2}{\pi} P_q \left|H^{EI}\right|^2 \left|\breve{i}_1(0,\omega)\right|^2 = \frac{1}{16\pi} \frac{Z_q}{A_{em}} \left(\frac{a_w}{\gamma\beta_z}\right)^2 \left|F^{EI}(\theta)\right|^2 eI_0 \qquad 3\text{-}60$$

Here $A_{em} = \frac{2P_q Z_q}{\left|E_{q\perp}\right|^2}$ is the effective cross-section area of the mode q and Z_q is the radiation mode impedance (in free space $Z_q = Z_0$).

We can now write an explicit expression for the spectral power of synchrotron undulator radiation spontaneous emission per mode (see [1]) (spontaneous emission of FEL in the low gain limit) using equation 3-47:

$$\frac{dP(L,\omega)}{d\omega} = \frac{1}{16\pi}\frac{eI_0 Z_q L^2}{A_{em}}\left(\frac{a_w}{\gamma_0 \beta_{0z}\Gamma}\right)^2 \mathrm{sinc}^2(\theta L/2) \qquad 3\text{-}61$$

and for the spectral power of SASE radiation (assuming single transverse mode operation [21]):

$$\frac{dP(L,\omega)}{d\omega} = \frac{1}{16\pi}\frac{eI_0 Z_q L^2}{A_{em}}\left(\frac{a_w}{\gamma_0 \beta_{0z}}\right)^2 \frac{1}{9}\exp(\sqrt{3}\Gamma L)\exp\left(-\frac{(\omega-\omega_0)^2}{(\Delta\omega_{HG})^2}\right) \qquad 3\text{-}62$$

because SASE FEL is commonly operated in high gain regime. The spectral power expressions can be written in general in the form:

$$\frac{dP(L,\omega)}{d\omega} = \left(\frac{dP_{NEP}}{d\omega}\right)^I G(\omega) \qquad 3\text{-}63$$

where $G(\omega)$ is the regular coherent electromagnetic radiation gain (Eq. 3-43):

$$G(\omega) = \frac{1}{9}\exp(\sqrt{3}\Gamma L)\exp\left(-\frac{(\omega-\omega_0)^2}{(\Delta\omega_{HG})^2}\right) \qquad 3\text{-}64$$

and the current shot-noise spectral density NEP (Noise Equivalent Power) is defined as:

$$\left(\frac{dP_{NEP}}{d\omega}\right)^I = \frac{1}{16\pi}\frac{eI_0 Z_q L^2}{A_{em}}\left(\frac{a_w}{\gamma\beta_z}\right)^2 \qquad 3\text{-}65$$

Taking into account the high gain spectral range ($-\int_0^\infty \exp\left(-\frac{(\omega-\omega_0)^2}{(\Delta\omega_{HG})^2}\right)d\omega \approx \sqrt{\pi}\Delta\omega_{HG}$ for $\omega_0 >> \Delta\omega_{HG}$), the total input effective power of the current shot-noise is:

$$(P_{NEP})^I = \frac{1}{16\sqrt{\pi}}\frac{eI_0 Z_q L^2}{A_{em}}\left(\frac{a_w}{\gamma\beta_z}\right)^2 \Delta\omega_{HG} \qquad 3\text{-}66$$

3.6 Seed injected FEL

A number of present day FELs are designed to operate at UV-X ray wavelengths. Because X-ray resonators are not available for use in FELs, the leading concept in current X-ray FELs is Self Amplified Spontaneous Emission (SASE). In SASE FELs, the amplified signal is the beam shot noise NEP that we calculated in the previous section (Eqs. 3-65 and 3-66). Naturally, the temporal coherence of such sources is limited (see Figure 3-2), but they are still extremely bright due to a significant feature of e-beam optical guiding, which makes it possible to establish transverse spatial coherence of the radiation wave in the high gain operating regime [93].

The possibility to use high gain FELs for amplification of a coherent input signal has been considered in recent years. A number of schemes were developed to overcome the coherence limitation of SASE FELs due to shot-noise. These include schemes of seed radiation injection, which were demonstrated first in the IR regime [94]. Such seed radiation injection has been demonstrated recently at UV wavelengths using High Harmonic Generation (HHG) by Lambert et al [23]. In this experiment, an intense laser pulse was focused on a xenon gas cell. The fifth harmonic at 160 nm generated in the gas cell was used as seed input signal for FEL.

Another seeding scheme is based on prebunching the e-beam by consecutive Harmonic Generation and High Gain amplification (HGHG) in wiggler structures, which has been demonstrated experimentally in the visible [25]. In both of these schemes, coherence is achieved if the coherent harmonic signal (of radiation or current modulation) is strong enough to significantly exceed SASE NEP (Noise Equivalent Power) which originates from shot noise.

Using the transfer matrix formulation (Eq. 3-39), it is possible to evaluate the coherent power generation in the high gain regime due to seed injection, and likewise evaluate the incoherent power generation due to noise (see equations 3-65 or 3-66) The comparison makes it possible to derive criteria for domination of the coherent power in the FEL emission.

Consider a general high gain FEL structure. Based on the coherent transfer matrix relation of an FEL in the linear regime (Eq. 3-39) and the FEL radiation power (Eq. 3-42), we obtain the solution of coherent radiation for radiation seed injection and for beam prebunching schemes respectively:

$$P(L_w,\omega) = P_q\left|\tilde{C}_q(L_w,\omega)\right|^2 = P_q\left|H^{EE}\right|^2\left|\tilde{C}_q(0,\omega)\right|^2$$

$$P(L_w,\omega) = P_q\left|\tilde{H}_{FEL}^{EI}(\omega)\tilde{i}(0) + \tilde{H}_{FEL}^{EV}(\omega)\tilde{V}(0)\right|^2$$

where $z = 0$ is the wiggler entrance plane and L_w is its length.

We now turn to calculate the incoherent (radiation - noise) output power of the FEL. We evaluate the spectral power density of incoherent radiation power (Eq. 3-58). It is convenient to define an incoherent radiation input (noise) effective

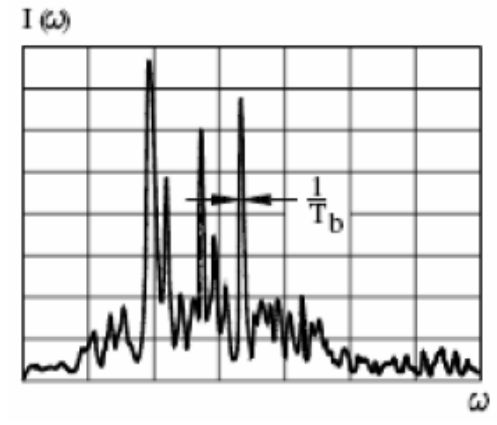

(a)

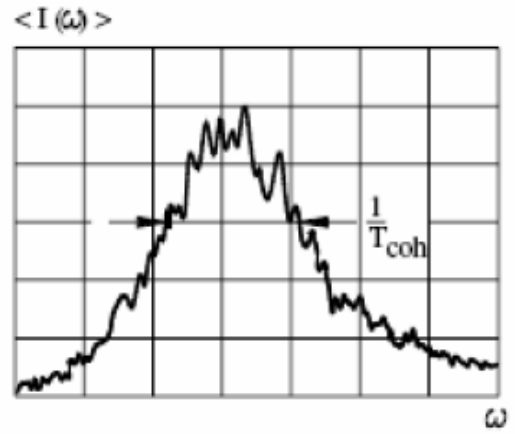

(b)

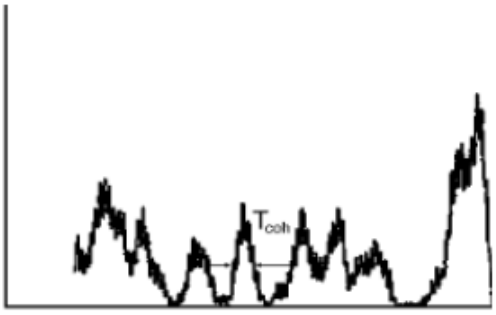

(c)

Figure 3-2 Simulation data of SASE radiative emission [95]: a) Single pulse spectral power, b) Spectral power averaged over many pulses , c) Time domain "Spiky" intensity distribution of a single pulse.

power (NEP), which lumps all effective incoherent input signal sources (the e-beam noise contributions due to random current, kinetic voltage and kinetic power and the EM-radiation noise at the FEL entrance plane):

$$\frac{dP_{NEP}}{d\omega}=\left(\frac{dP(L_w)}{d\omega}\right)_{incoh}\Big/\left|H^{EE}\right|^2 \qquad 3\text{-}67$$

where the total incoherent spectral power at the FEL output is given in equation 3-58.

In conventional FEL theory, it is customary to ignore any beam micro-dynamic process in the beam transport sections preceding the FEL, and assume that the velocity and current noises are not correlated. Therefore, for such a case, we apply marker "zero-length drift section before the wiggler" (L_d = 0). Substituting the classical expression for the uncorrelated spectral current shot noise (Eq. 2-113), velocity noise (Eq. 2-114) and kinetic power noise (Eq. 2-115), one obtains that the e-beam effective radiation input noise power is composed, in the conventional (uncorrelated) case, of four contributions:

$$\frac{dP_{NEP}}{d\omega}=\left(\frac{dP_{NEP}}{d\omega}\right)^{E}+\left(\frac{dP_{NEP}}{d\omega}\right)^{I}_{L_d=0}+\left(\frac{dP_{NEP}}{d\omega}\right)^{V}_{L_d=0}+\left(\frac{dP_{NEP}}{d\omega}\right)^{IV}_{L_d=0}$$

where $\left(\frac{dP_{NEP}}{d\omega}\right)^{E}$ is the ambient temperature blackbody radiation feeding the FEL input radiation mode (Eq. 3-59),

$$\left(\frac{dP_{NEP}}{d\omega}\right)^{I}_{L_d=0}=\frac{2P_q}{\pi}\left|\frac{H^{EI}}{G(\omega)}\right|^2\overline{\left|\breve{I}(0,\omega)\right|^2}=\frac{eI_0Z_q}{16\pi A_{em}}\left(\frac{a_w}{\gamma_0\beta_{0z}\Gamma}\right)^2 \qquad 3\text{-}68$$

$$\left(\frac{dP_{NEP}}{d\omega}\right)^{V}_{L_d=0}=\frac{2P_q}{\pi}\left|\frac{H^{EV}}{G(\omega)}\right|^2\overline{\left|\breve{V}(0,\omega)\right|^2}=\frac{Z_q}{16\pi A_{em}}\left(\frac{a_w}{\gamma_0\beta_{0z}}\frac{\theta_{prw}}{W_w}\frac{1}{\Gamma^2}\right)^2\left(\frac{mc^2}{e}\delta\gamma_{ef}\right)^2\frac{e}{I_0}=$$
$$=\left(\frac{\theta_{prw}}{\Gamma}\right)^2\left(\frac{mc^2\delta\gamma_{ef}}{eI_0W_w}\right)^2\left(\frac{dP_{NEP}}{d\omega}\right)^{I}_{L_d=0}=\left(\frac{\theta_{prw}}{\Gamma}\right)^2\left(\frac{W_d}{W_w}\right)^2N^2\left(\frac{dP_{NEP}}{d\omega}\right)^{I}_{L_d=0} \qquad 3\text{-}69$$

$$\left(\frac{dP_{NEP}}{d\omega}\right)^{IV}_{L_d=0}=\frac{2P_q}{\pi}\frac{2\,\mathrm{Re}\left(H^{EI}\left(H^{EV}\right)^*\right)}{G^2(\omega)}\overline{\breve{V}_z(0,\omega)\breve{I}^*(0,\omega)}=$$
$$=\frac{1}{16\pi}\frac{Z_q}{A_{em}}\left(\frac{a_w}{\gamma_0\beta_{0z}\Gamma}\right)^2\frac{\theta_{prw}}{\Gamma W_w}mc^2\delta\gamma_{ef}\frac{\delta\beta_{th}}{\beta_z}= \qquad 3\text{-}70$$
$$=\frac{\theta_{prw}}{\Gamma}\frac{mc^2\delta\gamma_{ef}}{eI_0W_w}\frac{\delta\beta_{th}}{\beta_{0z}}\left(\frac{dP_{NEP}}{d\omega}\right)^{I}_{L_d=0}=\frac{\delta\beta_{th}}{\beta_{0z}}\frac{\theta_{prw}}{\Gamma}\frac{W_d}{W_w}N\left(\frac{dP_{NEP}}{d\omega}\right)^{I}_{L_d=0}$$

If an FEL operates in the high gain cold tenuous beam regime ($\frac{\theta_{prw}}{\Gamma}<<1$) and the beam injected into the wiggler is shot-noise dominated:

$N^2 = \left(\frac{mc^2 \delta\gamma_{ef}}{eI_0 W_d} \right)^2 << 1$, the noise equivalent spectral power of the current noise (Eq. 3-68) dominants over that of the kinetic voltage noise (Eq. 3-69) and kinetic power (Eq. 3-70) (it is evident that $\frac{\delta\beta_{th}}{\beta_{0z}} << 1$):

$$\left(\frac{dP_{NEP}}{d\omega} \right)^{I}_{L_d=0} >> \left(\frac{dP_{NEP}}{d\omega} \right)^{V}_{L_d=0} >> \left(\frac{dP_{NEP}}{d\omega} \right)^{IV}_{L_d=0} \qquad 3\text{-}71$$

which means that the SASE power is determined in the common case by the beam current shot noise only, as is usually assumed in the literature [20].

To obtain a coherent output signal in an FEL amplifier (seed injected FEL), the input coherent signal power should exceed a threshold higher than the current noise NEP. Thus, with the assumptions of conventional FEL 1-D linear theory (all noise contributions except for current shot-noise are negligible), the input signal threshold conditions for attaining FEL coherence are:

$$P_{seed}(0) \left(= \left(\frac{dP}{d\omega} \right)_{seed} \Delta\omega_{seed} \right) >> \frac{eI_0 Z_q}{16\pi A_{em}} \left(\frac{a_w}{\gamma_0 \beta_{0z} \Gamma} \right)^2 \Delta\omega, \qquad 3\text{-}72$$

$$\left| \tilde{i}(0) \right|^2 >> eI_0 \Delta\omega \qquad 3\text{-}73$$

for seed radiation injection and e-beam prebunching schemes respectively. Here $\Delta\omega$ is the frequency bandwidth of the gain curve, ($\Delta\omega = \Delta\omega_{HG}$, see Eq. 3-46) if the entire spectral bandwidth of the SASE radiation is considered. If optical filtering can be employed to filter out the wideband without SASE radiation, then $\Delta\omega$ is the filter bandwidth. In a pulse of duration t_p , the bandwidth is Fourier transform limited: $\Delta\omega \approx \pi / t_p$. The noise power is determined by the smallest of this bandwidth.

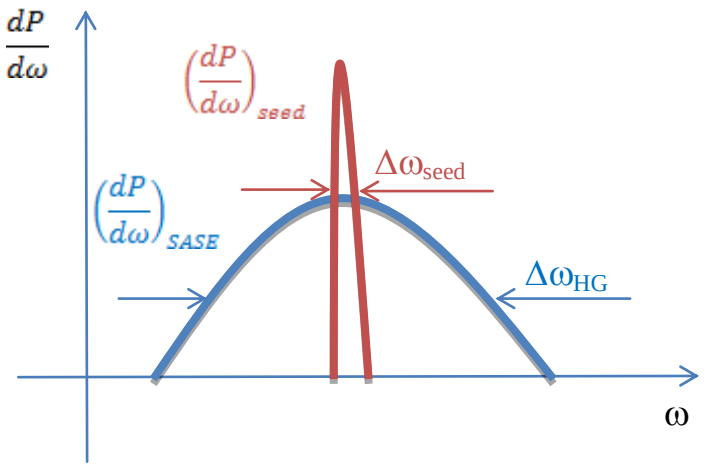

Figure 3-3 Comparing an FEL gain curve (blue curve) with the filtered seed injection signal (red curve).

4 The Coherence limits of FEL

In the previous chapter we evaluated the radiant emission power of FEL – both coherent and incoherent. In the linear regime, the coherent output power of an FEL amplifier is proportional to the coherent input power. The incoherent output power is proportional to the beam and radiation noise sources, which can be conveniently defined at the FEL input point $z = 0$ in terms of equivalent incoherent input power parameters (NEP). In this approach, the determination of whether the FEL radiation output is coherent, or the degree of its coherence, is made at its input. In general, the dominant input noise source of FELs is the current shot-noise. Therefore, according to conventional theory, the condition for FEL coherence is the requirement (in pre-bunched FELs) that the coherent beam prebunching current at the FEL input exceeds the classical current shot-noise (Eq. 3-73). In the case of seed radiation injection, the requirement is that the coherent radiation input power (seed injection) into the FEL exceeds the noise equivalent power (NEP) of the current shot-noise (Eq. 3-72).

In Chapter 2 we showed that the dominance of the current shot-noise over all other sources of noise is not an absolute physical limitation, and that it is possible to suppress it by proper control of the beam micro-dynamics in the transport line preceding the FEL wiggler. This means that by taking advantage of this process, the conditions for coherent output of the conventional theory for the injected coherent seed signal (Eqs. 3-73 and 3-74) can be relaxed. Alternatively, the degree of coherence of a seed injected FEL can be enhanced by controlling and suppressing the beam noise NEP.

Taking advantage of the formulations derived in Chapters 2 and 3, the goal in this chapter is to define the new limits of FEL coherence when the pre-injection microdynamics of the beam is controlled.

4.1 Electron beam microdynamic and radiation noise development in a system consisting of a drift section followed by a wiggler

We combine the analysis of the beam noise propagation from the cathode (or a general "I-V-independence plane" $z = z_c$) up to the wiggler entrance $z = 0$, and through the wiggler up to its end ($z = L_w$), together with the analysis of the incoherent radiation noise generation and propagation along the wiggler from its entrance ($z = 0$) to its end ($z = L_w$).

In our model, depicted in Figure 4-1, the system is composed of two sections: a drift section $z_c < z < 0$ of length L_d and a wiggler section $0 < z < L_w$ of length L_w. In principle, the first section could be composed of any of the electron optical elements that were treated in Chapter 2 (free drift, accelerator, dispersive sections). However, for the sake of simplicity, we assume here that this section is only a free drift section, but we allow the beam to propagate at different energies in the drift section (γ_{0d}) and the wiggler section (γ_0). This means that fast acceleration

sections, in which the collective micro-dynamics is frozen, may be incorporated right at the entrance to the drift section and at its end.

We define the electron beam parameters at the I-V no correlation point (z_c) by:

a) γ_{0c} - the start energy relativistic Lorenz factor,

b) δu_{0c} - the velocity distribution spread,

c) I_0 - the beam current.

d) A_e – the beam cross section area.

After acceleration, the electrons enter the drift section with an energy corresponding to a relativistic factor γ_{0d}. At the end of the drift section, the electrons are (optionally) accelerated again and are injected into the wiggler with an energy corresponding to a longitudinal relativistic Lorenz factor γ_{0z}. We assume that all other parameters of the set-up (such as the wiggler magnetic field, wiggler period and e-beam radius) are known.

Using these model definitions, all other parameters can be evaluated:

- At the I-V-independence plane - the kinetic voltage noise ($\overline{\left|\breve{V}(z_c)\right|^2}$, see Eq. 2-114), the current noise ($\overline{\left|\breve{I}(z_c)\right|^2}$, see Eq. 2-113), ($\theta_{pr}(z_c)$, see Eqs. 2-29 and 2-43),
- In the drift section - (θ_{prd}) and (W_d, see Eq. 2-67)
- In the wiggler - the plasma wave number (θ_{prw}, see Eq. 3-22), and the e-beam wave impedance (W_w, see Eq. 3-24).

The conditions for neglecting collective interaction microdynamics in the acceleration sections are:

$L_{acc}\theta_{pr}(z_c) << 1$ and $L_{acc}\theta_{pr}(L_d) << 1$.

$\theta_{pr}(z_c)L_{acc} < kA_e\theta_{pr}(z_c) < 1/\ \theta_{pr}(z_c)L_{acc}$

$\theta_{pr}(L_d)L_{acc} < kA_e\theta_{pr}(L_d) < 1/\ \theta_{pr}(L_d)L_{acc}$

Under these conditions, the transfer matrices of the acceleration sections may be represented by a unit matrix:

$$\mathbf{M}_{acc} = \begin{pmatrix} 1 & 0 \\ 0 & 1 \end{pmatrix}.$$

In order to find the complete transfer matrix of the combined system, we multiply the transfer matrix of the wiggler ($\tilde{\mathbf{H}}_{FEL}$) by that of the drift section ($\tilde{\mathbf{H}}_T$):

$$\tilde{\mathbf{H}}_{TOT} = \tilde{\mathbf{H}}_{FEL}\tilde{\mathbf{H}}_T \qquad 4\text{-}1$$

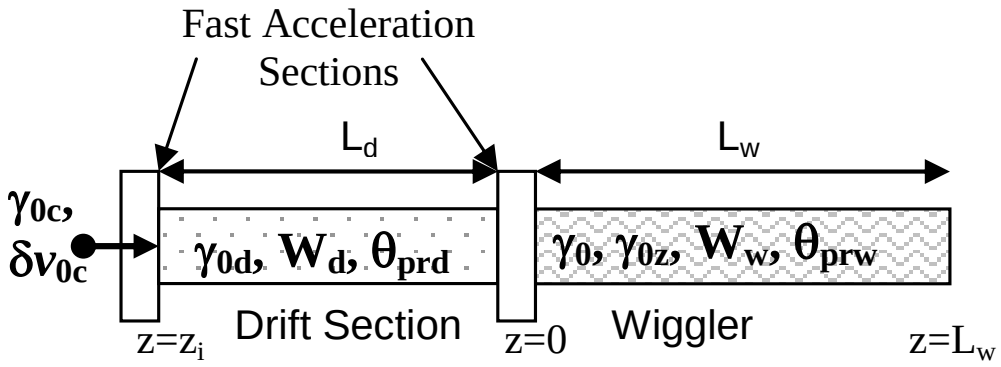

Figure 4-1 An FEL system composed of a free drift e-beam transport section and a radiating wiggler section.

where $\tilde{\mathbf{H}}_T$ is the general 3x3-transfer matrix of a non-dissipative drift section defined by:

$$\tilde{\mathbf{H}}_T = \begin{pmatrix} 1 & 0 & 0 \\ 0 & & \\ 0 & & \tilde{\mathbf{M}}_T \end{pmatrix} \qquad 4\text{-}2$$

where $\tilde{\underline{\underline{\mathbf{M}}}}_T$ is the 2x2 transfer matrix of a non-dissipative section (Eq. 2-68).

The total incoherent spectral power at the FEL output, described by equation 3-58, now becomes:

$$\left(\frac{dP(L_w,\omega)}{d\omega}\right) = \frac{2P_q}{\pi}\overline{\left|\breve{C}_q(L_w,\omega)\right|^2} = \frac{2P_q}{\pi}\left(\left|\tilde{H}_{FEL}^{TOT}\right|^2\overline{\left|\breve{C}_q(0)\right|^2} + \right.$$
$$\left|\tilde{H}_{TOT}^{EI}(\omega)\right|^2\overline{\left|\breve{i}(z_c)\right|^2} + \left|\tilde{H}_{TOT}^{EV}(\omega)\right|^2\overline{\left|\breve{V}(z_c)\right|^2} +$$
$$\left. + 2\,\mathrm{Re}\left(\tilde{H}_{TOT}^{EI}(\omega)\tilde{H}_{TOT}^{EV*}(\omega)\right)\mathrm{Re}\left(\overline{\breve{i}(z_c)\breve{V}^*(z_c)}\right) - 2\,\mathrm{Im}\left(\tilde{H}_{TOT}^{EI}(\omega)\tilde{H}_{TOT}^{EV*}(\omega)\right)\mathrm{Re}\left(\overline{\breve{i}(z_c)\breve{V}^*(z_c)}\right)\right)$$

4-3

In our previous analysis of noise dynamics in a drifting electron beam (see Sect. 2.3.2), we showed, based on equation 2-117, that for a drift distance

$$L_d = \pi/2\theta_{pr} \qquad 4\text{-}4$$

the initial beam velocity noise transforms into current noise and vice versa:

$$\overline{\left|\breve{i}(L_d)\right|^2} = \overline{\left|\breve{V}(z_c)\right|^2}\Big/W_d^2 \qquad 4\text{-}5$$

$$\overline{\left|\breve{V}(L_d)\right|^2} = W_d^2\overline{\left|\breve{i}(z_c)\right|^2} \qquad 4\text{-}6$$

As indicated earlier, usually the noise of a high quality relativistic electron beam, used in FELs, is dominated by current shot-noise. Namely:

$$N^2 << 1 \qquad 4\text{-}7$$

where we defined the noise dominance parameter N:

$$N^2 \equiv \frac{\overline{\left|\breve{V}(z_c)\right|^2}}{W_d^2\overline{\left|\breve{i}(z_c)\right|^2}};$$

For this case, the current shot noise in a uniformly transported beam, drifting a quarter plasma wavelength oscillation length (Eq. 4-4), is reduced by a factor N^2. Since in a conventional SASE FEL, the radiation power is dominated by the input current shot-noise, a scheme such as in Figure 4-1 with quarter plasma oscillation drift length (Eq. 4-4) might have been expected to enable maximal suppression of the SASE radiation noise power. However, since there is continued beam noise evolution dynamics also within the FEL interaction region, it is necessary to solve the problem of noise evolution in the entire system consisting of the beam transport section and the wiggler. The combined system analysis should

result in a more accurate expression for radiation noise suppression and for the optimal drift length for SASE noise output minimization.

As in Chapter 3-5, it is convenient to compare and analyze the noise level at the wiggler entrance point ($z = 0$) by defining a total beam-noise equivalent power (NEP) at the entrance to the wiggler as:

$$\frac{dP_{NEP}}{d\omega} = \left(\frac{dP(L_w, \omega)}{d\omega} \right) \Big/ G \qquad 4\text{-}8$$

Using equation 4-3, this NEP is composed of all e-beam shot-noise contributions (current, velocity and kinetic power), to which we add radiation input noise that originates from quantum spontaneous emission, and the ambient temperature black-body radiation at the FEL entrance plane (similarly to previous Section 3.4). This modeling of the incoherent and coherent input power source of the FEL is illustrated by Figure 4-2

$$\frac{dP_{NEP}}{d\omega} = \left(\frac{dP_{NEP}}{d\omega} \right)^{E} + \left(\frac{dP_{NEP}}{d\omega} \right)^{I} + \left(\frac{dP_{NEP}}{d\omega} \right)^{V} + \left(\frac{dP_{NEP}}{d\omega} \right)^{IV} \qquad 4\text{-}9$$

The explicit expressions of the last three (beam noise NEP) terms in the absence of a drift section were derived in the previous section (Eqs. 3-69 - 3-70). We now show that by proper control of the e-beam plasma dynamics in the non-radiative (drift) section of the transport line, it is possible to control the contributions of the different beam noise sources to the NEP, and specifically to reduce the current noise contribution (normally dominant) so that the total incoherent SASE power of the FEL would be suppressed.

Taking into account the drift section micro-dynamics by using Eqs. 4-3 and 4-8, the drift section modified NEPs of the current noise, velocity noise and kinetic power noise at the wiggler input can be written then in terms of the corresponding conventional (no drift section) NEPs (Eqs. 3-69 - 3-71) in a compact way (see Appendix 5.10):

$$\left(\frac{dP_{NEP}(L_d)}{d\omega} \right)^{I} = \left(\frac{dP_{NEP}}{d\omega} \right)^{I}_{L_d=0} \left| \cos(\phi_{prd}) - S \exp\left(-i\frac{\pi}{6} \right) \sin(\phi_{prd}) \right|^2 \qquad 4\text{-}10$$

$$\left(\frac{dP_{NEP}(L_d)}{d\omega} \right)^{V} = \left(\frac{dP_{NEP}}{d\omega} \right)^{V}_{L_d=0} \left| \cos(\phi_{prd}) + \frac{1}{S} \sin(\phi_{prd}) \exp\left(i\frac{\pi}{6} \right) \right|^2 \qquad 4\text{-}11$$

$$\left(\frac{dP_{NEP}(L_d)}{d\omega} \right)^{IV} = \left(\frac{dP_{NEP}}{d\omega} \right)^{IV}_{L_d=0} \cos(2\phi_{prd}) \qquad 4\text{-}12$$

Here $\phi_{prd} = \theta_{prd} L_d$ is the plasma phase in the free drift section and the noise suppression parameter S is:

$$S = \frac{W_d \theta_{prw}}{W_w \Gamma} \qquad 4\text{-}13$$

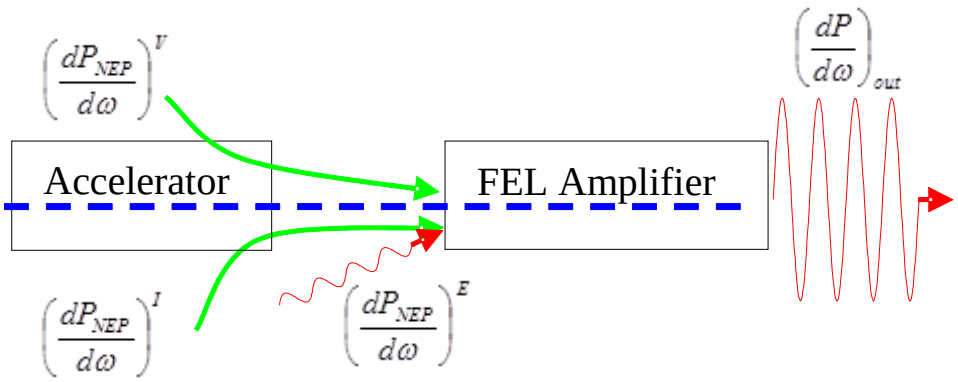

Figure 4-2 Scheme of different noise sources for radiation in Free Electron Laser.

It can be seen that Eqs. 4-10 – 4-11 reduce to the original Eqs. 3-69 – 3-70 in the limit $\phi_{prd} = 0$.

Equations 4-10 and 4-11 are rewritten as:

$$\left(\frac{dP_{NEP}(L_d)}{d\omega}\right)^I = \left(\frac{dP_{NEP}}{d\omega}\right)^I_{L_d=0}\left(\frac{1+S^2}{2} + \frac{1-S^2}{2}\cos(2\phi_{prd}) - \frac{\sqrt{3}S}{2}\sin(2\phi_{prd})\right) =$$
$$= \left(\frac{dP_{NEP}}{d\omega}\right)^I_{L_d=0}\frac{1}{2}\left(1+S^2+\sqrt{1+S^2+S^4}\cos(2\phi_{prd}+\varphi)\right) \qquad 4\text{-}14$$

$$\left(\frac{dP_{NEP}(L_d)}{d\omega}\right)^V = \left(\frac{dP_{NEP}}{d\omega}\right)^V_{L_d=0}\frac{1}{2S^2}\left(1+S^2-\left[\left(1-S^2\right)\cos(2\phi_{prd}) - \sqrt{3}S\sin(2\phi_{prd})\right]\right) =$$
$$= \left(\frac{dP_{NEP}}{d\omega}\right)^V_{L_d=0}\frac{1}{2S^2}\left(1+S^2-\sqrt{1+S^2+S^4}\cos(2\phi_{prd}+\varphi)\right) \qquad 4\text{-}15$$

where we defined $\varphi(S)$ by $\cos\varphi = \left(\frac{1-S^2}{\sqrt{1+S^2+S^4}}\right)$ and $\sin\varphi = \left(\frac{\sqrt{3}S}{\sqrt{1+S^2+S^4}}\right)$.

By inspection of 4-14, we observe that the current NEP obtains its minimum when the plasma phase accumulated in the drift section is:

$$\phi_{prd} = \frac{\pi}{2} - \frac{\varphi(S)}{2} \qquad 4\text{-}16$$

Note that this is a different condition from the condition required to attain minimum current noise at the end of the drift section ($\phi_{prd} = \pi/2$). However, in the most common case, we may assume that $W_d \le W_w$ and that the FEL operates in the high gain tenuous beam limit ($\theta_{prw} << \Gamma$). Consequently, the parameter S (Eq. 4-13) satisfied the condition $S << 1$, and first order expansion of $\varphi(S)$ results in that the plasma phase condition for minimum current NEP is:

$$\phi_{prd} = \frac{\pi}{2} - \frac{\sqrt{3}}{2}S \qquad 4\text{-}17$$

Namely, this is slightly below the point of minimum current noise at the end of the drift section.

Letting S still attain any value, substitution of the minimal NEP phase (Eq. 4-16) in equation 4–14 gives the expression for the minimum attainable current NEP:

$$\left(\frac{dP_{NEP}(L_d)}{d\omega}\right)^I = \left(\frac{dP_{NEP}}{d\omega}\right)^I_{L_d=0}\frac{1}{2}\left(1+S^2-\sqrt{1+S^2+S^4}\right) \qquad 4\text{-}18$$

However, note that at the same time the input radiation power originating from the velocity noise (the kinetic voltage NEP, see Eq. 4-15) attains a maximum value:

$$\left(\frac{dP_{NEP}(L_d)}{d\omega}\right)^V = \left(\frac{dP_{NEP}}{d\omega}\right)^V_{L_d=0} \frac{1}{2S^2}\left(1+S^2+\sqrt{1+S^2+S^4}\right) \qquad 4\text{-}19$$

The interesting question is: What is the minimum of the total NEP attainable when one considers both current noise and velocity noise contributions? To answer this question, we look into the sum of these two contributions (Eq. 4-14 and Eq. 4-15). Taking into account the relation 3-69, we obtain:

$$\frac{dP_{NEP}}{d\omega} = \frac{1}{2}\left(\frac{dP_{NEP}}{d\omega}\right)^I_{L_d=0}\left[\left(1+S^2+\sqrt{1+S^2+S^4}\cos(2\phi_{prd}+\varphi)\right)+\right.$$
$$\left.+N^2\left(1+S^2-\sqrt{1+S^2+S^4}\cos(2\phi_{prd}+\varphi)\right)\right]$$

This can be rewritten as:

$$\frac{dP_{NEP}}{d\omega} = \frac{1}{2}\left(\frac{dP_{NEP}}{d\omega}\right)^I_{L_d=0}\left(\left(1+S^2\right)\left(1+N^2\right)+\left(1-N^2\right)\sqrt{1+S^2+S^4}\cos(2\phi_{prd}+\varphi)\right) \qquad 4\text{-}20$$

Evidently, this result indicates that also the total NEP attains it minimum at the condition 4-16 and is given by:

$$\frac{dP_{NEP}}{d\omega} = \frac{1}{2}\left(\frac{dP_{NEP}}{d\omega}\right)^I_{L_d=0}\left(\left(1+S^2\right)\left(1+N^2\right)-\left(1-N^2\right)\sqrt{1+S^2+S^4}\right)$$

In the case of interest of SASE noise suppression, one may always assume $N, S << 1$, and this expression simplifies to a very compact and useful expression for the minimum spectral NEP that can be attainable with our proposed scheme:

$$\frac{dP_{NEP}}{d\omega} = \left(\left(\frac{S}{2}\right)^2+N^2\right)\left(\frac{dP_{NEP}}{d\omega}\right)^I_{L_d=0} \qquad 4\text{-}21$$

The first term in this equation is the contribution to the NEP due to the initial current shot-noise, as can be verified directly from Eq. 4-18 in the limit $S << 1$:

$$\left(\frac{dP_{NEP}(L_d)}{d\omega}\right)^I \approx \frac{1}{2}\left(1+S^2-\left(1+\frac{S^2}{2}\right)\right)\left(\frac{dP_{NEP}}{d\omega}\right)^I_{L_d=0} = \left(\frac{S}{2}\right)^2\left(\frac{dP_{NEP}}{d\omega}\right)^I_{L_d=0} \qquad 4\text{-}22$$

The second term in Eq. 4-21 is the contribution to NEP due to the initial velocity noise, as can be verified by taking Eq. 4-19 into the same limit:

$$\left(\frac{dP_{NEP}(L_d)}{d\omega}\right)^V \approx \frac{1}{S^2}\left(\frac{dP_{NEP}}{d\omega}\right)^V_{L_d=0} = N^2\left(\frac{dP_{NEP}}{d\omega}\right)^I_{L_d=0} \qquad 4\text{-}23$$

where the second part of the equation results from the relation 3-69: $\left(\frac{dP_{NEP}}{d\omega}\right)^V_{L_d=0} = S^2N^2\left(\frac{dP_{NEP}}{d\omega}\right)^I_{L_d=0}$

Note that we have neglected the kinetic power NEP (Eq. 4-12 and 3-71) which is negligible for any practical case. The radiation NEP contribution will be considered in a subsequent subsection (4.1.3).

4.1.1 Suppressed radiation power still limited by shot-noise

Since both inequalities $N << 1$ and $S << 1$ are valid, we need to examine separately two cases. If $N << S/2$, we have from equation 4-21 that the total NEP is:

$$\frac{dP_{NEP}}{d\omega} = \left(\frac{S}{2}\right)^2 \left(\frac{dP_{NEP}}{d\omega}\right)^I_{L_d=0} \qquad 4\text{-}24$$

and it means that the total NEP is still limited by the current noise, but is suppressed by a factor $(S/2)^2 << 1$. Its explicit expression (substituting Eqs. 2-122 and 3-69) is:

$$\frac{dP_{NEP}}{d\omega} \approx \left(\frac{dP_{NEP}}{d\omega}\right)^I_{L_d=0} \frac{S^2}{4} = \frac{eI_0 Z_q}{64\pi A_{em}} \left(\frac{a_w}{\gamma_0 \beta_z \Gamma}\right)^2 \left(\frac{W_d}{W_w} \frac{\theta_{prw}}{\Gamma}\right)^2 \qquad 4\text{-}25$$

Note that from 4-24, it seems that it is desirable to decrease the parameter S (for example by operating with small beam energy in the drift section). However, there is limit to the benefit of decreasing S when we exceed the condition $N << S/2$. At this point, the second term in equation 4-21 becomes dominant.

4.1.2 Suppressed radiation power limited by velocity noise

In the case $N >> S/2$, the contribution of the initial velocity noise becomes dominant over the current shot-noise contribution, because of the velocity noise taking place enhancement (gain) by dynamics in the drift section:

$$\left(\frac{dP_{NEP}(L_d)}{d\omega}\right)^V >> \left(\frac{dP_{NEP}(L_d)}{d\omega}\right)^I \qquad 4\text{-}26$$

The total NEP is then (from Eq. 4-21)

$$\frac{dP_{NEP}}{d\omega} = N^2 \left(\frac{dP_{NEP}}{d\omega}\right)^I_{L_d=0}$$

Note that also in this case the total NEP is suppressed relative to the conventional SASE radiation power, but by a factor $N^2 << 1$ (see Eq. 4-7). After substitutions, we find that the effective input radiation noise of the FEL in this case is determined by the initial beam axial velocity spread (and *not* by its shot-noise):

$$\frac{dP_{NEP}}{d\omega} = \left(\frac{mc^2 \gamma_0 \gamma_{0z}^2 \beta_0 \delta\beta_z}{eW_d}\right)^2 \frac{eZ_q}{I_0 16\pi A_{em}} \left(\frac{a_w}{\gamma_0 \beta_{0z} \Gamma}\right)^2 \qquad 4\text{-}27$$

Note that the spread of the axial velocities $\delta\beta_z$ may be caused by energy spread (then $\gamma_0 \gamma_{0z}^2 \beta_0 \delta\beta_z = \Delta\gamma$) or (and)by emittance (then $\delta\beta_z = \frac{\beta_{0z}}{2}\left(\frac{\varepsilon_n}{\gamma_{0z} r_b}\right)^2$).

If conditions for this case are satisfied, the effective incoherent input power is limited by the beam longitudinal velocity noise (namely, by its energy spread and emittance). The suppressed noise level limited by axial velocity spread may be realized with present-day accelerator parameters at optical frequencies. Extension to the UV and soft X-ray regime is plausible, but may require further technological improvement of beam quality parameters.

4.1.3 The radiation quantum noise limit of FEL

The Bose-Einstein radiation input noise term (3-59) assumes the value $k_B T_A$ at low frequencies, up to the THz regime (for an ambient temperature of $T_A = 300^{o}$K). At higher frequencies, it results in a radiation quantum noise limit expression:

$$\left(\frac{dP_{NEP}}{d\omega}\right)^{E} = \hbar\omega \qquad (4\text{-}28)$$

In the high (X-UV) frequency regime, this term can be quite large. Yet it has never been expected that FEL coherence may be governed by this quantum limit, and the fundamental FEL coherence limit has been considered always to be the current shot-noise. Theoretically, at high enough frequencies, the quantum radiation input noise (4-29) can become dominant over the electron beam NEP terms (4-21):

$$\hbar\omega >> \left(\frac{dP_{NEP}}{d\omega}\right)^{I} + \left(\frac{dP_{NEP}}{d\omega}\right)^{V}$$

and the FEL coherence becomes quantum-noise limited. With the present-day state of the art of accelerator technology, it is still early to predict if this limit can be attained.

*In all of these cases, the seed radiation coherence condition (*Eq. 3-72*) is relaxed:*

$$P_{seed}(0) = \left(\frac{dP}{d\omega}\right)_{seed} \Delta\omega_{seed} >> \frac{dP_{NEP}(L_d)}{d\omega}\Delta\omega,$$

where the suppressed NEP power on the right hand side is given by (4-21), (4-25), (4-27) or (4-28). The degree of temporal coherence of the FEL is then determined by the strength of the inequality.

4.2 Conclusions

The conditions for coherent operation of seeded high gain FELs and for operation of FELs with coherence beyond the shot-noise limit were derived. The analysis is based on a single Langmuir mode fluid plasma linear response theory of the electron beam employed in the wiggler and in a drift section preceding the wiggler.

We obtained a new expression for the low limit of the suppressed beam-noise radiation equivalent input power (NEP) of FEL. The incoherent radiation (SASE power) can be reduced by the sum of two factors, both much smaller than one. One factor is $(S/2)^2$, which is always less than 1 for any high gain FEL operating in the tenuous beam regime. The other factor is N^2 , which satisfied the condition $N^2 << 1$ when the accelerated beam is cold enough and is shot-noise dominated (which is the case in most high quality accelerated beams used for FEL). If the first factor is dominant, the reduced SASE power is still limited by the residual suppressed current shot-noise contribution. In the opposite case, the reduced SASE power is limited by the beam initial energy spread.

In practice, a variety of effects may limit the validity of our model and may impede the attainment of the theoretically predicted coherence limits. E-beam instabilities and aberrations in the accelerator and in electron-optical components, electron Coulomb collisions (at low energies - the Boersch effect [96]), and wake-field interactions along the transport line, may increase the electron axial velocity spread, and may interfere with the plasma wave oscillation process. Excitation of multiple transverse (Langmuir) plasma waves may also make it difficult to control the SASE noise power with a single parameter ϕ_p. As discussed in [28], a single transverse mode Langmuir plasma wave may be attained by proper design of the drift section parameters. Furthermore, a 3-D Vlasov equation analysis indicates that higher order transverse plasma waves may be damped due to transverse Landau damping [64]. However, in any practical operating regime, it is necessary to verify that electron-optical and beam transport imperfections do not corrupt the collective noise suppression process in the drift section, and that 3D effects do not overshadow the process [29].

At present, noise suppression has been demonstrated already at optical frequencies in two independent experiments by our group [31], and by LCLS/SLAC [97]. With the present state of the art, it may be difficult to attain optical current shot-noise suppression at short wavelength (X-UV), and to use it to enhance the coherence of *seed radiation* injected FELs at these frequencies. However, in *prebunching* schemes, such as HGHG, the noise suppression scheme may be effective even at such short wavelengths, since the main contribution to the high frequency shot-noise in this case is due to harmonic generation and high gain amplification of the shot-noise at the fundamental harmonic frequency in the optical regime, where shot-noise suppression seems feasible.

We conclude that theoretical considerations predict the possibility of very high coherence and *spectral* brightness of FELs operating at optical frequencies. Coherence enhancement may possibly also be attained in the future in X-UV FELs,

though there is still controversy over the attainable short wavelength limit [98]. Appropriate design and technological improvements of the non-radiating sections of the FEL transport line can provide control and reduction of shot noise power in SASE. If coherence beyond the current shot-noise limit is attained, the FEL coherence will be limited by the beam velocity noise determined by its (slice) energy spread. The ultimate coherence limit of FELs is the *quantum noise limit*. It is theoretically attainable at X-UV frequencies, but its attainment is dependent on progress in the technological state of the art, which at present has not yet been reached. However, the identification of this limit will serve at present as a fundamental limit yard-stick of progress, similar to the Schawlow-Townes limit for atomic laser oscillators [17].

Appendices

1. Vlasov equation

In this appendix we present a derivation of the Vlasov kinetic equation. It is well-known that the Vlasov equation describes a system's evolution based on a single particle distribution function. Here we demonstrate a procedure: how we can simplify a description of charged multi-particle systems and mention all assumptions which had been made.

The kinetic description of a charged particle system is used for many areas of science. For example, the next formalism was presented in [99].

A system of charged particles may be described in phase space by canonical space (**r**) and momentum (**p**) coordinates of the *i* particles ($\mathbf{r_i}$ and $\mathbf{p_i}$ correspondingly) with the help of the probability density function $D(\mathbf{r_1},\ldots, \mathbf{r_{Ne}}, \mathbf{p_1},\ldots, \mathbf{p_{Ne}}, t)$ (N_e is the total number of particles in the system). Thus $D\mathrm{d}\mathbf{r_1},\ldots,\mathrm{d}\mathbf{r_{Ne}},\mathrm{d}\mathbf{p_1},\ldots, \mathrm{d}\mathbf{p_{Ne}}$ is a probability that at the time *t* the particles are in a volume element $dV = \mathrm{d}\mathbf{r_1},\ldots,\mathrm{d}\mathbf{r_{Ne}},\mathrm{d}\mathbf{p_1},\ldots,\mathrm{d}\mathbf{p_{Ne}}$

Here we assume a statistical ensemble of identical systems (identical in the sense of dynamic characteristics). Of course, the probability density has been normalized:

$$\int_{-\infty}^{\infty} D(\mathbf{r}_1,\ldots,\mathbf{r}_{Ne},\mathbf{p}_1,\ldots,\mathbf{p}_{Ne},t)d\mathbf{r}_1,\ldots,\mathbf{r}_{Ne},\mathbf{p}_1,\ldots,\mathbf{p}_{Ne} = 1$$

Liouville's theorem tells us that the probability density function satisfies a continuity equation in phase space:

$$\left(\frac{\partial}{\partial t} + \sum_{i=1}^{Ne} \frac{\partial}{\partial \mathbf{r}_i}\dot{\mathbf{r}}_i\right) D = 0 \qquad \text{A0-1}$$

Here it must be reminded that the phase space formulation is based on canonical coordinates and momentum of charged particles. Therefore, the motion of each particle may be described by the Hamilton equation:

$$\dot{\mathbf{r}}_i = \frac{\partial H}{\partial \mathbf{p}_i}$$

$$\dot{\mathbf{p}}_i = -\frac{\partial H}{\partial \mathbf{r}_i}$$

where *H* is the Hamiltonian of the charged particle system and it takes into account both external electromagnetic fields and the fields of the charged particles in the system:

$$H = \sum_{i=1}^{Ne}\left(\frac{p_i^2}{2m_i} + q_i\varphi(\mathbf{r}_i, t)\right) + \frac{1}{2}\sum_{i\neq i'}^{Ne}\left(\frac{q_i q_{i'}}{4\pi\varepsilon_0|\mathbf{r}_i - \mathbf{r}_{i'}|}\right)$$

Based on this, the continuity equation A0-1 for the probability density function may be modified to:

$$\frac{\partial}{\partial t}D + \{H, D\} = 0 \qquad \text{A0-2}$$

where $\{H, D\} = \sum_{i=1}^{Ne}\left(\frac{\partial H}{\partial \mathbf{p}_i}\cdot\frac{\partial D}{\partial \mathbf{r}_i} - \frac{\partial H}{\partial \mathbf{r}_i}\cdot\frac{\partial D}{\partial \mathbf{p}_i}\right)$ are the Poison brackets.

Evidently, this is a full detailed microscopic description of a system with a large number of particles. In practice, the system may be described with fewer details. We can use information about the motion of one particle (or some number). It is given by a single particle distribution function f_1:

$$f_1(\mathbf{r}_1, \mathbf{p}_1, t) = N_e\int_{-\infty}^{\infty} D(\mathbf{r}_1, \ldots, \mathbf{r}_{Ne}, \mathbf{p}_1, \ldots, \mathbf{p}_{Ne}, t)d\mathbf{r}_2, \ldots, \mathbf{r}_{Ne}, \mathbf{p}_2, \ldots, \mathbf{p}_{Ne}$$

or multi-particle distribution function:

$$f_s(\mathbf{r}_1, \ldots, \mathbf{r}_s, \mathbf{p}_1, \ldots, \mathbf{p}_s, t) = (N_e)^s\int_{-\infty}^{\infty} D(\mathbf{r}_1, \ldots, \mathbf{r}_{Ne}, \mathbf{p}_1, \ldots, \mathbf{p}_{Ne}, t)d\mathbf{r}_{s+1}, \ldots, \mathbf{r}_{Ne}, \mathbf{p}_{s+1}, \ldots, \mathbf{p}_{Ne}$$

Note: in these equations the subscript near the coordinate (**r** or **p**) shows the number of a particle in the system (particles in the system are numbered arbitrarily), the subscript near the particle distribution function (*f*) shows the total number of particles which we use for the system description.

Now we can integrate the continuity equation (Eq. A0-2) with respect to variables $\mathbf{r}_{s+1},\ldots,\mathbf{r}_{Ne},\mathbf{p}_{s+1},\ldots,\mathbf{p}_{Ne}$. Finally, according to the definition of the multi-particle distribution function:

$$\frac{\partial f_s}{\partial t} + (N_e)^s\sum_{i=1}^{Ne}\int_{-\infty}^{\infty}\{H_i, D\}d\mathbf{r}_{s+1}, \ldots, \mathbf{r}_{Ne}, \mathbf{p}_{s+1}, \ldots, \mathbf{p}_{Ne} +$$

$$+ (N_e)^s\sum_{1\leq i<i'\leq Ne}\int_{-\infty}^{\infty}\{\varphi_{i,i'}, D\}d\mathbf{r}_{s+1}, \ldots, \mathbf{r}_{Ne}, \mathbf{p}_{s+1}, \ldots, \mathbf{p}_{Ne} = 0$$

where

$$\varphi_{i,i'} = \frac{q_i q_{i'}}{4\pi\varepsilon_0|\mathbf{r}_i - \mathbf{r}_{i'}|} \qquad \text{A0-3}$$

is the energy of interaction between *i*-th and *i'*-th particles in the system. Taking into account $\int \{\mathrm{H}_i D\} d\mathbf{r}_i = 0$ and $\int_{-\infty}^{\infty} \{\varphi_{i,i'} D\} d\mathbf{r}_i, d\mathbf{r}_{i'}, d\mathbf{p}_i, d\mathbf{p}_{i'} = 0$, we get:

$$\frac{\partial f_s}{\partial t} + \sum_{i=1}^{s} \int_{-\infty}^{\infty} \{H_i, f_s\} + \sum_{1 \le i < i' \le Ne} \int_{-\infty}^{\infty} \{\varphi_{i,i'}, f_s\} + \sum_{i=1}^{s} \int_{-\infty}^{\infty} \{\varphi_{i,s+1}, f_{s+1}\} d\mathbf{r}_{s+1} d\mathbf{p}_{s+1} = 0$$

It is a set of integral-differential equations which links the multi-particle distribution function f_s to f_{s+1}. This set is named BBGKY hierarchy (Bogolubov [100], Born [101], Green [101], Kirkwood [102], Yvon [103]).

If the Coulomb interaction between any two particles has long range character (a free path length is larger than the distance between particles), then the two-particle distribution function can be represented as the product of two single-particle distribution function:

$f_2(\mathbf{r}_1,\mathbf{r}_2,\mathbf{p}_1,\mathbf{p}_2) = f_1(\mathbf{r}_1,\mathbf{p}_1)*\mathrm{f}_1(\mathbf{r}_2,\mathbf{p}_2)$.

Substituting this relation into the first equation of the BBGKY hierarchy gives us the kinetic Vlasov equation [104]:

$$\left(\frac{\partial}{\partial t} + \mathbf{v}_1 \frac{\partial}{\partial \mathbf{r}_1} + q(\mathbf{E}_{ext} + \mathbf{v}_1 \times \mathbf{B}_{ext}) \frac{\partial}{\partial \mathbf{p}_1} - \int_{-\infty}^{\infty} \frac{1}{4\pi\varepsilon_0} \frac{\partial}{\partial \mathbf{r}_1} \frac{q^2}{|\mathbf{r}_1 - \mathbf{r}'|} f_1(\mathbf{r}', \mathbf{p}') d\mathbf{r}' d\mathbf{p}' \frac{\partial}{\partial \mathbf{p}_1} \right) f_1(\mathbf{r}_1, \mathbf{p}_1) = 0 \qquad \text{A0-4}$$

where $\mathbf{E}_{\mathrm{ext}}$ and $\mathbf{B}_{\mathrm{ext}}$ are the external electric and the magnetic fields respectively (sources of these fields do not depend on the motion of the charged particles).

We define a space charge density of the system $\rho_{self}(\mathbf{r},t)$ and a charged particle current density $\mathbf{J}_{\mathrm{self}}(\mathbf{r},t)$ as:

$$\rho_{self}(\mathbf{r},t) = q \int_{-\infty}^{\infty} f_1(\mathbf{r},\mathbf{p},t) d\mathbf{p} \qquad \text{A0-5}$$

$$J_{self}(\mathbf{r},t) = q \int_{-\infty}^{\infty} \mathbf{v} f_1(\mathbf{r},\mathbf{p},t) d\mathbf{p} \qquad \text{A0-6}$$

Thus, based on Gauss's law in integral form [105]:

$$\mathbf{E}_{self} = -\frac{1}{4\pi\varepsilon_0} \int_{-\infty}^{\infty} \frac{\partial}{\partial \mathbf{r}} \frac{\rho_{self}(\mathbf{r}')}{|\mathbf{r} - \mathbf{r}'|} d\mathbf{r}',$$

the integral term in the Vlasov equation (A0-4) has a similar physical interpretation: this is an electric field which is produced by the system of charged particles. This field is named the self-field (or space-charge field). The evolution of the single particle distribution function depends on the electric field which is defined by this distribution function. Note, the interaction between particles is represented only by an electric reciprocity (A0-3), whilst the magnetic one is ignored, thus in the obtained form of the kinetic Vlasov equation (A0-4), only the self electric field is presented.

It means that the kinetic Vlasov equation and Maxwell's equations are the full set of equations for a description of electron motion. In the case when the charged particles move in a space free from external charges and currents, we obtain:

$$\left(\frac{\partial}{\partial t}+\mathbf{v}\frac{\partial}{\partial \mathbf{r}}+q(\mathbf{E}_{tot}+\mathbf{v}\times\mathbf{B}_{tot})\frac{\partial}{\partial \mathbf{p}}\right)f_1(\mathbf{r},\mathbf{p})=0 \qquad \text{A0-7}$$

where $\mathbf{E}_{\text{tot}}$ and $\mathbf{B}_{\text{tot}}$ are the total (sum of the external and the self fields) electric and magnetic fields respectively and defined by:

$$\operatorname{div}\mathbf{E}_{tot}=\frac{\rho_{self}}{\varepsilon_0}$$

$$\operatorname{rot}\mathbf{E}_{tot}=-\frac{\partial\mathbf{B}_{tot}}{\partial t}$$

$$\operatorname{div}\mathbf{B}_{tot}=0$$

$$\operatorname{rot}\mathbf{B}_{tot}=\mu_0\mathbf{J}_{self}+\varepsilon_0\mu_0\frac{\partial\mathbf{E}_{tot}}{\partial t}$$

2. Transformation from the kinetic equation to the moment equation

Instead of a distribution function, the evolution of the system of charged particles may be described by the evolution of its moments: the current density $\mathbf{J}_{\text{self}}(\mathbf{r},t)$ (Eq. A0-6), the density of charged particles $n(\mathbf{r},t)$ and the average velocity $\mathbf{u}$:

$$n(\mathbf{r},t)=\frac{\rho_{self}(\mathbf{r},t)}{q}=\int_{-\infty}^{\infty} f_1(\mathbf{r},\mathbf{p},t)d\mathbf{p} \qquad \text{A0-8}$$

$$\mathbf{u}(\mathbf{r},t)=\int_{-\infty}^{\infty}\frac{\mathbf{v}f_1(\mathbf{r},\mathbf{p},t)}{n(\mathbf{r},t)}d\mathbf{p} \qquad \text{A0-9}$$

It is evident that we may choose as independent functions only two out of the three moments of the distribution function. The third moment is defined from:

$$\mathbf{J}(\mathbf{r},t)=qn(\mathbf{r},t)\mathbf{u}(\mathbf{r},t)$$

Integrating the kinetic Vlasov equation (Eq. A0-7) with respect to momentum $\mathbf{p}$, we obtain the zero-moment of the kinetic equation:

$$\frac{\partial}{\partial t}\int_{-\infty}^{\infty} f_1(\mathbf{r},\mathbf{p},t)d\mathbf{p}+\frac{\partial}{\partial \mathbf{r}}\int_{-\infty}^{\infty}\mathbf{v}f_1(\mathbf{r},\mathbf{p},t)d\mathbf{p}+q\int_{-\infty}^{\infty}(\mathbf{E}_{tot}+\mathbf{v}\times\mathbf{B}_{tot})\frac{\partial}{\partial \mathbf{p}}f_1(\mathbf{r},\mathbf{p},t)d\mathbf{p}=0 \qquad \text{A0-10}$$

Or, using the definitions A0-8 and A0-9 and taking into account that:

$$\int_{-\infty}^{\infty}(\mathbf{E}_{tot}+\mathbf{v}\times\mathbf{B}_{tot})\frac{\partial}{\partial \mathbf{p}}f_1(\mathbf{r},\mathbf{p},t)d^3\mathbf{p}=\mathbf{E}_{tot}\int_S f_1(\mathbf{r},\mathbf{p},t)d^2\mathbf{S}_p-\int_{-\infty}^{\infty}f_1(\mathbf{r},\mathbf{p},t)\frac{\partial}{\partial \mathbf{p}}\mathbf{v}\times\mathbf{B}_{tot}d^3\mathbf{p}=0$$

because the distribution function f_1 vanishes for infinite momentum, we obtain that the zero-moment of the kinetic Vlasov equation is the continuity equation:

$$\frac{\partial n(\mathbf{r},t)}{\partial t}+\frac{\partial n(\mathbf{r},t)\mathbf{u}(\mathbf{r},t)}{\partial \mathbf{r}}=0 \qquad \text{A0-11}$$

Multiplying the kinetic Vlasov equation (Eq. A0-7) by the momentum

$$\mathbf{p}=\sum_{j=1}^{3}\hat{e}_j p_j=\sum_{j=1}^{3}\hat{e}_j\gamma m v_j$$

and integrating with respect to $\mathbf{p}$, we obtain:

$$\sum_{j=1}^{k}\left(\frac{\partial}{\partial t}\int_{-\infty}^{\infty}\hat{e}_j p_j f_1(\mathbf{r},\mathbf{p},t)d^3\mathbf{p}+\hat{e}_j\frac{\partial}{\partial \mathbf{r}}\int_{-\infty}^{\infty}p_j\mathbf{v}f_1(\mathbf{r},\mathbf{p},t)d^3\mathbf{p}+\right.$$
$$\left.+q\hat{e}_j\int_{-\infty}^{\infty}p_j\left((\mathbf{E}_{tot}+\mathbf{v}\times\mathbf{B}_{tot})\cdot\frac{\partial}{\partial \mathbf{p}}f_1(\mathbf{r},\mathbf{p},t)\right)d^3\mathbf{p}\right)=0 \quad .$$

Following the definitions A0-8 and A0-9, we obtain:

$$\sum_{j=1}^{3}\left(\hat{e}_j \frac{\partial}{\partial t}\gamma m n(\mathbf{r},t)u_j(\mathbf{r},t) + \hat{e}_j \frac{\partial}{\partial \mathbf{r}}\left(\gamma m n(\mathbf{r},t)\mathbf{u}(\mathbf{r},t)u_j(\mathbf{r},t)\right)\right) - qn(\mathbf{r},t)\left(\mathbf{E}_{tot} + \mathbf{u}\times\mathbf{B}_{tot}\right) = 0$$

Now, using the zero-moment of the kinetic Vlasov equation (Eq. A0-11), we obtain:

$$\frac{\partial}{\partial t}\gamma m\mathbf{u}(\mathbf{r},t) + \left(\mathbf{u}(\mathbf{r},t)\cdot\frac{\partial}{\partial \mathbf{r}}\right)\gamma m\mathbf{u}(\mathbf{r},t) = q\left(\mathbf{E}_{tot} + \mathbf{u}(\mathbf{r},t)\times\mathbf{B}_{tot}\right)$$

Thus, the second moment of the kinetic Vlasov equation is the force equation for the average system momentum.

3. Symmetry properties of the transfer matrix

Now, applying Chu's theorem (Eq. 2-42) to a matrix representation of the solution (Eq. 2-58) we get that:

$$\left|\tilde{i}(0)\right|^2 \mathrm{Re}\left(CA^*\right)+\left|\tilde{v}(0)\right|^2 \mathrm{Re}\left(DB^*\right)+\mathrm{Re}\left(CB^*\tilde{i}(0)\tilde{v}^*(0)+DA^*\tilde{i}^*(0)\tilde{v}(0)\right)=\mathrm{Re}\left(\tilde{i}^*(0)\tilde{v}(0)\right)$$

Since the ABCD-matrix elements are independent of the beam's parameters ($\tilde{v}$ and $\tilde{i}$), and Chu's theorem is valid for arbitrary values of the current modulation and kinetic-voltage amplitudes (including zero), we get that the matrix terms must be satisfied for three conditions:

$$A^*C+C^*A=0 \qquad \text{A0-12}$$

$$B^*D+D^*B=0 \qquad \text{A0-13}$$

$$C^*B+D^*A=1 \qquad \text{A0-14}$$

If we express the ABCD-matrix elements in terms of an absolute value and phase: for example $A = |A|exp(i\phi_A)$, then the first and the second conditions for the matrix terms give us:

$$\phi_C-\phi_A=\pm\pi/2$$

$$\phi_D-\phi_B=\pm\pi/2$$

Taking into account these phase-dependencies, we receive that the third condition is transformed to:

$$\left(\pm|A||D|\mp|C||B|\right)i\exp\left(i(\phi_B-\phi_A)\right)=1 \qquad \text{A0-15}$$

This may be satisfied only when ϕ_A-ϕ_B = $\pm\pi/2$:

		ϕ_C-ϕ_A = $+\pi/2$	ϕ_C-ϕ_A = $-\pi/2$
ϕ_D-ϕ_B = $+\pi/2$	ϕ_A-ϕ_B = $+\pi/2$	$\|A\|\|D\|$-$\|C\|\|B\|$=1	$\|A\|\|D\|+\|C\|\|B\|=1$
	ϕ_A-ϕ_B = $-\pi/2$	-$\|A\|\|D\|$+$\|C\|\|B\|$=1	-$\|A\|\|D\|$-$\|C\|\|B\|$=1 Not realizable
ϕ_D-ϕ_B = $-\pi/2$	ϕ_A-ϕ_B = $+\pi/2$	-$\|A\|\|D\|$-$\|C\|\|B\|$=1 Not realizable	-$\|A\|\|D\|$+$\|C\|\|B\|$=1
	ϕ_A-ϕ_B = $-\pi/2$	$\|A\|\|D\|$+$\|C\|\|B\|$=1|	$\|A\|\|D\|$-$\|C\|\|B\|$=1

Based on the obtained phase-dependence between the transfer matrix elements, we get six possible matrix forms (here we assume that ϕ_A = 0):

		$\phi_C = \pi/2$	$\phi_C = -\pi/2$
$\phi_D - \phi_B = +\pi/2$	$\phi_B = -\pi/2$	$\begin{pmatrix} \lvert A(z)\rvert & -i\lvert B(z)\rvert \\ i\lvert C(z)\rvert & \lvert D(z)\rvert \end{pmatrix}$	$\begin{pmatrix} \lvert A(z)\rvert & -i\lvert B(z)\rvert \\ -i\lvert C(z)\rvert & \lvert D(z)\rvert \end{pmatrix}$
	$\phi_B = \pi/2$	$\begin{pmatrix} \lvert A(z)\rvert & i\lvert B(z)\rvert \\ i\lvert C(z)\rvert & -\lvert D(z)\rvert \end{pmatrix}$	Not realizable
$\phi_D - \phi_B = -\pi/2$	$\phi_B = -\pi/2$	Not realizable	$\begin{pmatrix} \lvert A(z)\rvert & -i\lvert B(z)\rvert \\ -i\lvert C(z)\rvert & -\lvert D(z)\rvert \end{pmatrix}$
	$\phi_B = \pi/2$	$\begin{pmatrix} \lvert A(z)\rvert & i\lvert B(z)\rvert \\ i\lvert C(z)\rvert & \lvert D(z)\rvert \end{pmatrix}$	$\begin{pmatrix} \lvert A(z)\rvert & i\lvert B(z)\rvert \\ -i\lvert C(z)\rvert & \lvert D(z)\rvert \end{pmatrix}$

Note that this relation is based on the general properties of linear differential equations and Chu's theorem only. We do not use here any other knowledge or assumptions about the electron beam propagation.

It is evident that the transfer matrix of zero-length ($z = 0$) is the unit matrix. However, a matrix which includes a diagonal term "$-|D(z)|$" can never reduce to be the unit matrix. From the rest of the matrix forms we conclude:

$$\phi_A = \phi_D$$

Consequently we conclude that only four matrix forms are physical and consistent with Chu's theorem (here we reintroduce the phase $\phi_A(z)$):

	$\phi_C - \phi_A = \pi/2$	$\phi_C - \phi_A = -\pi/2$
$\phi_A - \phi_B = +\pi/2$	$\begin{pmatrix} \lvert A(z)\rvert & -i\lvert B(z)\rvert \\ i\lvert C(z)\rvert & \lvert D(z)\rvert \end{pmatrix}\exp(i\phi_A(z))$	$\begin{pmatrix} \lvert A(z)\rvert & -i\lvert B(z)\rvert \\ -i\lvert C(z)\rvert & \lvert D(z)\rvert \end{pmatrix}\exp(i\phi_A(z))$
$\phi_A - \phi_B = -\pi/2$	$\begin{pmatrix} \lvert A(z)\rvert & i\lvert B(z)\rvert \\ i\lvert C(z)\rvert & \lvert D(z)\rvert \end{pmatrix}\exp(i\phi_A(z))$	$\begin{pmatrix} \lvert A(z)\rvert & i\lvert B(z)\rvert \\ -i\lvert C(z)\rvert & \lvert D(z)\rvert \end{pmatrix}\exp(i\phi_A(z))$

Note that the absolute value squared of the determinants for these four matrix forms are equivalent to the third condition (Eq. A0-14). Thus, the matrix determinant equals to 1 for each matrix relation:

$\left|\left(|A||D| + |C||B|\right)\exp(i\phi_A(z))\right|^2 = 1$ when $\phi_C - \phi_A = \mp\pi/2$ and $\phi_A - \phi_B = \pm\pi/2$

$\left|\left(|A||D| - |C||B|\right)\exp(i\phi_A(z))\right|^2 = 1$ when $\phi_C - \phi_A = \pm\pi/2$ and $\phi_A - \phi_B = \mp\pi/2$

Therefore, we found that when Chu's theorem is valid, the general transfer matrix for the set of two linear differential equations may be represented by one of

two kinds of functions – ordinary trigonometric or hyperbolic. We define three real functions $\varphi(z)$, $K(z)$ and $W(z)$ as:

$|A(z)||D(z)| = \cos^2(\varphi(z))$ when $\phi_C - \phi_A = \mp\pi/2$ and $\phi_A - \phi_B = \pm\pi/2$

$|A(z)||D(z)| = \cosh^2(\varphi(z))$ when $\phi_C - \phi_A = \pm\pi/2$ and $\phi_A - \phi_B = \mp\pi/2$

$\frac{|A(z)|}{|D(z)|} = K^2(z)$ and $\frac{|C(z)|}{|B(z)|} = W^2(z)$

where $K(z)$ and $W(z)$ are positive functions: $0 < K(z) < \infty$ and $0 < W(z) < \infty$

Finally, the transfer matrix may always be written in the general form:

$$M(z) = \begin{pmatrix} K(z)\cos(\varphi(z)) & \mp\frac{i}{W(z)}\sin(\varphi(z)) \\ \mp iW(z)\sin(\varphi(z)) & \frac{1}{K(z)}\cos(\varphi(z)) \end{pmatrix} \exp(i\phi_A(z)) \qquad \text{A0-16}$$

$$M(z) = \begin{pmatrix} K(z)\cosh(\varphi(z)) & \mp\frac{i}{W(z)}\sinh(\varphi(z)) \\ \pm iW(z)\sinh(\varphi(z)) & \frac{1}{K(z)}\cosh(\varphi(z)) \end{pmatrix} \exp(i\phi_A(z)) \qquad \text{A0-17}$$

This form presents the general symmetry properties of a charged particle beam system that conserves kinetic power (satisfies Chu's theorem).

If we pay attention to the slow-varying amplitude set of differential equations (Eqs. 2-53 and 2-54), then we find that the sign of the non-diagonal terms (B and C) must be the same. Therefore, the "ordinary trigonometric" form of the transfer matrix (Eq. A0-16) gives us the solution of the charged beam propagation. The sign of the non-diagonal terms depends on the phasor relation definition: for a "$-i\omega t$"-process the sign is "minus". The presented relation is also true for the "fast"-amplitude set of differential equations.

4. The transfer matrix of an acceleration section

Here we derive an explicit expression for the transfer matrix of "fast acceleration" corresponding to the 1st order iteration matrix (Eq. 2-75), and assuming a constant acceleration gradient model (Eq. 2-78):

$$\mathbf{M}_{acc}^{(1)}(L_{acc}) = \begin{pmatrix} 1 - \int_0^{L_{acc}} z'\theta_{pr}^2(z')dz' & -i\frac{kA_e}{Z_0}\int_0^{L_{acc}} \theta_p^2(z')dz' \\ -ir_p^2\frac{Z_0}{kA_e}L_{acc} & 1 - \int_0^{L_{acc}}\int_0^{z'} \theta_{pr}^2(z'')dz''dz' \end{pmatrix} \qquad \text{A0-18}$$

$$\theta_p^2(z) = \frac{I_0 Z_0}{\frac{mc^2}{e}A_e(z)}\frac{1}{(\gamma_0(z)\beta_0(z))^3} = \frac{I_0 Z_0}{\frac{mc^2}{e}A_e(z)}\frac{1}{\left((\gamma_0(0)+\gamma' z)^2 - 1\right)^{3/2}} \qquad \text{A0-19}$$

In the limit of zero acceleration gradient ($\gamma' = 0$), $\theta_{pr}(z) = const$, and trivial integrations in (Eq. A0-18) result in:

$$\mathbf{M}_{acc}^{(1)}(L_{acc}) = \begin{pmatrix} 1 - \frac{\theta_{pr}^2 L_{acc}^2}{2} & -i\frac{kA_e\theta_{pr}}{Z_0 r_p^2}\theta_{pr}L_{acc} \\ -i\frac{Z_0 r_p^2}{kA_e\theta_{pr}}\theta_{pr}L_{acc} & 1 - \frac{\theta_{pr}^2 L_{acc}^2}{2} \end{pmatrix} \qquad \text{A0-20}$$

This form is nothing but the Taylor expansion of the transfer matrix (Eq. 2-68) for a drift section of length L_{acc}. Now, for non-zero constant acceleration gradient ($\gamma' = const$), we substitute in equations A0-18 and A0-19:

$$\gamma_0(0) + \gamma' z = \gamma$$

$$dz = \frac{d\gamma}{\gamma'}$$

and use the immediate integral identities (for $x > 1$):

$$\int \frac{dx}{\left(x^2-1\right)^{3/2}} = -\frac{x}{\left(x^2-1\right)^{1/2}}$$

$$\int \frac{xdx}{\left(x^2-1\right)^{3/2}} = -\frac{1}{\left(x^2-1\right)^{1/2}}$$

$$\int \frac{xdx}{\left(x^2-1\right)^{1/2}} = \left(x^2-1\right)^{1/2}$$

Thus, we obtain for the matrix elements:

$$M_{acc_{11}} = 1 - \int_0^{L_{acc}} z'\theta_{pr}^2(z')dz' = 1 - \left(\frac{I_0 Z_0 r_p^2}{\frac{mc^2}{e} A_e (\gamma')^2}\right) \int_{\gamma_0(0)}^{\gamma_0(L_{acc})} \frac{\gamma - \gamma_0(0)}{(\gamma^2 - 1)^{3/2}} d\gamma =$$

$$= 1 - \left(\frac{I_0 Z_0 r_p^2}{\frac{mc^2}{e} A_e (\gamma')^2}\right) \left[\int_{\gamma_0(0)}^{\gamma_0(L_{acc})} \frac{\gamma}{(\gamma^2 - 1)^{3/2}} d\gamma - \int_{\gamma_0(0)}^{\gamma_0(L_{acc})} \frac{\gamma_0(0)}{(\gamma^2 - 1)^{3/2}} d\gamma \right] =$$

$$= 1 - \left(\frac{I_0 Z_0 r_p^2}{\frac{mc^2}{e} A_e (\gamma')^2}\right) \left[-\frac{1}{(\gamma^2 - 1)^{1/2}} \Bigg|_{\gamma_0(0)}^{\gamma_0(L_{acc})} + \gamma_0(0) \left(\frac{\gamma}{(\gamma^2 - 1)^{1/2}}\right) \Bigg|_{\gamma_0(0)}^{\gamma_0(L_{acc})} \right] = \quad \text{A0-21}$$

$$= 1 - \left(\frac{I_0 Z_0 r_p^2}{\frac{mc^2}{e} A_e (\gamma')^2}\right) \left(\frac{\gamma_0(0)\gamma_0(L_{acc}) - 1}{(\gamma_0^2(L_{acc}) - 1)^{1/2}} - (\gamma_0^2(0) - 1)^{1/2} \right)$$

$$M_{acc_{12}} = -i\frac{kA_e}{Z_0} \int_0^{L_{acc}} \theta_p^2(z')dz' = -i\frac{kA_e}{Z_0} \left(\frac{I_0 Z_0}{\frac{mc^2}{e} A_e \gamma'}\right) \int_{\gamma_0(0)}^{\gamma_0(L_{acc})} \frac{1}{(\gamma^2 - 1)^{3/2}} d\gamma =$$

$$= i\frac{kA_e}{Z_0} \left(\frac{I_0 Z_0}{\frac{mc^2}{e} A_e \gamma'}\right) \left[\left(\frac{\gamma}{(\gamma^2 - 1)^{1/2}}\right) \Bigg|_{\gamma_0(0)}^{\gamma_0(L_{acc})} \right] = i\frac{kA_e}{Z_0} \left(\frac{I_0 Z_0}{\frac{mc^2}{e} A_e \gamma'}\right) \left(\frac{\gamma_0(L_{acc})}{(\gamma_0(L_{acc})^2 - 1)^{1/2}} - \frac{\gamma_0(0)}{(\gamma_0(0)^2 - 1)^{1/2}} \right)$$

A0-22

$$M_{acc_{22}} = 1 - \int_0^{L_{acc}} \int_0^{z'} \theta_{pr}^2(z'')dz''dz' = 1 + \frac{I_0 Z_0 r_p^2}{\frac{mc^2}{e} A_e \gamma'} \int_0^{L_{acc}} \left(\frac{\gamma_0(0) + \gamma' z'}{((\gamma_0(0) + \gamma' z')^2 - 1)^{1/2}} - \frac{\gamma_0(0)}{(\gamma_0(0)^2 - 1)^{1/2}} \right) dz' =$$

$$= 1 + \frac{I_0 Z_0 r_p^2}{\frac{mc^2}{e} A_e (\gamma')^2} \int_{\gamma_0(0)}^{\gamma_0(L_{acc})} \frac{\gamma}{(\gamma^2 - 1)^{1/2}} d\gamma - \frac{I_0 Z_0 r_p^2}{\frac{mc^2}{e} A_e \gamma'} \frac{\gamma_0(0) L_{acc}}{(\gamma_0(0)^2 - 1)^{1/2}} =$$

$$= 1 + \frac{I_0 Z_0 r_p^2}{\frac{mc^2}{e} A_e (\gamma')^2} (\gamma^2 - 1)^{1/2} \Big|_{\gamma_0(0)}^{\gamma_0(L_{acc})} - \frac{I_0 Z_0 r_p^2}{\frac{mc^2}{e} A_e \gamma'} \frac{\gamma_0(0) L_{acc}}{(\gamma_0(0)^2 - 1)^{1/2}} =$$

$$= 1 + \frac{I_0 Z_0 r_p^2}{\frac{mc^2}{e} A_e \gamma'} \left(\frac{(\gamma_0(L_{acc})^2 - 1)^{1/2} - (\gamma_0(0)^2 - 1)^{1/2}}{\gamma'} - \frac{\gamma_0(0) L_{acc}}{(\gamma_0(0)^2 - 1)^{1/2}} \right)$$

A0-23

For the case when the e-beam is relativistic before and after an accelerator ($\gamma_0(0) >> 1$ and $\gamma_0(L_{acc}) >> 1$), we define small parameters $x_0 = 1/\gamma_0(0)$ and $x_1 = 1/\gamma_0(L_{acc})$. Keeping the second term only, we obtain:

$$M_{acc_{11}} = 1 - \int_0^{L_{acc}} z'\theta_{pr}^2(z')dz' = 1 - \left(\frac{I_0 Z_0 r_p^2}{\frac{mc^2}{e} A_e (\gamma')^2}\right) \left(\frac{\gamma_0(0)\gamma_0(L_{acc}) - 1}{(\gamma_0^2(L_{acc}) - 1)^{1/2}} - (\gamma_0^2(0) - 1)^{1/2} \right) =$$

$$= 1 - \left(\frac{I_0 Z_0 r_p^2}{\frac{mc^2}{e} A_e}\right) \frac{L_{acc}^2}{(\gamma_0(L_{acc}) - \gamma_0(0))^2} \gamma_0(0) \left(\frac{1 - x_0 x_1}{(1 - x_1^2)^{1/2}} - (1 - x_0^2)^{1/2} \right) \cong$$

$$\cong 1 - \left(\frac{I_0 Z_0 r_p^2}{\frac{mc^2}{e} A_e}\right) \frac{L_{acc}^2}{(\gamma_0(L_{acc}) - \gamma_0(0))^2} \gamma_0(0) \left(\frac{x_0^2}{2} + \frac{x_1^2}{2} - x_0 x_1 \right) = 1 - \left(\frac{I_0 Z_0 r_p^2}{\frac{mc^2}{e} A_e}\right) \frac{L_{acc}^2}{2\gamma_0(0)\gamma_0^2(L_{acc})}$$

A0-24

$$M_{acc_{12}} = -i\frac{kA_e}{Z_0}\int_0^{L_{acc}}\theta_{pr}^2(z')dz' = i\frac{kA_e}{Z_0}\left(\frac{I_0Z_0}{\frac{mc^2}{e}A_e\gamma'}\right)\left(\frac{\gamma_0(L_{acc})}{\left(\gamma_0(L_{acc})^2-1\right)^{1/2}}-\frac{\gamma_0(0)}{\left(\gamma_0(0)^2-1\right)^{1/2}}\right)=$$

$$= i\frac{kA_e}{Z_0}\left(\frac{I_0Z_0}{\frac{mc^2}{e}A_e}\frac{L_{acc}}{\gamma_0(L_{acc})-\gamma_0(0)}\right)\left(\frac{1}{\sqrt{1-x_1^2}}-\frac{1}{\sqrt{1-x_{10}^2}}\right)\cong$$

$$\cong i\frac{kA_e}{Z_0}\left(\frac{I_0Z_0}{\frac{mc^2}{e}A_e}\frac{L_{acc}}{\gamma_0(L_{acc})-\gamma_0(0)}\right)\left(\frac{x_1^2}{2}-\frac{x_0^2}{2}\right) = -i\frac{kA_e}{2Z_0}\left(\frac{I_0Z_0}{\frac{mc^2}{e}A_e}\frac{L_{acc}\left(\gamma_0(L_{acc})+\gamma_0(0)\right)}{\gamma_0^2(L_{acc})\gamma_0^2(0)}\right)$$

A0-25

$$M_{acc_{22}} = 1-\int_0^{L_{acc}}\int_0^{z'}\theta_{pr}^2(z'')dz''dz' = 1+\frac{I_0Z_0r_p^2}{\frac{mc^2}{e}A_e\gamma'}\left(\frac{\left(\gamma_0^2(L_{acc})-1\right)^{1/2}-\left(\gamma_0^2(0)-1\right)^{1/2}}{\gamma'}-\frac{\gamma_0(0)L_{acc}}{\left(\gamma_0^2(0)-1\right)^{1/2}}\right)=$$

$$= 1+\frac{I_0Z_0r_p^2L_{acc}^2}{\frac{mc^2}{e}A_e}\left(\frac{\gamma_0(L_{acc})\sqrt{1-x_1^2}-\gamma_0(0)\sqrt{1-x_0^2}}{\left(\gamma_0(L_{acc})-\gamma_0(0)\right)^2}-\frac{1}{\left(\gamma_0(L_{acc})-\gamma_0(0)\right)\sqrt{1-x_0^2}}\right)\cong$$

$$\cong 1+\frac{I_0Z_0r_p^2L_{acc}^2}{\frac{mc^2}{e}A_e}\left(\frac{\gamma_0(L_{acc})\left(1-\frac{x_1^2}{2}\right)-\gamma_0(0)\left(1-\frac{x_0^2}{2}\right)}{\left(\gamma_0(L_{acc})-\gamma_0(0)\right)^2}-\frac{1+\frac{x_0^2}{2}}{\left(\gamma_0(L_{acc})-\gamma_0(0)\right)}\right)=$$

$$= 1-\frac{I_0Z_0r_p^2}{\frac{mc^2}{e}A_e}\frac{L_{acc}^2}{2\gamma_0(L_{acc})\gamma_0^2(0)}$$

A0-26

or, in the matrix form, in terms of the plasma wave number ($\theta_{pr}(0)$) and using the e-beam wave impedance ($W_d(0)$) at the entrance to the accelerator, we obtain:

$$\mathbf{M}_{acc}^{(1)}(L_{acc}) = \begin{pmatrix} 1-\frac{\theta_{pr}^2(0)L_{acc}^2}{2}\frac{\gamma_0^2(0)\beta_0^3(0)}{\gamma_0^2(L_{acc})} & -i\frac{\theta_{pr}(0)L_{acc}}{W_d(0)}\left(\frac{\gamma_0(0)}{\gamma_0(L_{acc})}\frac{\left(\gamma_0(L_{acc})+\gamma_0(0)\right)}{2\gamma_0(L_{acc})}\beta_0^3(0)\right) \\ -iW_d(0)\theta_{pr}(0)L_{acc} & 1-\frac{\theta_{pr}^2(0)L_{acc}^2}{2}\frac{\gamma_0(0)\beta_0^3(0)}{\gamma_0(L_{acc})} \end{pmatrix}$$

The same result in terms of the plasma wave number and the e-beam wave impedance at the end of the accelerator ($\theta_{pr}(L_{acc})$, $W_d(L_{acc})$) is given by:

$$\mathbf{M}_{acc}^{(1)}(L_{acc}) = \begin{pmatrix} 1-\frac{\theta_{pr}^2(L_{acc})L_{acc}^2}{2}\frac{\gamma_0(L_{acc})\beta_0^3(L_{acc})}{\gamma_0(0)} & -i\frac{\theta_{pr}(L_{acc})L_{acc}}{W_d(L_{acc})}\left(\frac{\gamma_0(L_{acc})}{\gamma_0(0)}\frac{\left(\gamma_0(L_{acc})+\gamma_0(0)\right)}{2\gamma_0(0)}\beta_0^3(L_{acc})\right) \\ -iW_d(L_{acc})\theta_{pr}(L_{acc})L_{acc} & 1-\frac{\theta_{pr}^2(L_{acc})L_{acc}^2}{2}\frac{\gamma_0^2(L_{acc})\beta_0^3(L_{acc})}{\gamma_0^2(0)} \end{pmatrix}$$

5. A new theorem for a sufficient condition for quarter plasma oscillation in free space e-beam transport

In this appendix we derive the conditions sufficient for obtaining quarter plasma oscillation in a free drift section of electron beam transport. We start from the K-V beam envelope equation of an e-beam transport in a section free from external fields [96]:

$$\frac{d^2 r_b(z)}{dz^2} - \frac{K}{r_b(z)} - \frac{\varepsilon^2}{r_b^3(z)} = 0 \qquad \text{A0-27}$$

where $r_b(z)$ is the beam radius, ε is the conventional emittance, and $K = 2I_0/I_A(\gamma\beta)^3$ is the relativistic perveance ($I_A = 4\pi\varepsilon_0 mc^3/e$ = 17 kA is the Alfven current). This equation is valid for a beam with flat top transverse current density distribution. The equation is approximately valid also for a Gaussian distribution (σ_x is the Gaussian beam radius, $\sigma_{x'}$ is the Gaussian beam transverse velocity spread) with replacements

$$r_b = \sqrt{2}\sigma_x, \varepsilon = 2\sigma_x\sigma_{x'}.$$

Neglecting reduction of the plasma wavenumber (r_p = 1), we define the phase shift ($\varphi_{p_{waist}}$) of a plasma wave passing through a beam waist (using the Eq. 2-29) as:

$$\varphi_{p_{waist}} = \int_{-z_{waist}}^{z_{waist}} \theta_p(z)dz = \int_{-z_{waist}}^{z_{waist}} \sqrt{\frac{I_0 Z_0}{\pi r_b^2(z)\frac{mc^2}{e}\beta_0^3\gamma_0^3}}dz \qquad \text{A0-28}$$

The solution of the equation A0-27 for the zero-emittance case, namely – space-charge dominated transport beam expansion in free–space, is given in [96]. If we denote the minimal beam radius at the waist r_0, then the beam radius as a function of distance (z) is given by:

$$r_b^{sch}(z) = r_0\left(1 + \frac{K}{2}\left(\frac{z}{r_0}\right)^2\right) \qquad \text{A0-29}$$

with the accuracy better than 3% (see Figure A0-1). Analogously to optic beams, we introduce the term "waist length" (z_{waist}) as a distance along the z-direction where the beam cross section area is twice as large. Therefore, for a space charge dominance regime, we obtain:

$$z_{waist}^{sch} = r_0\sqrt{\frac{2(\sqrt{2}-1)}{K}} \qquad \text{A0-30}$$

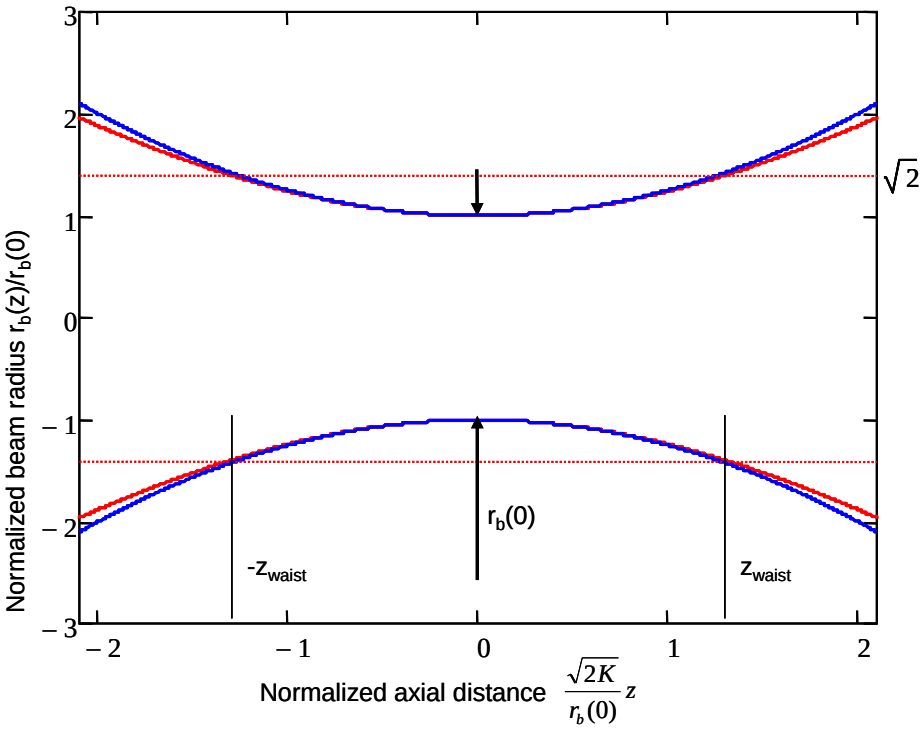

Figure A0-1 Beam envelope in a space charge dominated case: numerical solution (red curve) and approximated analytical solution (blue curve).

Substituting these definitions (Eqs. A0-29 and A0-30) to equation A0-28, we obtain:

$$\varphi_{p_{waist}}^{sch} = \int_{-z_{waist}}^{z_{waist}} \frac{1}{(2r_0^2 + \frac{2I_0}{I_A\beta_0^3\gamma_0^3} z^2)} \sqrt{\frac{4r_0^2 I_0 Z_0}{\pi \frac{mc^2}{e} \beta_0^3\gamma_0^3}} dz = 2\sqrt{\frac{cZ_0 4\pi\varepsilon_0}{\pi}} \operatorname{atan}\left(z_{waist} \sqrt{\frac{\frac{2I_0}{I_A\beta_0^3\gamma_0^3}}{2r_0^2}} \right) =$$

$$= 4\operatorname{atan}\left(\sqrt{(\sqrt{2}-1)} \right) = \frac{\pi}{2}$$

A0-31

Thus we obtained that if the beam propagates in the space charge dominance regime, then the phase of the plasma wave in the waist is always equal to π/2, independently of the beam parameters.

The space charge dominance regime is defined by:

$$K >> \frac{\varepsilon^2}{r_0^2}$$ A0-32

This sets a condition on the emittance or the beam radius required for quarter wavelength longitudinal plasma oscillation in free space drift.

The physical significance of this theorem is that the process of homogenization of longitudinal density bunches that takes place within the quarter plasma oscillation time, occurs at the same rate as the beam envelope expansion due to the Coulomb forces. In the beam frame of reference both processes are seen as the same.

Since the beam is approximately uniform along the waist, the uniform beam model expression (Eqs. 2-51 and 2-52) is quite valid. This leads to a quite significant conclusion: If the beam is initially current noise dominated, and transported in the space-charge dominance regime (Eq. A0-32), then a sufficient condition for its noise suppression is to have it pass through through a waist in the sense defined above (Eq. A0-31).

It is interesting to evaluate the plasma phase propagation also in the emittance dominated transport regime ($K << \varepsilon^2/r_0$, opposite case to Eq. A0-32). In this case the solution of the beam envelope equation (Eq. A0-27) is (see Figure A0-2):

$$r_b^{\varepsilon}(z) = r_0 \sqrt{1 + \left(\frac{\varepsilon z}{r_0^2} \right)^2}$$ A0-33

Thus the waist length in an emittance dominated regime can be defined as:

$$z_{waist}^{\varepsilon} = \frac{r_0^2}{\varepsilon}$$ A0-34

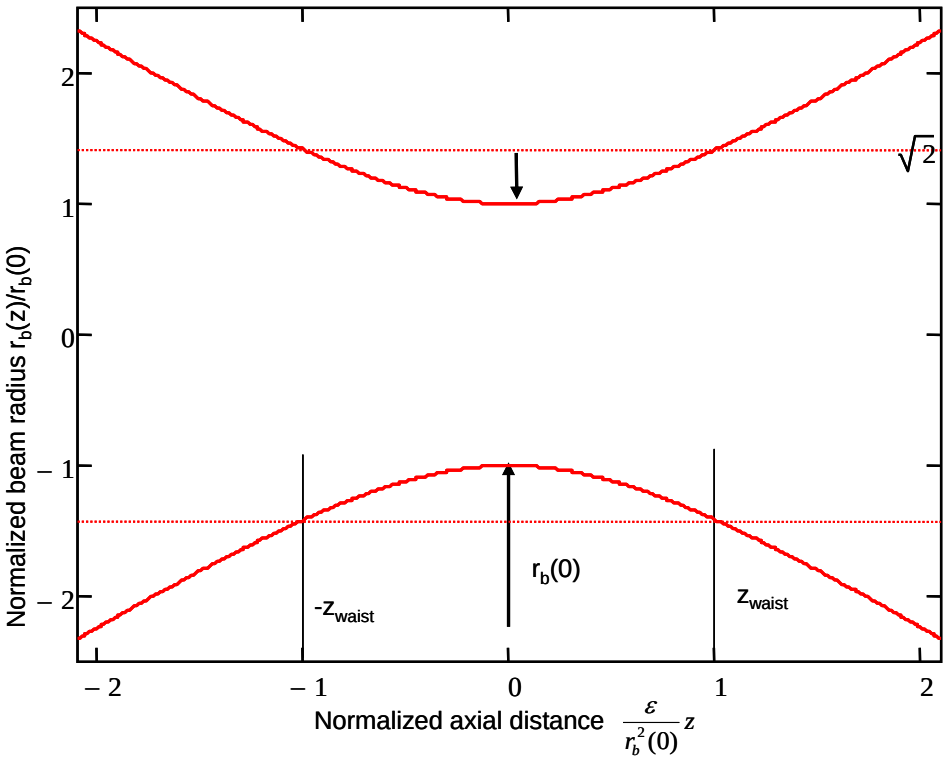

Figure A0-2 Beam envelope in an emittance dominated case. Analytical solution.

Substituting these definitions (Eqs. A0-33 and A0-34) into equation A0-28, we obtain:

$$\varphi_{p_{waist}}^{\varepsilon}=\sqrt{\frac{I_0 Z_0}{\pi r_0^2\,\frac{mc^2}{e}\,\beta_0^3\gamma_0^3}}\int_{-z_{waist}^{\varepsilon}}^{z_{waist}^{\varepsilon}}\sqrt{\frac{1}{\left(1+\left(\frac{\varepsilon\, z}{r_0^2}\right)^2\right)}}dz=\sqrt{\frac{I_0 Z_0 r_0^2}{\pi\,\frac{mc^2}{e}\,\beta_0^3\gamma_0^3\varepsilon^2}}\int_{-z_{waist}^{\varepsilon}}^{z_{waist}^{\varepsilon}}\sqrt{\frac{1}{\left(\frac{r_0^4}{\varepsilon^2}+z^2\right)}}dz=$$

$$=\sqrt{\frac{I_0 Z_0 r_0^2}{\pi\,\frac{mc^2}{e}\,\beta_0^3\gamma_0^3\varepsilon^2}}\ln\left(\frac{\sqrt{\left(z_{waist}^{\varepsilon}\right)^2+\frac{r_0^4}{\varepsilon^2}}+z_{waist}^{\varepsilon}}{\sqrt{\left(z_{waist}^{\varepsilon}\right)^2+\frac{r_0^4}{\varepsilon^2}}-z_{waist}^{\varepsilon}}\right)=2\sqrt{\frac{I_0 Z_0 r_0^2}{\pi\,\frac{mc^2}{e}\,\beta_0^3\gamma_0^3\varepsilon^2}}\ln\left(\sqrt{2}+1\right)$$

A0-35

Thus, taking into account the relativistic perveance definition (*K*), we obtain:

$$\varphi_{p_{waist}}^{\varepsilon}==2\sqrt{\frac{2Kr_0^2}{\varepsilon^2}}\ln\left(\sqrt{2}+1\right)\approx 2.5\sqrt{\frac{Kr_0^2}{\varepsilon^2}}\approx 1.76\frac{\theta_p r_0^2}{\varepsilon}=1.76\,\theta_p z_{waist}^{\varepsilon}$$

A0-36

Obviously, having significant emittance may have significant axial velocity noise, and attainment of quarter plasma oscillation this way may not correspond to noise suppression.

6. Optical Transition Radiation

Optical Transition Radiation (OTR) is a commonly used particle beam diagnostic tool. The radiation effect, produced at the moment when a charged particle crosses the boundary between two different media, was theoretically predicted by Frank and Ginzburg [106] (see Figure A0-3). The solution for the intensity of the radiation field from one charged particle was found from Maxwell's equation by applying necessary field boundary conditions on the dielectric surface [107, 108]:

$$\frac{d^2 I(\Theta,\omega)}{d\omega d\Omega} = \frac{e^2\beta^2\sqrt{\varepsilon_2}\sin^2\Theta\cos^2\Theta}{\pi^2 c}\times \\ \times\left|\frac{(\varepsilon_1-\varepsilon_2)(1-\beta^2\varepsilon_2-\beta\sqrt{\varepsilon_1-\varepsilon_2\sin^2\Theta})}{(1-\beta^2\varepsilon_2\cos^2\Theta)(1-\beta\sqrt{\varepsilon_1-\varepsilon_2\sin^2\Theta})(\varepsilon_1\cos\Theta+\sqrt{\varepsilon_1\varepsilon_2-\varepsilon_2^2\sin^2\Theta})}\right| \qquad \text{A0-37}$$

where Θ is the angle between the forward OTR wave-vector and the beam axis, ε_1 and ε_2 are the dielectric permittivities of the media (Figure A0-4).

When OTR is used for beam diagnostics, it provides information about the e-beam transverse current distribution. In the case where electrons are incident on the screen independently of each other, and their entrance times are uncorrelated, the radiation pattern is an incoherent sum of the radiation energies from each electron. OTR screens actually measure in general current noise, and they are used for current distribution diagnostics only under the assumption that the current noise at the OTR screen plane is uncorrelated and proportional to the current density [109]. Only then the intensity of OTR is proportional to the current density.

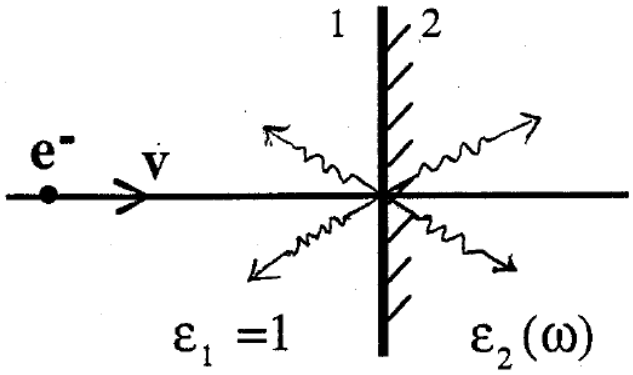

Figure A0-3. The Optical Transition Radiation. Radiation scheme. (Taken from CAA-Tech-Note-internal report #24 by Beth Gitter)

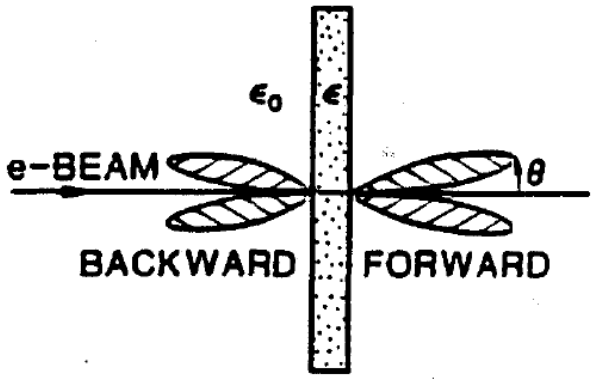

Figure A0-4 Transition Radiation patterns in the case of normal electron incidence on a boundary. (Taken from CAA-Tech-Note-internal report #24 by Beth Gitter).

7. Spectral power density of radiation modes

We shall develop here a suitable, simple, mathematical formulation for quantifying the spectral characteristics of partially coherent radiation modes. This formulation deals with systems having known behavior regarding coherency and statistical probability in the time-space domain. It is based on the description of a system in the "phase-space" which is defined as the space containing the space-time variable $(\mathbf{r},t)$, and their Fourier transform variables in the space-frequency variable $(\mathbf{r},\omega)$.

We derive here an expression for the spectral radiation power per radiation mode within the framework of the general radiation mode expansion model (Eqs. 3-8 and 3-9). At this point we still restrict the analysis to finite energy radiation signals that are Fourier transformable.

We keep the previous definition of the Fourier transform (Eq. 2-104). Thus, the Fourier transform of the electric field (**E**(**r**,*t*)) and the magnetic field (**H**(**r**,*t*)) are:

$$\breve{\mathbf{E}}(\mathbf{r},\omega)=\int_{-\infty}^{\infty}\mathbf{E}(\mathbf{r},t)e^{i\omega t}dt$$

$$\breve{\mathbf{H}}(\mathbf{r},\omega)=\int_{-\infty}^{\infty}\mathbf{H}(\mathbf{r},t)e^{i\omega t}dt$$

and the inverse Fourier transforms of the fields are:

$$\mathbf{E}(\mathbf{r},t)=\frac{1}{2\pi}\int_{-\infty}^{\infty}\breve{\mathbf{E}}(\mathbf{r},\omega)e^{i\omega t}d\omega$$

$$\mathbf{H}(\mathbf{r},t)=\frac{1}{2\pi}\int_{-\infty}^{\infty}\breve{\mathbf{H}}(\mathbf{r},\omega)e^{i\omega t}d\omega$$

Since the fields in the time-space domain are real functions (imaginary part equal to zero), we can use a property of Fourier transforms: the transforms of such functions satisfy a reality condition (the real part of the Fourier transform is an even function of frequency, the imaginary part is an odd function of frequency):

$$\breve{\mathbf{E}}(-\omega)=\breve{\mathbf{E}}^{*}(\omega) \qquad \text{A0-38}$$

$$\breve{\mathbf{H}}(-\omega)=\breve{\mathbf{H}}^{*}(\omega) \qquad \text{A0-39}$$

We identify

$$\mathbf{S}(\mathbf{r},t)=\mathbf{E}(\mathbf{r},t)\times\mathbf{H}(\mathbf{r},t)$$

as the Poynting vector in the time domain, and

$$\breve{\mathbf{S}}(\mathbf{r},\omega)=\frac{1}{2\pi}\breve{\mathbf{E}}(\mathbf{r},\omega)\times\breve{\mathbf{H}}^{*}(\mathbf{r},\omega) \qquad \text{A0-40}$$

as the Poynting vector in the frequency domain. Based on the reality condition (Eqs. A0-38, A0-39), it is evident that the spectral Poynting vector **S** satisfies the reality condition too:

$$\breve{\mathbf{S}}(-\omega)=\breve{\mathbf{S}}^{*}(\omega) \qquad \text{A0-41}$$

Employing the Parseval theorem in the time-frequency dimensions (the total energy transfer in the time domain is equal to the sum of energies over all frequencies), we find the total energy (W) transferred (energy flow) to the +z-direction as:

$$W(z)=\int\int\int_{-\infty}^{\infty}\breve{\mathbf{S}}(\mathbf{r},\omega)\cdot\hat{\mathbf{e}}_z\,dxdyd\omega=\int\int\int_{-\infty}^{\infty}\mathbf{S}(\mathbf{r},t)\cdot\hat{\mathbf{e}}_z\,dxdydt \qquad \text{A0-42}$$

Or, using the field relation

$$W(z)=\int\int\int_{-\infty}^{\infty}\frac{1}{2\pi}\left[\breve{\mathbf{E}}(\mathbf{r},\omega)\times\breve{\mathbf{H}}^{*}(\mathbf{r},\omega)\right]\cdot\hat{\mathbf{e}}_z\,dxdyd\omega=\int\int\int_{-\infty}^{\infty}\left[\mathbf{E}(\mathbf{r},t)\times\mathbf{H}(\mathbf{r},t)\right]\cdot\hat{\mathbf{e}}_z\,dxdydt$$

It is now possible to express the radiation energy flow in terms of integration over positive frequencies only (taking into account A41):

$$W(z)=\int\int\int_{-\infty}^{\infty}\breve{\mathbf{S}}(\mathbf{r},\omega)\cdot\hat{\mathbf{e}}_z\,dxdyd\omega=\int\int\int_{-\infty}^{0}\breve{\mathbf{S}}(\mathbf{r},\omega)\cdot\hat{\mathbf{e}}_z\,dxdyd\omega+\int\int\int_{0}^{\infty}\breve{\mathbf{S}}(\mathbf{r},\omega)\cdot\hat{\mathbf{e}}_z\,dxdyd\omega=$$

$$\int\int\int_{0}^{\infty}\breve{\mathbf{S}}(\mathbf{r},-\omega)\cdot\hat{\mathbf{e}}_z\,dxdyd\omega+\int\int\int_{0}^{\infty}\breve{\mathbf{S}}(\mathbf{r},\omega)\cdot\hat{\mathbf{e}}_z\,dxdyd\omega=\int\int\int_{0}^{\infty}2\,\mathrm{Re}\left(\breve{\mathbf{S}}(\mathbf{r},\omega)\right)\cdot\hat{\mathbf{e}}_z\,dxdyd\omega$$

This suggests that in the positive frequencies spectral domain definition, the spectral energy density flow (Pointing vector) should be defined as:

$$\breve{\mathbf{S}}^{p}(\mathbf{r},\omega)=2\,\mathrm{Re}\,\breve{\mathbf{S}}(\mathbf{r},\omega)$$

and consequently, the positive frequency spectral energy flow can be written as:

$$\frac{dW^{p}(z,\omega)}{d\omega}=\iint\mathbf{S}^{p}(\mathbf{r},\omega)dxdy=\frac{1}{\pi}\,\mathrm{Re}\iint\left[\breve{\mathbf{E}}(\mathbf{r},\omega)\times\breve{\mathbf{H}}^{*}(\mathbf{r},\omega)\right]\cdot\hat{\mathbf{e}}_z\,dxdy \qquad \text{A0-43}$$

We now focus our spectral formulation to the case when the radiation field is expressed in terms of mode expansion. For calculating axial flow of radiative energy, only transverse components of the fields need to be taken into account. Using the modal expansion formalism, we represent the fields in terms of a complete set of forward and backward propagating transverse modes q propagating in the z-direction):

$$\breve{\mathbf{E}}_{\perp}(\mathbf{r},\omega)=\sum_{q}\breve{C}_q(z,\omega)\tilde{\mathbf{E}}_{q\perp}(\mathbf{r}_{\perp},\omega)\exp\left(ik_{qz}z\right)+\breve{C}_{-q}(z,\omega)\tilde{\mathbf{E}}_{-q\perp}(\mathbf{r}_{\perp},\omega)\exp\left(-ik_{qz}z\right)$$

$$\breve{\mathbf{H}}_{\perp}(\mathbf{r},\omega)=\sum_{q}\breve{C}_q(z,\omega)\tilde{\mathbf{H}}_{q\perp}(\mathbf{r}_{\perp},\omega)\exp\left(ik_{qz}z\right)+\breve{C}_{-q}(z,\omega)\tilde{\mathbf{H}}_{-q\perp}(\mathbf{r}_{\perp},\omega)\exp\left(-ik_{qz}z\right)$$

where $\breve{C}_q, k_{qz}, \tilde{\mathbf{E}}_{q\perp}, \tilde{\mathbf{H}}_{q\perp}$ are. Respectively. the slow-varying amplitude, the wave number, and the electric and magnetic field transverse profile functions of the electromagnetic mode q. Mode "–q" propagates in the "–z"-direction. Note, that the profile amplitudes define a q-mode normalization power P_q as:

$$P_q = \frac{1}{2}\mathrm{Re}\iint\left[\tilde{\mathbf{E}}_q \times \tilde{\mathbf{H}}_q^*\right]\cdot \hat{e}_z dxdy$$

and "*–q"*-mode normalization power as:

$$P_{-q} = \frac{1}{2}\mathrm{Re}\iint\left[\tilde{\mathbf{E}}_q \times \tilde{\mathbf{H}}_{-q}^*\right]\cdot \hat{\mathbf{e}}_z dxdy$$

Substituting this formulation into equation A0-43, and using the orthogonality relation of the expansion mode profiles, we obtain:

$$\frac{dW^p(z,\omega)}{d\omega} = \frac{1}{\pi}\mathrm{Re}\iint\left(\sum_{\pm q}\breve{C}_q\tilde{\mathbf{E}}_q\right)\cdot\left(\sum_{\pm q'}\breve{C}_q^*\tilde{\mathbf{H}}_q^*\right)\cdot\hat{\mathbf{e}}_z dxdy =$$

$$= \frac{1}{\pi}\mathrm{Re}\sum_q\left|\breve{C}_q\right|^2\int\tilde{\mathbf{E}}_q\times\tilde{\mathbf{H}}_q^*\cdot\hat{\mathbf{e}}_z dxdy + \left|\breve{C}_{-q}\right|^2\int\tilde{\mathbf{E}}_{-q}\times\tilde{\mathbf{H}}_q^*\cdot\hat{\mathbf{e}}_z dxdy =$$

$$= \frac{2}{\pi}P_q\left(\left|\breve{C}_q\right|^2 - \left|\breve{C}_{-q}\right|^2\right)$$

If the electromagnetic wave is known to propagate only in the +z-direction ($\breve{C}_{-q} = 0$), then:

$$\frac{dW^p(z,\omega)}{d\omega} = \frac{2}{\pi}P_q\left|\breve{C}_q\right|^2$$

8. Landau damping in relativistic e-beams

In non-relativistic plasma physics there is a well-known effect called Landau damping. If some electrons in the system are synchronous with a plasma wave of frequency ω_p and wavenumber k_p (their velocity u_e is about equal to the phase velocity of the plasma wave):

$$u_e = \frac{\omega_p}{k_p}$$

Subsequently, there can be a significant energy swap from the wave to the kinetic energy of these electrons. This effect makes propagation of a short wavelength plasma wave into the system impossible. The increment of the Landau damping (γ_L) is proportional to the derivative of the electron distribution function in terms of velocity at the point of synchronism and is given by:

$$\gamma_L(\omega) = -\frac{\pi}{2}\frac{\omega_p^3}{k_p^2 n_0}\left.\frac{\partial f}{\partial u}\right|_{u=\frac{\omega_p}{k_p}}$$

For a Gaussian velocity distribution, the increment of Landau damping attains a maximum when the electrons have thermal velocities: $u_e \sim u_{th}$.

The Landau damping effect was analyzed first by Lev Landau in the context of stationary plasma [79]. His kinetic model, based on the solution of the Vlasov equation in 1-D, was employed to stationary plasma (zero average velocity) with Maxwellian velocity distribution of standard deviation σ_v. Instead of the pure sinusoidal oscillation solution at plasma frequency ω_p , which is the solution of the fluid plasma equation, it was found in the kinetic model solution, that the frequency ω has an imaginary part:

$$\omega = \mathrm{Re}(\omega) + i\,\mathrm{Im}(\omega)$$

therefore the sinusoidal wave solution decays exponentially with a decay constant $\gamma_L = \mathrm{Im}(\omega)$

Citing the solution of Jackson [80] (which includes some numerical factor correction to Landau's formula), the frequency decay constant and the plasma wave dispersion equation are given in the case of stationary Maxwellian distribution plasma by approximate analytical expressions:

$$\frac{\mathrm{Im}\,\omega}{\omega_p} = \sqrt{\frac{\pi}{8}}\left(\frac{k_D}{k_p}\right)^{-3}\exp\left(-\frac{k_D^2}{2k^2}\right)\exp\left(-\frac{3}{2}\right) \qquad \text{A0-44}$$

$$\frac{\mathrm{Re}\,\omega}{\omega_p} = \sqrt{1+\frac{3k_p^2}{k_D^2}} \qquad \text{A0-45}$$

Here $k_D = \omega_p/\sigma_u$, and the analytical solution is only valid in the range $N_D = k_p/k_D < 0.5$.

Clearly the Landau damping effect is negligible when the decay constant is small relative to the oscillation frequency ($\mathrm{Im}\omega < \omega \cong \omega_p$). As can be seen from equation A0-44, this happens in the limit $N_D = k_p/k_D << 1$.

Obviously the Landau damping effect would take place also in a drifting plasma (and particularly in a relativistic electron beam with axial velocity spread). Equations A0-44 and A0-45 certainly apply in the beam frame of reference. The time decay in this frame is viewed then in the Lab frame as spatial decay in the z coordinate of the stationary sinusoidal plasma wave solution of wavenumber $\omega/u \pm \theta_{pr}$ (here we use θ_{pr} instead θ_p to take into account the plasma reduction factor in a finite width beam). Based on the principle of phase invariance under Lorentz transformation, the spatial decay constant ($\mathrm{Im}k_z$) in the lab frame can be evaluated by a Lorentz transformation of equations A0-44 and A0-45 back to the lab frame. Alternatively, the entire Vlasov equation derivation can be carried out in the lab frame with a velocity distribution of a drifting Maxwellian [65]. This results in the same expression like equation A0-44 for the spatial decay constant $\mathrm{Im}k_z = \mathrm{Im}\omega/u_0$ with $N_D = k/k_D$ evaluated in the lab frame.

In this appendix we show that the Landau decay neglect condition is $N_D << 1$ using a simple lab frame explanation. Figure A0-5 describes the dispersion diagram of plasma waves propagating on an electron beam with velocity u_0, velocity spread u_{th} and plasma frequency ω_{pr} (all parameters are evaluated in the lab frame). Electrons with velocity $u = u_0 \pm u_{th}$ will be synchronous with the plasma wave when the following dispersion lines intersect:

$$\omega \pm \omega_{pr} = k_z u_0$$

$$\omega = k_z \left(u_0 \pm u_{th} \right)$$

Thus, we obtain a synchronism condition between the electrons in the beam and plasma wave propagated on the beam as:

$$k_z = \frac{\omega_{pr}}{\beta_{th} c} = k_D$$

or in terms of the plasma wavenumber:

$$k_z = k_D = \theta_{pr} \frac{\beta_0}{\beta_{th}}$$

or in terms of energy spread ($\delta\gamma = \gamma_0^3 \beta_0 \beta_{th}$):

$$k_z = \theta_{pr} \frac{\gamma_0}{\delta\gamma} \gamma_0^2 \beta_0^2 .$$

Therefore, Landau damping is negligible in the range

$$k << k_D$$

where intersection of the curves is avoided.

For the example of the LCLS injector (E_k = 135 MeV, δE_k = 3 keV, θ_{pr} = 0.318 rad/m), we obtain Landau damping for a wavelength less than

$$\lambda < 6\ nm$$

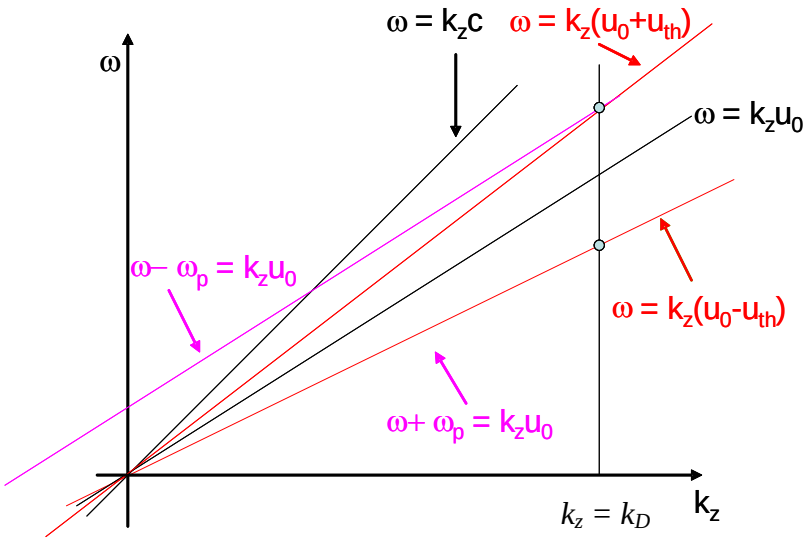

Figure A0-5 Scheme of the dispersion diagram for Landau damping in an e-beam. Landau damping occurs in the case where the dispersion lines of the fast and slow plasma waves (magenta curves) intersect the dispersion lines of the thermal electrons of the beam (red curves).

9. Derivatives of the Pierce equation roots

Here some mathematical expressions of the roots of Pierce dispersion equation are calculated. They are being used in the analysis of the FEL transfer matrix in Chapter 3.

The Pierce equation (Eq. 3-23) is:

$$\Delta = s\left(\left(s - i\theta\right)^2 + \theta_{prw}^2\right) - i\Gamma^3 = 0 \qquad \text{A0-46}$$

Let S_j is a root of the Pierce dispersion equation. Thus, using the Implicit function theorem, we define:

$$\frac{dS_j}{d\theta} = -\frac{\dfrac{\partial\Delta}{\partial\theta}}{\dfrac{\partial\Delta}{\partial s}} = \frac{2is^2 + 2\theta s}{3s^2 - 4i\theta s + \theta_{prw}^2 - \theta^2} \qquad \text{A0-47}$$

$$\frac{dS_j}{d\theta_{prw}} = -\frac{\dfrac{\partial\Delta}{\partial\theta_{prw}}}{\dfrac{\partial\Delta}{\partial s}} = \frac{-2\theta_{prw} s}{3s^2 - 4i\theta s + \theta_{prw}^2 - \theta^2} \qquad \text{A0-48}$$

Based on these results, the higher order derivatives are given as:

$$\frac{d^2S_j}{d\theta^2} = \frac{d}{d\theta}\left(\frac{dS_j}{d\theta}\right) = \frac{2s}{3s^2 - 4i\theta s + \theta_{prw}^2 - \theta^2} - \frac{\left(2is^2 + 2\theta s\right)\left(-4is - 2\theta\right)}{\left(3s^2 - 4i\theta s + \theta_{prw}^2 - \theta^2\right)^2} \qquad \text{A0-49}$$

$$\frac{d^2S_j}{d\theta_{prw}^2} = \frac{d}{d\theta_{prw}}\left(\frac{dS_j}{d\theta_{prw}}\right) = \frac{-2s}{3s^2 - 4i\theta s + \theta_{prw}^2 - \theta^2} - \frac{-4\theta_{prw}^2 s}{\left(3s^2 - 4i\theta s + \theta_{prw}^2 - \theta^2\right)^2} \qquad \text{A0-50}$$

$$\frac{d^2S_j}{d\theta_{prw}d\theta} = \frac{d}{d\theta_{prw}}\left(\frac{dS_j}{d\theta}\right) = -\frac{\left(2is^2 + 2\theta s\right)2\theta_{prw}}{\left(3s^2 - 4i\theta s + \theta_{prw}^2 - \theta^2\right)^2} \qquad \text{A0-51}$$

For the synchronism condition (θ = 0), neglecting the space charge effect (θ_{prw} = 0), the roots of the Pierce equation are:

$$S_{1_0} = \frac{\sqrt{3} + i}{2}\Gamma$$

$$S_{2_0} = \frac{-\sqrt{3} + i}{2}\Gamma$$

$$S_{3_0} = -i\Gamma$$

Substituting these results into equations A0-47 - A0-51, we obtain:

$$\left.\frac{dS_j}{d\theta}\right|_{\substack{\theta=0 \\ \theta_{prw}=0}} = \frac{2i}{3}$$

$$\left.\frac{dS_j}{d\theta_{prw}}\right|_{\substack{\theta=0\\ \theta_{prw}=0}} = 0$$

$$\left.\frac{d^2S_j}{d\theta^2}\right|_{\substack{\theta=0\\ \theta_{prw}=0}} = -\frac{2}{9S_{j0}}$$

$$\left.\frac{d^2S_j}{d\theta_{prw}^2}\right|_{\substack{\theta=0\\ \theta_{prw}=0}} = -\frac{2}{3S_{j_0}}$$

$$\left.\frac{d^2S_j}{d\theta_{prw}d\theta}\right|_{\substack{\theta=0\\ \theta_{prw}=0}} = 0$$

Thus, the roots of the Pierce equation in the Tailor expansion are:

$$S_j = S_{j_0} + \frac{2i}{3}\theta + 0\cdot\theta_{prw} - \frac{1}{9S_{j_0}}\theta^2 - \frac{1}{3S_{j_0}}\theta_{prw}^2 + 0\cdot\theta_{prw}\theta + \ldots$$

Comparison of this result with the exact calculation based on Cardano's formula (Figure A0-6) demonstrates a good agreement near the synchronism frequency ($\theta/\Gamma < 1$).

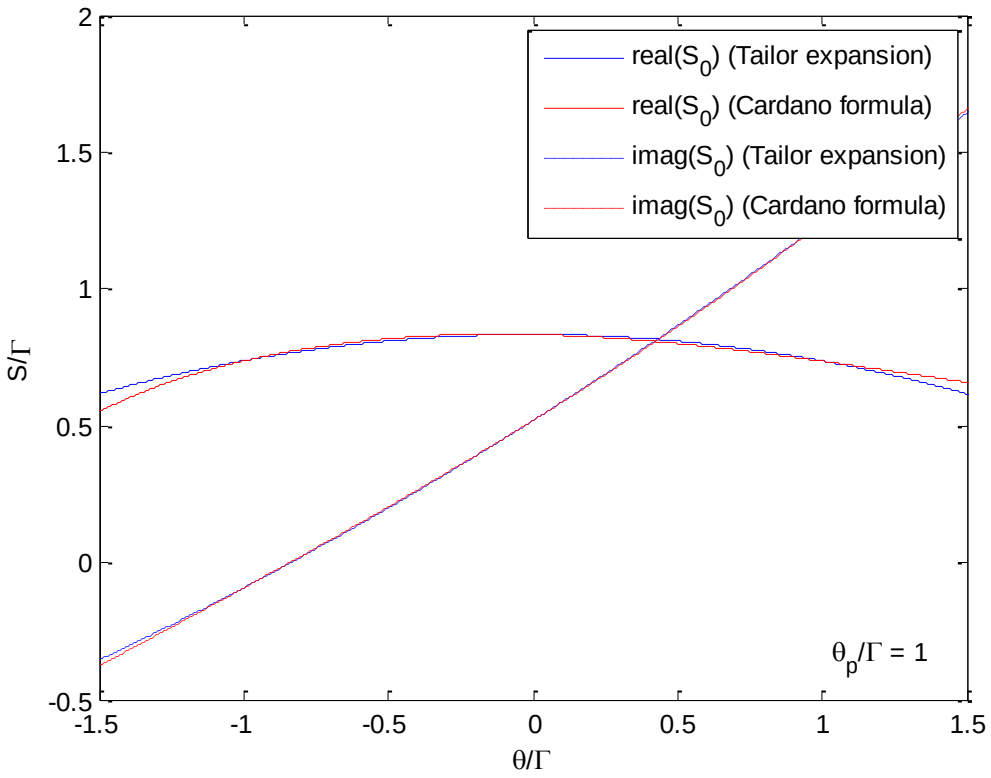

Figure A0-6. The Pierce equation's root with a positive real part calculated by the Tailor expansion (blue lines) and by the exact Cardano's equation (red lines).

10. The Radiation Noise Equivalent Power of an FEL considering the collective microdynamic process in a preceding e-beam drift section

In order to find the noise equivalent power parameters (NEP) of the combined system (free drift and wiggler) of an FEL in the high gain regime, we multiply the transfer matrix of the FEL - $\tilde{\tilde{\mathbf{H}}}_{FEL}$, (see Eqs. 3-30, 3-39 and 3-40) by the 3x3 transfer matrix of the e-beam drift section - $\tilde{\tilde{\mathbf{H}}}_{T}$ (see Eqs. 2-68 and 4-2):

$$\tilde{\mathbf{H}}_{TOT}=\tilde{\mathbf{H}}_{FEL}\tilde{\mathbf{H}}_{T}=\begin{pmatrix} h^{EE}f^{EE} & \cos(\theta_{prd}L_d)h^{EI}f^{EI}-iW_d\sin(\theta_{prd}L_d)h^{EV}f^{EV} & \frac{-i}{W_d}\sin(\theta_{prd}L_d)h^{EI}f^{EI}+\cos(\theta_{prd}L_d)h^{EV}f^{EV} \\ h^{IE}f^{IE} & \cos(\theta_{prd}L_d)h^{II}f^{II}-iW_d\sin(\theta_{prd}L_d)h^{IV}f^{IV} & \frac{-i}{W_d}\sin(\theta_{prd}L_d)h^{II}f^{II}+\cos(\theta_{prd}L_d)h^{IV}f^{IV} \\ h^{VE}f^{VE} & \cos(\theta_{prd}L_d)h^{VI}f^{VI}-iW_d\sin(\theta_{prd}L_d)h^{VV}f^{VV} & \frac{-i}{W_d}\sin(\theta_{prd}L_d)h^{VI}f^{VI}+\cos(\theta_{prd}L_d)h^{VV}f^{VV} \end{pmatrix}$$

Thus, we obtain:

$$\tilde{H}^{EI}_{TOT}=\cos(\theta_{prd}L_d)h^{EI}f^{EI}-iW_d\sin(\theta_{prd}L_d)h^{EV}f^{EV}=$$

$$=-\cos(\theta_{prd}L_d)\frac{E^{*}_{q\perp}}{8P_q}\frac{a_w}{\gamma_0\beta_z\Gamma}\exp\left(-i\frac{\pi}{6}\right)-iW_d\sin(\theta_{prd}L_d)\frac{iE^{*}_{q\perp}}{8P_q}\frac{a_w}{\gamma_0\beta_z\Gamma}\frac{\theta_{prw}}{W_w\Gamma}\exp\left(-i\frac{\pi}{3}\right)=$$

$$=-\frac{E^{*}_{q\perp}}{8P_q}\frac{a_w}{\gamma_0\beta_z\Gamma}\exp\left(-i\frac{\pi}{6}\right)\left(\cos(\theta_{prd}L_d)-\sin(\theta_{prd}L_d)\frac{W_d\theta_{prw}}{W_w\Gamma}\exp\left(-i\frac{\pi}{6}\right)\right)=$$

$$=H^{EI}_{FEL}\left(\cos(\theta_{prd}L_d)-\sin(\theta_{prd}L_d)\frac{W_d\theta_{prw}}{W_w\Gamma}\exp\left(-i\frac{\pi}{6}\right)\right)$$

$$\tilde{H}^{EV}_{TOT}=\frac{-i}{W_d}\sin(\theta_{prd}L_d)h^{EI}f^{EI}+\cos(\theta_{prd}L_d)h^{EV}f^{EV}=$$

$$=\frac{-i}{W_d}\sin(\theta_{prd}L_d)\frac{-E^{*}_{q\perp}}{8P_q}\frac{a_w}{\gamma_0\beta_z\Gamma}\exp\left(-i\frac{\pi}{6}\right)+\cos(\theta_{prd}L_d)\frac{iE^{*}_{q\perp}}{8P_q}\frac{a_w}{\gamma_0\beta_z\Gamma}\frac{\theta_{prw}}{W_w\Gamma}\exp\left(-i\frac{\pi}{3}\right)=$$

$$=\frac{iE^{*}_{q\perp}}{8P_q}\frac{a_w}{\gamma_0\beta_z\Gamma}\frac{\theta_{prw}}{W_w\Gamma}\exp\left(-i\frac{\pi}{3}\right)\left(\frac{W_w\Gamma}{W_d\theta_{prw}}\sin(\theta_{prd}L_d)\exp\left(i\frac{\pi}{6}\right)+\cos(\theta_{prd}L_d)\right)=$$

$$=H^{EV}_{FEL}\left(\frac{W_w\Gamma}{W_d\theta_{prw}}\sin(\theta_{prd}L_d)\exp\left(i\frac{\pi}{6}\right)+\cos(\theta_{prd}L_d)\right)$$

Substituting these expressions into the second, third and fourth terms of equation 4-3 results in the following three NEP contributions to the total NEP power (Eq. 4-9) :

1. The current noise equivalent power is:

$$\left(\frac{dP_{NEP}(L_d)}{d\omega}\right)^{I}=\left(\frac{dP_{NEP}}{d\omega}\right)^{I}_{L_d=0}\left|\cos(\theta_{prd}L_d)-S\exp\left(-i\frac{\pi}{6}\right)\sin(\theta_{prd}L_d)\right|^2 \qquad \text{A0-52}$$

2. The kinetic voltage noise equivalent power is:

$$\left(\frac{dP_{NEP}(L_d)}{d\omega}\right)^{V} = \left(\frac{dP_{NEP}}{d\omega}\right)^{V}_{L_d=0}\left|\cos(\theta_{prd}L_d) + \frac{1}{S}\sin(\theta_{prd}L_d)\exp\left(i\frac{\pi}{6}\right)\right|^2 \qquad \text{A0-53}$$

3. The kinetic power noise equivalent power is:

$$\left(\frac{dP_{NEP}(L_d)}{d\omega}\right)^{IV} = \frac{2}{\pi}\frac{P_q}{G^2}2\,\mathrm{Re}\left[H^{EI}_{FEL}\left(\cos(\theta_{prd}L_d) - \sin(\theta_{prd}L_d)S\exp\left(-i\frac{\pi}{6}\right)\right)\cdot\right.$$

$$\left.\cdot\left(H^{EV}_{FEL}\right)^{*}\left(\frac{1}{S}\sin(\theta_{prd}L_d)\exp\left(-i\frac{\pi}{6}\right) + \cos(\theta_{prd}L_d)\right)\right]\overline{\breve{V}(0,\omega)\breve{I}^{*}(0,\omega)} =$$

$$-2\left(\frac{dP_{NEP}(L_d)}{d\omega}\right)^{IV}_{L_d=0}\mathrm{Re}\left[\exp\left(i\frac{2\pi}{3}\right)\left(\cos^2(\theta_{prd}L_d) - \sin^2(\theta_{prd}L_d)\exp\left(-i\frac{\pi}{3}\right) - \right.\right.$$

$$\left.\left. - \cos(\theta_{prd}L_d)\sin(\theta_{prd}L_d)\exp\left(-i\frac{\pi}{6}\right)S\left(1 - 1/S\right)\right)\right] =$$

$$-2\left(\frac{dP_{NEP}(L_d)}{d\omega}\right)^{IV}_{L_d=0}\left(-\frac{\cos^2(\theta_{prd}L_d)}{2} + \frac{\sin^2(\theta_{prd}L_d)}{2}\right) = \left(\frac{dP_{NEP}(L_d)}{d\omega}\right)^{IV}_{L_d=0}\cos(2\theta_{prd}L_d)$$

A0-54

where the equations 3-69 – 3-71 are used to define the corresponding NEP expressions for $L_d = 0$, and the noise suppression parameter S is defined by:

$$S = \frac{W_d\theta_{prw}}{W_w\Gamma} \qquad \text{A0-55}$$

With simplifying assumptions that the beam cross-section area (A_e) and the plasma reduction factor (r_p) are the same in the free drift and the wiggler sections, the noise suppression parameter may be written as:

$$S = \left(\frac{\gamma_{0d}^3\beta_{0d}^3}{\gamma_0\gamma_{0z}^2\beta_{0z}^3}\right)^{\frac{1}{2}}\frac{\theta_{prw}}{\Gamma} \qquad \text{A0-56}$$

References

1 A. Gover, "Lasers: Free Electron Lasers", Encyclopedia of Modern Optics, p. 431, Ed. R. D. Guenther, D. G. Steel and L. Bayvel, Elsevier, Oxford (2005)

2 P.O'Shea, H.Freund, "Free-Electron Lasers: Status and Applications", Science, **292**, p.1853 (2001)

3 C. W. Roberson, P. Sprangle, "A review of free electron lasers", NRL (1989)

4 Zhirong Huang, Kwang-Je Kim, "Review of x-ray free-electron laser theory", Phys. Rev. ST-AB, **10**, p.034801 (2007)

5 B.W.J. McNeil, N.R. Thompson, "X-ray free electron lasers", Nature Photonics, **4**, p.814 (2010)

6 S.Khan, "Free Electron Lasers", Journal of Modern Optics, **55**, p.3467 (2008)

7 Data based in part on H.P. Freund, V.L. Granatstein, "Long wavelength free-electron lasers in 1998", Nucl. Instrum. Methods Phys. Res. A, **429**, p.33 (1999),.

8 W. Colson, "Short wavelength free electron lasers in 2000", Nucl. Instrum. Methods Phys. Res. A **475**, p.397, (2001)

9 Dr. R. Willingale Lecture Notes, University of Leicester, Department of Physics and Astronomy Lasers and Quantum Optics

10 P. Emma, et al. "First lasing and operation of an ångstrom-wavelength free-electron laser", Nature Photonics, **4**, p.6417 (2010)

11 H. Wabnitz, et al, "Multiple ionization of atom clusters by intense soft X-rays from a free-electron laser",Nature, **420**, p.482 (2002).

12 M. Meyer, et al, "Two-color photoionization in XUV free-electron and visible laser fields", Phys. Rev. A, **74**, p.011401 (2006).

13 A. A.Sorokin, et al, "Multi-photon ionization of molecular nitrogen by femtosecond soft x-ray FEL pulses", Journal of Physics B: Atomic, Molecular and Optical Physics, **39**, L.299 (2006).

14 R. Sobierajski, et al, "Experimental station to study the interaction of intense femtosecond vacuum ultraviolet pulses with matter at TTF1 free electron laser", Review of Scientific Instruments, v.76, p.013909 (2005).

15 H. Chapman, et al, "Femtosecond diffractive imaging with a soft-X-ray free-electron laser", Nature Physics, **2**, p.839 (2006).

16 A. Gover, A. Amir, L. R. Elias "Laser Line Broadening Due to Classical and Quantum Noise and the Free-Electron-Laser Linewidth", Phys. Rev. A **35**, 164-173 (1987).

17 A.L. Schawlow and C.H. Townes, "Infrared and optical masers", Phys. Rev. **112**, p.1940 (1958)

18 K.J. Kim, “Three-Dimensional Analysis of Coherent Amplification and Self-Amplified Spontaneous Emission in Free-Electron Lasers”, Phys. Rev. Lett., **57**, p.1871 (1986).

19 S. Krinsky and L.H. Yu, “Output power in guided modes for amplified spontaneous emission in a single-pass free-electron laser”, Phys. Rev. A **35**, p.3406 (1987).

20 E.L. Saldin, E.A. Schneidmiller, M.V. Yurkov, “The Physics of Free Electron Lasers”, Springer, Berlin-Heidelberg (2000)

21 E. Hemsing, A. Gover, J. Rosenzweig, “Virtual dielectric waveguide mode description of a high-gain free-electron laser. I. Theory”, Phys. Rev. A, **77**, p063830 (2008)

22 E. Hemsing, A. Gover, J. Rosenzweig, “Virtual dielectric waveguide mode description of a high-gain free-electron laser. II. Modeling and numerical simulations”, Phys. Rev. A, **77**, p.063831 (2008)

23 G. Lambert et al, “Injection of harmonics generated in gas in a free-electron laser providing intense and coherent extreme-ultraviolet light”, Nature Physics **4**, p.296 (2008).

24 L. DiMauro, et al, “First SASE and seeded FEL lasing of the NSLS DUV FEL at 266 and 400 nm”, Nucl. Instrum. Methods Phys. Res. A, **507**, p.15 (2003).

25 L. H. Yu et al. “High-Gain Harmonic-Generation Free-Electron Laser”, Science, **289**, p.932 (2000).

26 A. Gover, E. Dyunin, “FEL Prize Lecture: Coherent Electron-Beam Radiation Sources and FELs: A Theoretical Overview”, Proceedings of FEL 2006, BESSY, Berlin, Germany http://cern.ch/AccelConf/f06/PAPERS/MOAAU01.PDF.

27 K.L. Jensen, et al, “A photoemission model for low work function coated metal surfaces and its experimental validation”, J.Appl. Phys. **99**, p.124905 (2006).

28 A. Gover, E. Dyunin, “Collective-Interaction Control and Reduction of Optical Frequency Shot Noise in Charged-Particle Beams”, Phys. Rev. Lett. **102**, p.154801 (2009)

29 A. Nause, E. Dyunin, A. Gover, “Optical frequency shot-noise suppression in electron beams: three-dimensional analysis”, J. Appl. Phys., **107**, p.103101 (2010)

30 A.Gover, E.Dyunin, T.Duchovni, A.Nause, “Collective microdynamics and noise suppression in dispersive electron beam transport”, Physics of Plasmas, **18**, p.123102 (2011)

31 A. Gover, A. Nause, E. Dyunin, M. Fedurin, “Beating the shot-noise limit”, Nature Physics, **8**, p.877 (2012)

32 E. Dyunin, A.Gover, “The general velocity and current modulation linear transfer matrix of FEL and control over SASE power in the collective regime”, Nucl. Instrum. Methods Phys. Res. A, **593**, p.49 (2008)

33 A. Gover, E. Dyunin, “Coherence limits of free electron lasers”, IEEE J. Quantum Electron., **46**, p. 1511 (2010)

34 J.R. Pierce, “Theory and design of electron beams”, 2nd ed. Toronto : Van Nostrand (1954)

35 J.R. Pierce, “Traveling-Wave tubes”, Toronto : Van Nostrand (1950)

36 H.A. Haus, L.D. Smullin, “Noise in electron devices”, New York : M.I.T. (1959)

37 F.B.Llewellyn, “Electron Inertia Effects”, Cambridge Univ. Press, Cambridge (1941)

38 F.B.Llewellyn, L.C.Peterson, “Vacuum tube network”, Proc. IRE, **32**,p.144 (1944)

39 S.Bloom, R.W.Peter, “Transmission line analog of a Modulated Electron Beam”, RCA Rev. **15**, p.95 (1954)

40 H.Haus, ”Limitations on the noise figure of microwave amplifiers of the beam type”, Trans. Inst. Radio Eng., **ED-1**, p.238, (1954)

41 F.N.H. Robinson, “Microwave shot noise in electron beams and the minimum noise factor of travelling wave tubes and klystrons”, J. Brit. Inst. Radio Engrs., **14**, p.79 (1954)

42 H. Nyquist, "Thermal Agitation of Electric Charge in Conductors", Phys. Rev. **32**, p.110 (1928)

43 H. T. Friis, “Noise figure of radio receivers”, Proc. Inst. Radio Eng., **32**, p.419 (1944)

44 J.R.Pierce, “A theorem Concerning noise in electron streams”, Journal of Appl. Phys, **25**, p.931 (1954)

45 C.C.Cutler, C.F.Quate, “Experimental verification of space charge and transit time reduction of noise in electron beam”, Phys. Rev. **80**, p.875 (1950)

46 H. Motz, “Applications of the Radiation from Fast Electron Beams”, J. Appl. Phys. **22,** p.527 (1951)

47 J.M.J. Madey, H.A. Schwettman, W.M. Fairbank, “A Free Electron Laser”, IEEE Trans. Nucl Sci., **NS-20**, p.980 (1973)

48 D.A.G. Deacon, et al, “First Operation of a Free-Electron Laser”, Phys.Rev.Lett, **38**, p.892 (1977)

49. H. Motz, W. Thon and R. N. Whitehurst, “Experiments on Radiation by Fast Electron Beams”, J. Appl. Phys. 24, 826 (1953) .

50 H. Motz and M. Nakamura, “Radiation of an electron in an infinitely long waveguide”, Annals of Physics, **7**, p.84 (1959)

51 H. Motz and M. Nakamura, “The Generation of Submillimeter Waves and Fast-Wave Amplification”, Proc. Symp. Millimeter Waves 1959, p.155, Polytechnic Press, Brooklyn, New York, (1960)

52 R. H. Pantell, G. Soncini, and H. E. Puthoff, “Stimulated photon-electron scattering”, IEEE J. Quantum Electronics **4**, p.905 (1968).

53. L. R. Elias, W. M. Fairbank, J. M. J. Madey, H. A. Schwettman, and T. I. Smith, “Observation of Stimulated Emission of Radiation by Relativistic Electrons in a Spatially Periodic Transverse Magnetic Field”, Phys. Rev. Lett. **36**, p.717 (1976).

54 A. Gover and P. Sprangle, “A Unified Theory of Magnetic-Bremsstrahlung, Electrostatic Bremsstrahlung, Compton-Raman Scattering and Cerenkov-Smith Purcell Free Electron Lasers”, IEEE J. of Quantum Electronics, **QE-17**, p.11965 (1981).

55 A.Gover, A.Yariv, "Collective and Single Electron Interactions of Electron Beam with Electromagnetic Waves, and Free-Electron Laser”, *Journal of Applied Physics*, **16**, p.121, 1978

56 Workshop on the Microbunching Instability, September 17–19, Trieste, Italy 2007. Links on presentations:
http://www.elettra.trieste.it/FERMI/index.php?n=Main.MicrobProgram

4th Microbunching Instability, Maryland, 2012, Links on presentations:
http://www.umer.umd.edu/events_folder/uBi12/PastUBIWorkshops/ubi12-Talks

57 Z.Huang et al, “Suppression of microbunching instability in the linac coherent light source”, Phys. Rev. ST-AB, **7**, p.074401 (2004)

58 R.A.Bosch, et al, “Modeling two-stage bunch compression with wakefields: Macroscopic properties and microbunching instability”, Phys. Rev. ST-AB, **11**, p.090702 (2008)

59 T.Shaftan, Z.Huang, “Experimental characterization of a space charge induced modulation in high-brightness electron beam”, Phys. Rev. ST-AB, **7**, p.080702 (2004)

60 L.A. Lugiato, F. Casagrande, L. Pizzuto, “Fluctuation theory in quantum-optical systems”, Phys. Rev. A, **26**, p.3438 (1982)

61 R. H. Dicke, “Coherence in Spontaneous Radiation Processes”, Phys. Rev. **93**, p.99 (1954)

62 J.B. Rosenzweig, et al, “Quasicrystalline beam formation in RF photoinjectors”, ADVANCED ACCELERATOR CONCEPTS: Proceedings of the Thirteenth Advanced Accelerator Concepts Workshop, AIP Conference Proceedings, **1086**, p.661 (2009)

63 V.N. Litvinenko, “Suppressingshot noise and spontaneouse radiation in electron beams”, Proceedings of FEL2009, TUOB05, Liverpool, UK (2009)

64 A. Marinelli, et al, “Three dimensional analysis of longitudinal plasma oscillations in a thermal relativistic electron beam”, Physics of Plasmas, **18**, p.103105 (2011)

65 A. Marinelli, et al, “Microscopic kinetic analysis of space-charge induced optical microbunching in a relativistic electron beam”, Phys. Rev. ST-AB, **13**, p.110703 (2010)

66 P. Musumeci , et al, “Nonlinear Longitudinal Space Charge Oscillations in Relativistic Electron Beams”, Phys. Rev. Lett., **106**, p.184801 (2011)

67 L. J. Chu, “A kinetic power theorem,” presented at the IRE-PGED Electron Tube Research Conference, Durham, New Hampshire, June, 1951.

68 Z. Huang, et al, “Suppression of microbunching instability in the linac coherent light source”, Phys. Rev. ST Accel. Beams 7, 074401 (2004).

69 D. Ratner, et al, “Analysis of shot noise suppression for electron beams”, Phys. Rev. ST Accel. Beams **14**, p.060710 (2011)

70 D. Ratner, A. Chao, and Z. Huang, “Three-Dimensional Analysis of Longitudinal Space Charge Microbunching Starting from Shot Noise”, in FEL Conf. Gieongju, Korea, 2008, http://www.slac.stanford.edu/cgi-wrap/getdoc/slac-pub-13392.pdf

71 R. Akre, et al, “Commissioning the Linac Coherent Light Source injector”, Phys. Rev. ST Accel. Beams **11**, p.030703 (2008)

72 H. Haus and F. N. H. Robinson, “The minimum noise figure of the microwave beam amplifier”, Proc. IRE **43**, p.981 (1955)

73 W. C. Hahn, “Small signal theory of velocity modulated electron beams”, Gen. Elec. Rev. **42**, p.258 (1939).

74 G.M. Brunch, T.G.Mihran, “Plasma Frequency Reduction Factors in Electron Beams”, IRE Transactions on Electron Device, **2**, p.3 (1955)

75 M. Venturini, “Models of longitudinal space-charge impedance for microbunching instability”, Phys. Rev. ST Accel. Beams **11**, p.034401 (2008).

76 M. Xie, “Exact and variational solutions of 3D eigenmodes in high gain FELs”, Nucl. Instrum. Methods Phys. Res. A **445**, p.59 (2000).

77 L. H. Yu, S. Krinsky, and R. L. Gluckstern, “Calculation of universal scaling function for free-electron-laser gain”, Phys. Rev. Lett. 64, p.3011 (1990)

78 J. B. Rosenzweig “Fundamental of beam physics”, Oxford University Press, 2003

79 L. Landau, “On the vibrations of the electronic plasma”, J. Phys. USSR **10**, p.25 (1946) or

L. Landau, “On the vibrations of the electronic plasma”, Zh. Eksp. Teor. Fiz. (JETP) **16**, p.574 (1946).

80 J.D. Jackson, “Longitudinal Plasma Oscillations” J. Nucl. Energy. Part C: Plasma Physics, **1**, p.171 (1960)

81 Prof.Gover Lecture Notes

82 R. Bonifacio and C. Pellegrini, “Collective instabilities and high-gain regime in a free electron laser”, Opt. Commun., **50**, p.373 (1984).

83 I. Schnitzer, A. Gover, “The prebunched free electron laser in various operating gain regimes”, Nucl. Instrum. Methods Phys. Res. A **237**, p.124 (1985)

84 B.Z. Steinberg, A. Gover, S. Rushin, “Three-dimensional theory of free-electron lasers in the collective regime”, Physical Review A **36**, p.147 (1987)

85 E. Jerby, A.Gover, “Investigation of the gain regimes and gain parameter of the free electron lasers dispersion equation”, IEEE Journal of Quantum Electronics, **QE-21**, p.1041 (1985)

86 R.Horn, C. Johnson, “Matrix Analysis”, (Chapter 5), UK, Cambridge: Cambridge University Press, (1985).

87 A. Gover, “Superradiant and stimulated-superradiant emission in prebunched electron-beam radiators. I. Formulation”, Physical Review Special Topics-Accelerators and Beams, **8**, p.030701 (2005)

88 A. Gover, E. Dyunin, Y. Lurie, Y.Pinhasi, M.V. Krongauz, “Superradiant and stimulated-superradiant emission in prebunched electron-beam II. Radiation enhancement schemes”, Physical Review Special Topics-Accelerators and Beams, **8**, p.030702 (2005)

89 I.B. Drobyazko, et al, “Lasing in visible and ultraviolet regions in an optical klystron installed on the VEPP-3 storage ring”, Nucl. Instrum. Methods Phys. Res., Sect. A**282**, p.424 (1989)

90 M. Arbel, et al, “Superradiant and stimulated superradiant emission in a prebunched beam free-electron maser”, Physical Review Letters, **86**, p.2561 (2001)

91 V. Zhaunerchyk, et al, “Selective amplification of the lower-frequency branch via stimulated super-radiance in a waveguided free electron laser oscillator driven by short electron bunches”, Applied Physics Letters, **97**, p.231109 (2010)

92 A. Friedman, “Spontaneous and stimulated emission from quasifree electrons”, Reviews of Modern Physics, **60**, p.471 (1988)

93 R. Mitzner, et al, “Spatio - temporal coherence of free electron laser pulses in the soft X-ray regime”, Optics Express, **16**, p.19909 (2008).

94 Juhao Wu, et al, “Exponential growth, superradiance, and tunability of a seeded free electron laser”, Optics Express, **16**, p.3255 (2008)

95 S. Krinski and R.L. Gluckstern, Phys.Rev. ST-AB, 6, 050701, (2003).

96 M. Reiser, “Theory and Design of Charged Particle Beam”, Wiley (1994).

97 D. Ratner and G. Stupakov, “Observation of Shot Noise Suppression at OpticalWavelengths in a Relativistic Electron Beam”, Physical Review Letters, **109**, p.034801 (2012)

98 R.R. Lindberg, K.-J. Kim, “Mode growth and competition in the X-ray free-electron laser oscillator start-up from noise”, Phys. Rev. ST Accel. Beams, **12**, p.070702 (2009)

99 A.I. Ahiezer and I.A. Ahiezer, “Plasma Electrodynamics”, Pergamon, New York (1974)

100 N. N. Bogoliubov. "Kinetic Equations", Journal of Physics USSR **10,** p.265 (1946).

101 M. Born and H. S. Green "A General Kinetic Theory of Liquids I. The Molecular Distribution Functions", Proc. Roy. Soc. A **188**, p.10 (1946)

102 John G. Kirkwood, "The Statistical Mechanical Theory of Transport Processes I. General Theory", The Journal of Chemical Physics **14**, p.180 (1946)

103 J. Yvon, “Theorie Statistique des Fluides et l'Equation d'Etat”, (in French), Actes sientifique et industrie. № 203. Paris: Hermann. (1935)

104 A. A. Vlasov "On Vibration Properties of Electron Gas", (in Russian). J. Exp. Theor. Phys. **8,** p.291 (1938).

105 J.D. Jackson, “Classical Electrodynamics”, 3rd Ed., Wiley (1998)

106 V.L Ginzburg and I.M. Frank, “On the Transition Radiation Theory”, Sov. Phys. J. Exp. Theor. Phys. **16**, p.15 (1946)

107 V.L Ginzburg and V.N. Tsytovich, “Several problems of the theory of transition radiation and transition scattering”, Phys. Rep. **49**, p.1 (1979)

108 V.E. Pafomov, “Radiation of a charged particle in the presence of a separating boundary”, Proceedings P.N. Lebedev Physics Institute, ed. by D.V. Skolbel'tsyn, **44,** p.25 (Consultants Bureau, New York, 1971).

109 A.Tremaine, et al, “Observation of Self-Amplified Spontaneous-Emission-Induced Electron-Beam Microbunching Using Coherent Transition Radiation”, Phys. Rev. Lett. **81**, p.5816 (1998).